

# **UNIVERSITY OF ALBERTA**

## **Experimental Investigation of the Effect of Elasticity on the Sweep Efficiency in Viscoelastic Polymer Flooding Operations**

by

**Tolkynay S. Urbissinova**

A thesis submitted to the Faculty of Graduate Studies and Research  
in partial fulfillment of the requirements for the degree of

**Master of Science**

**in**

**Petroleum Engineering**

Department of Civil and Environmental Engineering

©Tolkynay S. Urbissinova

Fall, 2010

Edmonton, Alberta

Permission is hereby granted to the University of Alberta Libraries to reproduce single copies of this thesis and to lend or sell such copies for private, scholarly or scientific research purposes only. Where the thesis is converted to, or otherwise made available in digital form, the University of Alberta will advise potential users of the thesis of these terms.

The author reserves all other publication and other rights in association with the copyright in the thesis and, except as herein before provided, neither the thesis nor any substantial portion thereof may be printed or otherwise reproduced in any material form whatsoever without the author's prior written permission.

## **Examining Committee**

Ergun Kuru, Civil and Environmental Engineering

Japan J. Trivedi, Civil and Environmental Engineering

Juliana Leung, Civil and Environmental Engineering

Phillip Choi, Chemical and Materials Engineering

## **ABSTRACT**

This study aims to investigate the effect of elastic properties of viscoelastic polymer solutions on the microscopic sweep efficiency in enhanced oil recovery (EOR) operations.

The effect of elasticity was studied as isolated from the shear viscosity effect using polymer blends with identical shear viscosity behavior but different elastic characteristics. Oil displacement results were compared and the individual effect of elasticity on the sweep efficiency was investigated.

A detailed rheological characterization of the polymer solutions was done to measure their viscoelastic properties. A series of polymer flooding experiments were performed using a radial core holder.

Results of the experiments indicated that the sweep efficiency of a polymeric fluid could be effectively improved by adjusting the molecular weight distribution (MWD) of the solution at constant shear viscosity and polymer concentration. An attempt was made to find a rheological parameter of polymer solutions that correlates better with the resultant oil recovery.

## **ACKNOWLEDGEMENTS**

It is a great pleasure to express my deepest gratitude and appreciation to my supervisors, Dr. Ergun Kuru and Dr. Japan J. Trivedi, whose highly professional and immensely valuable advice, mentorship, guidance and encouragement throughout the research study made this thesis possible. I am much obliged to them for they could always make their time available to listen to my questions and to provide helpful and valuable answers.

I am heartily thankful to Mr. Stephen Gamble for his support in constructing the experimental set-up and solving other technical issues. I would also like to thank Tao Guo, Shishir Shivhare and Santhosh Kumar, who kindly gave me a helping hand in conducting the experiments as and when needed.

I would also like to make a special reference to Mr. Hassan Dehghanpour, who provided his helpful advice and suggestions with regard to the research study.

It is an honor for me to acknowledge the financial support provided by the Bolashak International Scholarship of the President of Kazakhstan, which offered a unique opportunity for me to study and pursue my academic ambitions at the University of Alberta. The financial support of the research study provided by the National Science and Engineering Research Council of Canada is also greatly appreciated.

Last but not least, I owe my sincere gratitude to my beloved mother and father, my brother, my three sisters, especially Gulder Urbissinova, who stayed in Edmonton this summer beside me to provide her immeasurable support in numerous ways, also my friends Noira Nigmatova, Yerzhan Dauletyarov, Jones Olumide, other friends and fellow students, who inspired, encouraged and morally supported me during my time at the university.

# TABLE OF CONTENTS

<b>1 INTRODUCTION.....</b>	<b>1</b>
1.1 Overview.....	1
1.2 Statement of the Problem.....	2
1.3 Objective and Scope of the Study.....	4
1.4 Structure of the Thesis.....	5
<b>2 LITERATURE REVIEW.....</b>	<b>7</b>
2.1 Polymer Flooding Technology.....	7
2.1.1 Polymer Flooding for Enhanced Oil Recovery Applications .....	7
2.1.2 Polymer Flooding Mechanisms and Principles.....	8
2.1.3 Screening Criteria for Polymer Flooding.....	13
2.2 Polymers Used in Enhanced Oil Recovery Operations.....	17
2.2.1 Synthetic Polymers.....	17
2.2.2 Biopolymers.....	19
2.2.3 Evaluation of Polymers for Enhanced Oil Recovery .....	21
2.3 Rheological Properties of Aqueous Polymer Solutions.....	26
2.3.1 Shear Viscosity.....	26
2.3.2 Normal Stress Difference.....	27
2.3.3 Extensional Viscosity.....	28

2.3.4	Trouton Ratio.....	30
2.4	Effect of Weight Average Molecular Weight and Molecular Weight Distribution on Rheological Properties of Polymer Solutions.....	32
2.4.1	Weight Average Molecular Weight.....	32
2.4.2	Molecular Weight Distribution.....	34
2.5	Rheological Behavior of Polymer Solutions in Porous Media.....	36
2.5.1	Rheological Models Describing the Rheological Behavior of Polymer Solutions.....	36
2.5.1.1	Power-Law Model.....	36
2.5.1.2	Carreau Model.....	38
2.5.2	Viscoelastic Models for Polymer Flow in Porous Media....	40
2.6	Viscoelasticity of Polymer Solutions in Polymer Flooding Operations....	47
2.6.1	Mobilization of Oil in Polymer Flooding.....	47
2.6.2	Effect of Viscoelasticity of Polymer Solutions on the Displacement Efficiency.....	50
<b>3</b>	<b>EXPERIMENTAL PROGRAM.....</b>	<b>53</b>
3.1	Materials Used in the Experimental Studies.....	54
3.2	Preparation of Polymer Solutions.....	56
3.2.1	Procedure for the Preparation of Polymer Solutions.....	55
3.2.2	Preparation of Polymer Solutions with Identical Shear Viscosity but Different Elastic Properties.....	59
3.3	Rheological Characterization of Polymer Solutions.....	61

3.3.1	Viscometry Tests.....	63
3.3.2	Oscillation Tests.....	64
3.3.2.1	Amplitude Sweep.....	64
3.3.2.2	Frequency Sweep.....	66
3.3.3	Creep/Recovery Tests.....	67
3.4	Polymer Flooding Experiments.....	68
3.4.1	Experimental Set-Up for Polymer Flooding Experiments.....	68
3.4.1.1	Radial Core Holder.....	70
3.4.1.2	Syringe Pump for Saturating the Core Holder with Mineral Oil.....	71
3.4.1.3	Positive Displacement Pump for Injecting Polymer Solutions.....	72
3.4.1.4	Data Acquisition System.....	73
3.4.2	Experimental Procedure.....	74
3.4.2.1	Core Holder Packing Procedure.....	74
3.4.2.2	Porosity Measurement.....	75
3.4.2.3	Absolute Permeability Measurement.....	75
3.4.2.4	Flow Rate Determination.....	77
3.4.2.5	Flooding Procedure.....	80

<b>4</b>	<b>EXPERIMENTAL RESULTS AND DISCUSSION (POLYETHYLENE OXIDE)</b> .....	<b>82</b>
4.1	Weight Average Molecular Weight and Polydispersity Indices of PEO Solutions.....	82
4.2	Rheological Characterization of PEO Solutions.....	84
4.2.1	Viscometry Test Results.....	84
4.2.2	Oscillation Test Results.....	88
4.2.2.1	Amplitude Sweep Results.....	88
4.2.2.2	Frequency Sweep Results.....	89
4.2.3	Creep/Recovery Test Results.....	92
4.3	Polymer Flooding Experiments with PEO Solutions.....	93
4.3.1	Pressure Drop During Polymer Flooding Experiments.....	93
4.3.2	Oil Displacement Results.....	95
4.3.3	Effluent Viscometry Results.....	97
4.3.4	Summary of Experimental Results.....	99
<b>5</b>	<b>EXPERIMENTAL RESULTS AND DISCUSSION (PARTIALLY HYDROLYZED POLYCRYLAMIDE)</b> .....	<b>101</b>
5.1	Weight Average Molecular Weight and Polydispersity Indices of HPAM Solutions.....	101
5.2	Rheological Characterization of HPAM Solutions.....	103
5.2.1	Viscometry Test Results.....	104
5.2.2	Oscillation Test Results.....	109

5.2.2.1	Amplitude Sweep Results.....	110
5.2.2.2	Frequency Sweep Results.....	113
5.2.3	Creep/Recovery Test Results.....	116
5.3	Polymer Flooding Experiments with HPAM Solutions.....	119
5.3.1	Pressure Drop During Polymer Flooding Experiments.....	119
5.3.2	Oil Displacement Results.....	121
5.3.3	Effluent Viscometry Results.....	125
5.3.4	Summary of Experimental Results.....	127
<b>6</b>	<b>EXPERIMENTAL RESULTS AND DISCUSSION (XANTHAN GUM).....</b>	<b>130</b>
6.1	Rheological Characterization of Xanthan Gum Solution.....	130
6.1.1	Viscometry Test Results.....	130
6.2	Polymer Flooding Experiment with Xanthan Gum Solution.....	133
6.2.1	Oil Displacement Results.....	133
6.2.2	Effluent Viscometry Results.....	135
6.2.3	Summary of Experimental Results.....	136
<b>7</b>	<b>COMPARISON OF EXPERIMENTAL DATA FOR PEO, HPAM AND XANTHAN GUM SOLUTIONS.....</b>	<b>138</b>
7.1	Comparison of Experimental Results of Xanthan Gum and HPAM Solutions.....	138
7.1.1	Comparison of Viscometry Test Results.....	138

7.1.2 Comparison of Polymer Flooding Results.....	142
7.2 Comparison of Experimental Data for PEO, HPAM and Xanthan Gum Solutions.....	144
<b>8 CONCLUSIONS AND RECOMMENDATIONS.....</b>	<b>151</b>
8.1 Conclusions.....	151
8.2 Recommendations.....	154
<b>REFERENCES.....</b>	<b>156</b>

## LIST OF TABLES

Table 2-1—Technical Screening Criteria for Polymer Flooding (Taber et al., 1997).....	16
Table 3-1—PEO Grades with Various Weight Average Molecular Weight Values.....	54
Table 3-2—HPAM Grades with Various Weight Average Molecular Weight Values.....	55
Table 4-1—Composition of PEO Samples 1 and 2.....	82
Table 4-2—Weight Average Molecular Weight and Polydispersity of PEO Samples 1 and 2.....	83
Table 4-3—Power-Law Parameters for PEO Samples 1 and 2.....	85
Table 4-4—Summary Table of Experimental Data for Polymer Flooding Experiments with PEO Samples 1 and 2.....	100
Table 5-1—Composition of HPAM Samples 1 and 2.....	101
Table 5-2—Weight Average Molecular Weight and Polydispersity of HPAM Samples 1 and 2.....	102
Table 5-3—Composition of HPAM Samples 3 and 4.....	103
Table 5-4—Weight Average Molecular Weight and Polydispersity of HPAM Samples 3 and 4.....	103
Table 5-5—Power-Law Parameters for HPAM Samples 1 and 2.....	106

Table 5-6—Power-Law Parameters for HPAM Samples 3 and 4.....	106
Table 5-7—Summary Table of Experimental Data for Polymer Flooding Experiments with HPAM Samples 1 and 2.....	128
Table 5-8—Summary Table of Experimental Data for Polymer Flooding Experiments with HPAM Samples 3 and 4.....	129
Table 6-1—Power-Law Parameters for Xanthan Gum Solution.....	131
Table 6-2— Summary Table of Experimental Data for Polymer Flooding Experiments with Xanthan Gum Solution.....	137
Table 7-1—Oil Recovery Data for Aqueous Solutions of PEO, HPAM and Xanthan Gum.....	145

## LIST OF FIGURES

Fig. 2-1—Cluster Type Residual Oil by Polymer Flooding and Waterflooding (Du and Guan, 2004).....	9
Figure 2-2—Influence of Viscosity Ratio on Oil Recovery Process According to Tunn (Littmann, 1988).....	11
Fig. 2-3—Polymer Flood Project Evaluation and Development Process (Kaminsky et al., 2007).....	14
Fig. 2-4—Extensional Viscosity of M1 as a Function of Strain Rate and Axial Location (James and Chandler, 1990).....	29
Fig. 2-5—Trouton Ratio of 20.0% w/w Casein and 35.0% w/w Waxy Maize Starch as a Function of Extensional Strain Rate at 25°C Compared to Purely Viscous Fluid (Chan, 2007).....	31
Fig. 2-6—Schematic Presentation of the Flow Behavior of Polymer Solutions (Heemskerk et al., 1984).....	37
Fig.2-7—Comparison of the Carreau and Power-Law Models (Sorbie, 1991)....	40
Fig. 2-8—Effect of the Main Practical Parameters on the Core Flow (Heemskerk et al., 1984).....	41
Fig. 2-9—Overview of Parameters for the Description of the Core Flow of Polyacrylamide Solutions (Heemskerk et al., 1984).....	43
Fig. 2-10—Relation Between Pressure Difference and Time for Viscoelastic Fluids (Ranjbar et al., 1992).....	44

Fig. 2-11—Schematic of Viscoelastic Flow in Porous Media.....	48
Fig. 2-12—Forces Acting on Residual Oil Film in Oil Wet Systems (Wang et al., 2007; Jiang et al., 2008).....	49
Fig. 2-13—Forces Acting on Residual Oil Droplet in Water Wet Systems (Wang et al., 2007).....	49
Fig. 2-14—Residual Oil in “Dead Ends” After Waterflooding and Polymer Flooding (Wang et al., 2001).....	51
Fig. 2-15—Mobilization of Residual Oil in Films (Wang et al., 2001).....	52
Fig. 3-1—Rotational Rheometer Used for Rheological Characterization of Polymer Solutions.....	62
Fig. 3-2—Viscometry Test (Bohlin Instruments, 2003).....	63
Fig. 3-3—Amplitude Sweep Test (Bohlin Instruments, 2003).....	65
Fig. 3-4—Frequency Sweep Test (Bohlin Instruments, 2003).....	66
Fig. 3-5—Creep/Recovery Tests (Bohlin Instruments, 2003).....	68
Fig. 3-6—Schematic Diagram of the Experimental Set-up.....	69
Fig. 3-7—Radial Core Holder.....	70
Fig. 3-8—Syringe Pump Used to Saturate the Core Holder with Mineral Oil.....	71
Fig. 3-9—Positive Displacement Pump with the Variable Frequency Drive Used to Inject Polymer Solutions into the Core Holder.....	72

Fig. 3-10—Calibration Curve for Positive Displacement Pump Flow Rate.....	73
Fig. 3-11—Data Logger.....	74
Fig. 3-12—Pressure Drop vs. Flow Rate Profile for Water Injection.....	76
Fig. 3-13—Shear Rate Envelope for the Polymer Flooding Experiments.....	80
Fig. 4-1—Shear Stress vs. Shear Rate Profiles for PEO Samples 1 and 2.....	85
Fig. 4-2—Shear Viscosity vs. Shear Rate for PEO Samples 1 and 2.....	86
Fig. 4-3—Normal Force vs. Shear Rate for PEO Samples 1 and 2.....	87
Fig. 4-4—Elastic Modulus vs. Shear Stress for PEO Samples 1 and 2.....	88
Fig. 4-5—Viscous Modulus vs. Angular Frequency for PEO Samples 1 and 2...	90
Fig. 4-6— Elastic Modulus vs. Angular Frequency for PEO Samples 1 and 2...	91
Fig. 4-7— Creep and Recovery Compliance vs. Time for PEO Samples 1 and 2... .....	92
Fig. 4-8—Pressure Drop During Injection of PEO Samples 1 and 2.....	94
Fig. 4-9—Cumulative Oil Recovery vs. Polymer Solution Injected for PEO Samples 1 and 2.....	95
Fig. 4-10—Breakthrough Recovery and Total Oil Recovery for PEO Samples 1 and 2.....	96
Fig. 4-11—Shear Viscosity vs. Shear Rate for Effluent Fluids of PEO Samples 1 and 2.....	98

Fig. 5-1—Shear Stress vs. Shear Rate Profiles for HPAM Samples 1 and 2.....	104
Fig. 5-2—Shear Stress vs. Shear Rate Profiles for HPAM Samples 3 and 4.....	105
Fig. 5-3—Shear Viscosity vs. Shear Rate Profiles for HPAM Samples 1 and 2.... .....	107
Fig. 5-4—Shear Viscosity vs. Shear Rate Profiles for HPAM Samples 3 and 4..... .....	107
Fig. 5-5—Normal Force vs. Shear Rate for HPAM Samples 1 and 2.....	108
Fig. 5-6—Normal Force vs. Shear Rate for HPAM Samples 3 and 4.....	108
Fig. 5-7—Elastic Modulus vs. Shear Stress for HPAM Samples 1 and 2.....	110
Fig. 5-8—Elastic Modulus vs. Shear Stress for HPAM Samples 3 and 4.....	111
Fig. 5-9—Viscous Modulus vs. Angular Frequency for HPAM Samples 1 and 2... .....	113
Fig. 5-10—Viscous Modulus vs. Angular Frequency for HPAM Samples 3 and 4.. .....	114
Fig. 5-11—Elastic Modulus vs. Angular Frequency for HPAM Samples 1 and 2.....	115
Fig. 5-12—Elastic Modulus vs. Angular Frequency for HPAM Samples 3 and 4.....	115
Fig. 5-13— Creep and Recovery Compliance vs. Time for HPAM Samples 1 and 2.....	117

Fig. 5-14— Creep and Recovery Compliance vs. Time for HPAM Samples 3 and 4.....	118
Fig. 5-15—Pressure Drop During Injection of HPAM Samples 3 and 4.....	120
Fig. 5-16—Cumulative Oil Recovery vs. Polymer Solution Injected for HPAM Samples 1 and 2.....	121
Fig. 5-17—Cumulative Oil Recovery vs. Polymer Solution Injected for HPAM Samples 3 and 4.....	122
Fig. 5-18—Breakthrough Recovery and Total Oil Recovery for HPAM Samples 1 and 2.....	123
Fig. 5-19—Breakthrough Recovery and Total Oil Recovery for HPAM Samples 3 and 4.....	124
Fig. 5-20—Shear Viscosity vs. Shear Rate for Effluent Fluids of HPAM Samples 1 and 2.....	125
Fig. 5-21—Shear Viscosity vs. Shear Rate for Effluent Fluids of HPAM Samples 3 and 4.....	126
Fig. 6-1—Shear Stress vs. Shear Rate Profile for the Xanthan Gum Solution...	131
Fig. 6-2—Shear Viscosity vs. Shear Rate for the Xanthan Gum Solution.....	132
Fig. 6-3—Normal Force vs. Shear Rate for the Xanthan Gum Solution.....	132
Fig. 6-4—Cumulative Oil Recovery vs. Polymer Solution Injected for the Xanthan Gum Solution.....	133

Fig. 6-5—Breakthrough Recovery and Total Oil Recovery for the Xanthan Gum Solution.....	134
Fig. 6-6—Shear Viscosity vs. Shear Rate for Effluent Fluids of the Xanthan Gum Solution .....	135
Fig. 7-1—Shear Stress vs. Shear Rate Profile for the Xanthan Gum Solution Compared to HPAM Samples 1 and 2.....	139
Fig. 7-2—Shear Viscosity vs. Shear Rate Profile for the Xanthan Gum Solution Compared to HPAM Samples 1 and 2.....	140
Fig. 7-3—Normal Force vs. Shear Rate for the Xanthan Gum Solution as Compared to HPAM Samples 1 and 2.....	141
Fig. 7-4—Cumulative Oil Recovery vs. Polymer Solution Injected for the Xanthan Gum Solution and HPAM Samples 1 and 2.....	142
Fig. 7-5—Breakthrough Recovery and Total Oil Recovery for the Xanthan Gum Solution and HPAM Samples 1 and 2.....	143
Fig. 7-6—Equivalent Trouton Ratio of Aqueous Solutions of PEO, HPAM and Xanthan Gum.....	146
Fig. 7-7—Total Oil Recovery vs. Equivalent Trouton Ratio of Aqueous Solutions of PEO, HPAM and Xanthan Gum at a Shear Rate of 20 1/s.....	148
Fig. 7-8—Total Oil Recovery vs. Equivalent Trouton Ratio of Aqueous Solutions of PEO, HPAM and Xanthan Gum at a Shear Rate of 14 1/s.....	149
Fig. 7-9—Total Oil Recovery vs. Equivalent Trouton Ratio of Aqueous Solutions of PEO, HPAM and Xanthan Gum at a Shear Rate of 100 1/s.....	149

## LIST OF NOMENCLATURE

### Roman Letters

A	Cross section area
b	Empirical constant (Eq. 2-15)
$C_1$	Initial concentration
$C_2$	Bulk solution concentration
$\overline{D}_p$	Average grain diameter
$De$	Deborah number
$E'$	Model index (Eq. 2-24)
$F_R$	Resistance factor
$F_{Rr}$	Residual resistance factor
$G^*$	Complex modulus
$G'$	Elastic modulus
$G''$	Viscous modulus
h	Height of the core
I	Polydispersity index
$k_o$	Permeability of the oil phase
$k_w$	Permeability of the water phase
K	Consistency index

$K$	Empirical constant (Eq. 2-13)
$M$	Mobility ratio
$M_w$	Weight average molecular weight
$M_{w,B}$	Weight average molecular weight of a blend
$M_{w,i}$	Weight average molecular weight of polymer grade $i$
$M_n$	Number average molecular weight
$N_v$	Viscosity number
$n$	Power-law index (or flow behavior index)
$n$	Empirical constant (Eq. 2-27)
$n_1$	Power-law exponent (Fig. 2-9)
$n_2$	Power-law exponent (Fig. 2-9)
$n_2$	Empirical constant (Eq. 2-27)
$\Delta P_t$	Pressure difference
$P'$	Pressure after reducing the injection rate (Eq. 2-24)
$P''$	Pressure by which the original pressure was reduced (Eq. 2-24)
$P_e$	Pressure at the external boundary
$P_w$	Pressure at the wellbore
$P_{11} - P_{22}$	First normal stress difference (Eq. 2-15)

$r_e$	Radius at the external boundary
$r_w$	Radius of the wellbore
$Q$	Flow rate
$S_{or}$	Residual oil saturation
$T_r$	Trouton ratio
$u$	Fluid velocity
$\bar{v}$	Average interstitial velocity
$V$	Volume
$(3n+1)/4n$	Non-Newtonian correction for power-law fluids or Rabinowitsch correction factor

## Greek Letters

$\alpha$	Empirical constant (Eq. 2-19 and Eq. 2-26)
$\alpha$	Material constant (Eq. 3-7)
$\alpha$	Intercept of a log-log plot of $N_v$ vs. pressure gradient (Eq. 2-25)
$\beta$	Slope of a log-log plot of $N_v$ vs. pressure gradient (Eq. 2-25)
$\beta$	Empirical constant (Eq. 2-12)
$\dot{\gamma}$	Rate of strain (or shear rate)
$\gamma_{eff}$	Effective shear rate
$\Gamma_s$	Surface excess
$\delta$	Phase angle
$\dot{\epsilon}$	Extensional rate
$\eta$	Apparent viscosity
$\eta_0$	Zero shear rate viscosity
$\eta_\infty$	High shear rate viscosity
$\eta_e$	Extensional viscosity
$\theta_{f_1}$	Longest relaxation time
$\lambda$	Mobility

$\lambda$	Time constant (Eq. 2-21)
$\lambda$	Empirical constant (Eq. 2-27)
$\lambda_2$	Empirical constant (Eq. 2-27)
$\mu$	Shear viscosity
$\mu_0$	Zero shear rate viscosity
$\mu_p^0$	Limiting Newtonian viscosity at the low shear limit
$\mu_\infty$	Limiting Newtonian viscosity at the high shear limit
$\mu_{\max}$	Empirical constant (Eq. 2-27)
$\sigma$	First normal stress difference
$\sigma'$	Second normal stress difference
$\sigma_{11}$	First principle stress
$\sigma_{22}$	Second principle stress
$\sigma_{33}$	Third principle stress
$\sigma_n$	Normal stress
$\tau$	Shear stress
$\tau_f$	Fluid relaxation time (Eq. 2-22)
$\phi$	Porosity
$\omega_i$	Weight fraction of polymer grade i

# CHAPTER 1

## INTRODUCTION

---

### 1.1 Overview

Polymer flooding is a chemical oil recovery method, which consists in adding high-molecular-weight polymers to thicken the injection water for the purpose of reducing its tendency to by-pass oil in less permeable portions of the reservoir, thus, improving the reservoir sweep efficiency.

Polymer flooding for EOR applications was first suggested in the early 1960s. Extensive research efforts that followed the early pioneering work on the polymer flooding technology have significantly contributed to the improvement of the polymer flooding process. Numerous successful lab-scale as well as field-scale projects have been carried out, among which a large-scale project in Daqing oil field located in the northern part of China is of special note. The polymer flooding technology is now considered a technically and economically proven EOR method, and it still attracts significant research efforts that aim to further improve the technology.

It has been widely reported in the literature that it is viscoelasticity of polymer solution that plays an important role in polymer flood operations. This can be explained by the specific nature of the viscoelastic fluid flow in porous media,

which is distinctively different from that of Newtonian fluids. Moreover, some authors have reported that the major mechanism in the polymer flooding process is the elasticity of polymer solution. They have indicated that the displacement efficiency can be significantly improved due to the elastic properties of the injected polymeric fluids, which can result in high incremental oil recovery.

Thus, there is an enormous incentive to investigate the elastic properties of polymeric fluids and their effect on the displacement efficiency. In this regard, the clear delineation of the effect of elasticity plays a pivotal role for EOR applications.

## **1.2 Statement of the Problem**

It is well-known that much oil usually remains in a reservoir even after primary and secondary recovery processes (usually waterflooding). Therefore, the development of improved oil recovery methods was a focus area of many researchers. It was identified that it is the high mobility ratio that makes waterflooding an inefficient recovery process and results in much oil bypassed and left behind in a reservoir. Even more oil remains in heterogeneous reservoirs, where conventional waterflooding also fails to efficiently displace and sweep oil. It is now well-known that these weaknesses of conventional waterflooding can be remedied by polymer-augmented waterflooding.

It stands to reason, that the polymer flooding process should be improved for the economic development of a reservoir. In this regard, selection of polymer solutions with optimum characteristics can play an important role. Numerous authors have investigated and presented laboratory results showing the effect of viscoelasticity on the displacement efficiency in polymer flood operations. Wang et al. (2001) reported results of the core flood tests conducted with viscoelastic polymer solutions indicating that elastic properties of the injected fluids substantially increased the displacement efficiency. The effect of viscoelastic properties of polymer solutions was also studied by Xia et al. (2004) and Wang et al. (2007), who, in agreement with the previously-mentioned studies, attributed the increase in oil recovery to elastic properties of polymer solutions.

Despite all the efforts, the individual effect of elasticity isolated from the viscosity effect has not been clearly distilled for a single viscoelastic polymer. In this study, the effect of elasticity of polymer-based fluids on the microscopic sweep efficiency is investigated. The individual effect of elasticity is studied by comparing the results of oil displacement by polymer blends having similar shear viscosity behavior but different elastic characteristics.

It is also very important to clearly identify a rheological parameter of a polymer solution that could be used for screening of polymers for EOR. Therefore, an attempt was made in this experimental study to find a rheological parameter that could be used as a general screening criterion for polymers in EOR operations independent of the polymer type, molecular weight, concentration, etc.

### **1.3 Objective and Scope of the Study**

The objective of this experimental study was to investigate the individual effect of elasticity on the microscopic sweep efficiency in viscoelastic polymer flood operations. This was done by injecting polymer solutions with identical weight average molecular weight (i.e. identical shear viscosity behavior) and different MWD (i.e. different elastic characteristics) into the radial core holder and comparing the resultant oil recovery.

The secondary objective of the study was to identify if there is any correlation between oil recovery and rheological properties of injected polymer solutions independent of the polymer type, molecular weight, concentration, etc. A rheological parameter was selected that is thought to be prospective for use as a general screening criterion for polymers in EOR operations.

To achieve the above-stated research objectives, the following tasks were defined and accomplished:

- 1) Literature review on the subject area;
- 2) Preparation of aqueous polymer solutions with similar weight average molecular weights and different MWD;
- 3) Rheological characterization of the polymer solutions, including the determination of shear viscosity behavior and the measurement of elastic properties of the solutions;

- 4) Polymer flooding experiments using a special core holder designed to simulate radial flow;
- 5) Analysis of experimental results, including breakthrough and total oil recovery for each type of polymer used in the experimental study;
- 6) Comparison of all experimental results regardless of the polymer type, molecular weight, concentration, etc.

#### **1.4 Structure of the Thesis**

Chapter 1 presents the overview of the research study. It also states the research problem as well as the scope and objectives of the research work.

Chapter 2 gives a literature review relevant to the subject of the research study. It provides a comprehensive theoretical background on the polymer flooding technology, rheological properties of polymer solutions, behavior of viscoelastic polymer solutions in porous media, and the effect of viscoelastic properties on the displacement efficiency in EOR operations.

Chapter 3 addresses the experimental program of the research work. It describes the materials, equipment and experimental procedures for polymer solution preparation, rheological characterization and flooding experiments. It also gives a detailed description of the rheological tests and the experimental set-up used in this study.

Chapter 4 provides the results of the rheological tests carried out on the polyethylene oxide (PEO) solutions, including the viscometry tests, oscillation tests, and creep/recovery tests. The chapter also discusses the results of polymer flooding experiments with the PEO solutions conducted in the radial core holder.

Chapter 5 presents and discusses the results of the rheological tests and polymer flooding experiments using the partially hydrolyzed polyacrylamide (HPAM) solutions.

Chapter 6 states the results of the rheological tests and the polymer flooding experiment carried out with the xanthan gum solution.

Chapter 7 compares the experimental results of all the polymer solutions used in the experimental study to identify a relation between the rheological properties of the injected polymer solutions and the resultant oil recovery independent of the polymer type, molecular weight, concentration, etc.

Chapter 8 concludes the thesis with a summary of the experimental results and recommendations for further research.

## **CHAPTER 2**

### **LITERATURE REVIEW**

---

#### **2.1 Polymer Flooding Technology**

##### **2.1.1 Polymer Flooding for Enhanced Oil Recovery Applications**

Polymer flooding, sometimes referred to as polymer-augmented waterflooding, is a chemical EOR method, which was suggested in the early 1960s to remedy the problems observed in conventional waterflooding associated with the high mobility ratio and the reservoir heterogeneity. Pye and Sandiford were the first to establish that water-soluble polymers added into the injection water can lead to better displacement of oil and, consequently, greater oil recovery compared to conventional waterflooding (Sorbie, 1991).

The early pioneering work on the polymer flooding technology was then followed by further research efforts, which improved the understanding of the non-Newtonian nature of polymer solutions and polymer flooding mechanisms (Clay and Menzie, 1966; Jennings et al., 1971; Chauveteau and Kohler, 1974; Hill et al., 1974; Szabo, 1975; Chang, 1978; Chauveteau, 1982; Martin et al., 1983). Later works on polymer flooding included works by Needham and Doe (1987), Castagno et al. (1987), Allen and Boger (1988), Gleasure and Phillips (1990), Hejri et al. (1991).

Polymer flooding has been used successfully for the improvement of the reservoir sweep (Taber et al., 1997). Primarily because of the low polymer cost, there have been conducted more polymer flooding projects than any other EOR method (Trivedi, 2009).

The interest in polymer flooding has increased especially after successful results were achieved in Daqing oil field located in the northern part of China. It was reported that an incremental oil recovery of 20% OIIP was obtained in Daqing due to high concentration polymer flooding (Wang et al., 2010).

Nowadays, it is generally known that the polymer flooding technology might be an economically efficient oil recovery method and a reasonable EOR choice. Moreover, EOR polymers are also used in surfactant/polymer and alkali/surfactant/polymer floods as mobility control agents.

### **2.1.2 Polymer Flooding Mechanisms and Principles**

The objective of polymer flooding is to provide better sweep efficiency and more efficient displacement of oil during waterflooding, which is achieved due to the following mechanisms as indicated by Taber et al. (1997):

- Decrease in the mobility of the injection water
- Increase in the viscosity of the injection water
- Contact with a larger reservoir volume.

The above mechanisms employed in polymer flooding operations lead to higher oil recovery compared to waterflooding. This is clearly shown in Fig. 2-1 by Du and Guan (2004), which compares the results of conventional waterflooding and polymer flooding.

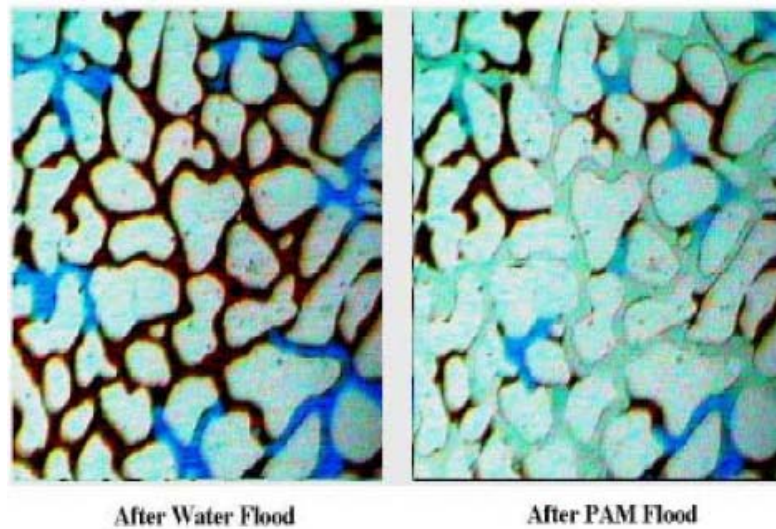


**Fig. 2-1—Cluster Type Residual Oil by Polymer Flooding and Waterflooding (Du and Guan, 2004)**

The discussion of the polymer flooding mechanisms would be insufficient without introducing the key concepts associated with polymer flooding, namely, the displacement efficiency, volumetric sweep efficiency, mobility ratio, resistance factor and residual resistance factor.

The displacement efficiency (local or microscopic sweep efficiency) is defined as the ratio of the amount of displaced oil to the amount of oil contacted by the displacing fluid.

It should be noted here that the terms “displacement efficiency” and “sweep efficiency” are interchangeably used herein to determine the ratio of the volume of oil recovered in a displacement process to the volume of oil initially in place (OIIP).

The volumetric sweep efficiency is defined as the ratio of the volume of oil contacted by the displacing fluid to the volume of OIIP.

Since EOR polymers are used as mobility control agents, the mobility ratio M is a central concept to all mechanisms of oil recovery by polymer flooding. It is given by:

$$M = \frac{\lambda_o}{\lambda_w} = \frac{[\mu_o / k_o]}{[\mu_w / k_w]} \quad 2-1$$

where:

$\lambda_o$  and  $\lambda_w$  are the mobility of the displaced fluid (oil) and the mobility of the displacing fluid (water), respectively;

$\mu_o$  and  $\mu_w$  are the viscosities of oil and water, respectively;

$k_o$  and  $k_w$  are the effective permeabilities of the oil phase and the water phase, respectively.

It is clear from the above expression that stable displacement occurs if the mobility ratio is unity or less. Thus, a water soluble EOR polymer is added to the

injection water to increase the viscosity of the displacing fluid with the purpose to reduce the mobility ratio, which leads to more efficient sweep and, consequently, greater oil recovery.

Fig 2-2 demonstrates the increase in oil recovery due to the increase in the viscosity of the displacing fluid.

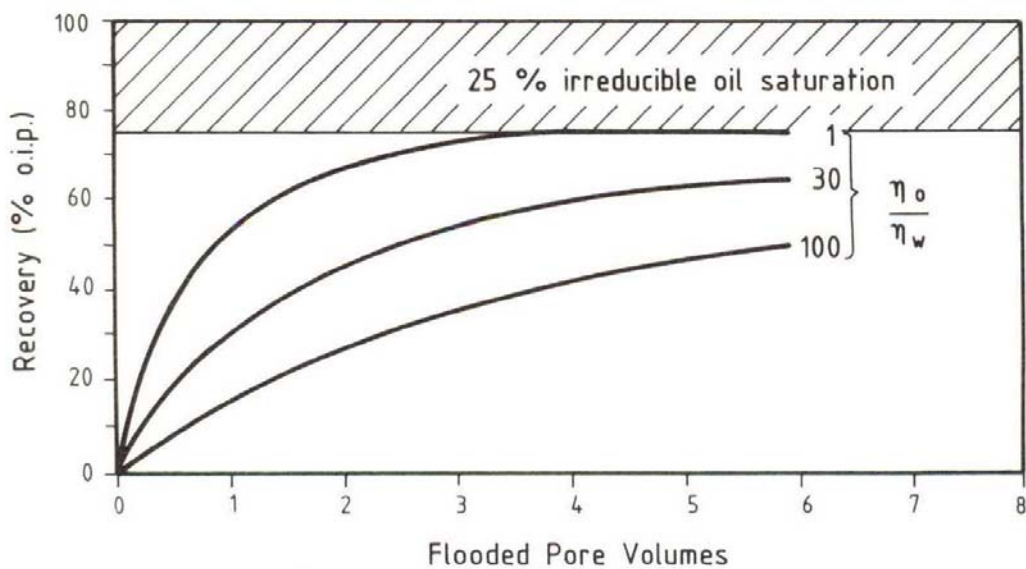


**Figure 2-2—Influence of Viscosity Ratio on Oil Recovery Process According to Tunn (Littmann, 1988)**

It should be mentioned here that the residual oil saturation  $S_{or}$  remains the same after a high number of injected pore volumes for all viscosity ratios. However, polymer flooding is still considered an efficient EOR process, because the residual oil saturation is reached more quickly, which makes polymer flooding an effective and economically attractive EOR process.

One more concept essential in polymer flooding operations is the resistance factor  $F_R$ . The resistance factor indicates the decrease in mobility of polymer solution in comparison with the flow of water or brine in which it is prepared, i.e. it is a measure of the relative mobility of polymer solution. Therefore, the resistance factor is defined as the ratio of water or brine mobility to the mobility of polymer solution in the same porous media and is expressed as follows:

$$F_R = \frac{\lambda_w}{\lambda_p} \tag{2-2}$$

which becomes

$$F_R = \frac{\mu_p}{\mu_w} \tag{2-3}$$

if there are no permeability alterations (Jennings et al., 1971).

The residual resistance factor  $F_{Rr}$ , in its turn, indicates the decrease in mobility of water that follows polymer solution relative to water flow before the flow of the polymer solution. It reflects the permanent permeability reduction and is given as:

$$F_{Rr} = \frac{\lambda_w(\text{initial})}{\lambda_p(\text{after polymer flow})} \tag{2-4}$$

### **2.1.3 Screening Criteria for Polymer Flooding**

Like any EOR method, polymer flooding has screening criteria to be applied to any polymer flood project for preliminary evaluation of reservoir candidates.

In this regard, it might be appropriate to review the overall process of polymer flood project evaluation.

The staged process of polymer flood project evaluation and development as suggested by Kaminsky et al. (2007) is given in Fig. 2-3.

As Fig. 2-3 shows, evaluating whether polymer flooding is suitable for a given field is a comprehensive process consisting of multiple stages prior to full-scale field implementation.

The first stage of this extensive process is preliminary screening, where the passing criterion is a favorable comparison of the rock and fluid properties with the general polymer flooding screening criteria. The first stage is followed by preliminary analysis and detailed analysis, both comprising Stage 2 of the process. This stage covers preliminary laboratory screening, for instance, to determine compatibility of brine with polymer, rheological behavior of polymer solution in porous media, as well as detailed laboratory investigation of polymer solutions to finalize the specific polymer choice and etc. The next stages include field testing, field pilot and, finally, commercial application.

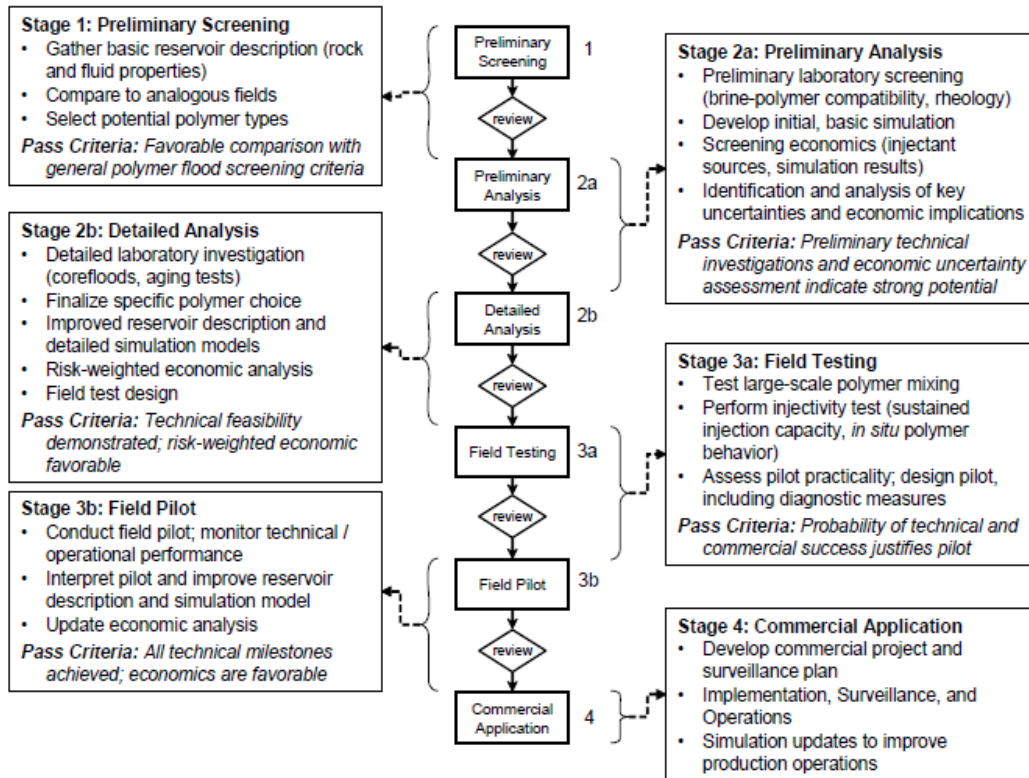


**Fig. 2-3—Polymer Flood Project Evaluation and Development Process (Kaminsky et al., 2007)**

The process of polymer flood project evaluation illustrated in Fig. 2-3 can be applied to any polymer flood project.

According to Sorbie (1991), there are two principal reasons for applying screening criteria for polymer flooding. They are as follows:

- Identify reservoirs with poor sweep efficiency due to high oil viscosity or due to large scale heterogeneity
- Determine whether the overall conditions in that reservoir are suitable for polymer flooding to remedy this problem.

It is clear, that identifying exact screening rules is impossible, however, there is some agreement which exists in the literature as to which criteria can be applied to candidate reservoirs for polymer flooding to select or, conversely, reject reservoirs as likely candidates for polymer flooding.

Technical screening criteria for polymer flooding as suggested by Taber et al. (1997) are given in Table 2-1.

TABLE 5—POLYMER FLOODING					
<b>Description</b>					
The objective of polymer flooding is to provide better displacement and volumetric sweep efficiencies during a waterflood. In polymer flooding, certain high-molecular-weight polymers (typically polyacrylamide or xanthan) are dissolved in the injection water to decrease water mobility. Polymer concentrations from 250 to 2,000 mg/L are used; properly sized treatments may require 25 to 60% reservoir PV.					
<b>Mechanisms</b>					
Polymers improve recovery by (1) increasing the viscosity of water; (2) decreasing the mobility of water; and (3) contacting a larger volume of the reservoir.					
<b>Technical Screening Guides*</b>					
	Wide-Range Recommendation			Range of Current Field Projects	
<b>Crude Oil</b>					
Gravity, °API	>15			14 to 43	
Viscosity, cp	<150 (preferably <100 and >10)			1 to 80	
Composition	Not critical				
<b>Reservoir</b>					
Oil saturation, % PV	>50			50 to 92	
Type of formation	Sandstones preferred but can be used in carbonates				
Net thickness	Not critical				
Average permeability, md	>10 md**			10 to 15,000	
Depth, ft	<9,000 (see Temperature)			1,300 to 9,600	
Temperature, °F	<200 to minimize degradation			80 to 185	
<b>Properties of Polymer-Flood Field Projects</b>					
Property	1980's median (171 projects)	Marmul	Oerrel	Courtenay	Daqing
Oil/water viscosity ratio at reservoir temperature	9.4	114	39	50	15
Reservoir temperature, °F	120	115	136	86	113
Permeability, md	75	15,000	2,000	2,000	870
% OOIP present at startup	76	≈ 92	81.5	78	71
WOR at startup	3	1	4	8	10
HPAM concentration, ppm	460	1,000	1,500	900	1,000
lbm polymer/acre-ft	25	373	162	520	271
Projected IOR, % OOIP	4.9	25***	≈ 13	30	11
Projected bbl oil/lbm polymer	1.1	1.2	≈ 1.4	0.96	0.57
Projected bbl oil/acre-ft	27	461	≈ 230	499	155
<b>Limitations/Problems</b>					
See text for limitations and recommendations for overcoming problems.					
*These screening guides are very broad. When identifying polymer-flood candidates, we recommend the reservoir characteristics and polymer-flood features be close to those of the four successful projects at the bottom of table.					
**In reservoirs where the rock permeability is less than 50 md, the polymer may sweep only fractures effectively unless the polymer molecular weight is sufficiently low.					
***IOR over primary production for this case only. For the others, IOR is incremental over waterflooding.					

**Table 2-1—Technical Screening Criteria for Polymer Flooding (Taber et al., 1997)**

## **2.2 Polymers Used in Enhanced Oil Recovery Operations**

There are two groups of water soluble polymers used for EOR process: synthetic polymers and biopolymers.

### **2.2.1 Synthetic Polymers**

The first group of EOR polymers are produced synthetically, compared to the other group of polymers, which are produced by bacterial fermentation processes.

The most widely used type of synthetic polymers is polyacrylamide. Polyacrylamides are water soluble polymers produced by many manufacturers in many ways and for different purposes.

Polyacrylamides are marketed in a variety of forms, including dry powder, liquid emulsion or dispersion, concentrated solutions and gels. This affects the procedure for polymer preparation, which shall be strictly followed to preserve appropriate polymer properties.

Polyacrylamides are co-polymers of acrylic acid and acrylamide. Polyacrylamides used in polymer flooding have undergone partial hydrolysis, which causes negatively charged carboxyl groups (--COO--) to be scattered along the backbone chain. Therefore, the polymers are referred to as partially hydrolyzed polyacrylamides or HPAM. The percentage of acrylic acid in the molecule chain gives the degree of hydrolysis. Typical degrees of hydrolysis are 30-35%

(Lake, 1989). Polymers with degrees of hydrolysis approximating 0% do not exhibit strong sensitivity to salts like polyacrylamides having higher degree of hydrolysis. In this regard, it should also be mentioned that hydrolysis of the amide continues at high temperatures. During flooding in a reservoir some hydrolysis always takes place, which shall be taken into consideration, since this may lead to changes in the chemical character of the polymer.

The degree of hydrolysis is selected to be 30-35% to optimize some properties of polymers such as water solubility, viscosity and retention. If the degree of hydrolysis is too low, the polymer will not be water soluble. And otherwise, if the degree of hydrolysis is too high, the polymer will be too sensitive to salinity and hardness.

Polyacrylamides can develop desired viscosity in fresh waters. The viscosity increasing property of polyacrylamides lies in its large molecular weight. However, as mentioned earlier, they show poor performance in high-salinity waters.

The method of synthesis of the two groups of EOR polymers gives different structural characteristics to the polymers, which, in its turn, affects the properties of solutions prepared from these polymers. HPAM molecules have a flexible coil structure, which gives viscoelastic properties that are of particular importance for many petroleum engineering applications.

Thus, the main disadvantage of polyacrylamides is that they cannot be used in high-salinity waters, especially if they are used at high temperatures. Also, they are more sensitive to mechanical degradation (shear degradation) as compared to biopolymers, which requires special considerations for polymer mixing and other operations.

On the other hand, in addition to other advantages of polyacrylamides as mentioned earlier herein, they are less expensive and show relatively good resistance to bacterial degradation as compared to biopolymers.

Due to the limitation in using polyacrylamides for EOR operations because of their sensitivity to salinity and hardness, other synthetic polymers were developed. These include, for instance, vinylsulfonate/vinylamide co-polymers that were originally developed for drilling fluids in high temperature wells. Some other synthetic polymers include polyethylene glycol, polyethylene oxide, polyvinyl acetate, polystyrene and polymethylmethacrylate (Littmann, 1988).

### **2.2.2 Biopolymers**

As mentioned above, biopolymers are another type of polymers used for EOR operations. Biopolymers are natural products from wood, seeds, etc. They are formed from the polymerization of saccharide molecules, a process of fermentation with bacteria or fungi. For this reason, these polymers are called polysaccharides. Molecular weights of polysaccharides are generally about  $2 \times 10^6$ .

Polysaccharides are marketed in a form of dry powder and liquid broths containing up to 15% active polymer (API RP 63: Recommended Practices for Evaluation of Polymers Used in Enhanced Oil Recovery Operations, 1990).

The method of the polymer synthesis gives the polymers different structural characteristics, while structural characteristics of polymers affect the properties of solutions prepared from these polymers. Biopolymers are characterized by rigidity of their molecules. This great stiffness of biopolymer molecules gives them excellent viscosifying power in high-salinity waters and resistance to mechanical degradation.

However, biopolymers are quite sensitive to bacterial attack. This necessitates using of biocides for surface handling of the polymer solutions, and if the reservoir temperature is not very high, biocides must be used along with the injected solutions to avoid biological degradation of the polymers. Both groups of polymers tend to chemically degrade at elevated temperatures.

One of the most widely used polysaccharide polymer is xanthan, which is produced by bacteria of the type *Xanthomonas Campestris*. The molecular weight of xanthan ranges from  $2 \times 10^6$  to  $50 \times 10^6$  (Sorbie, 1991).

### **2.2.3 Evaluation of Polymers for Enhanced Oil Recovery**

Hill et al. (1974) studied the behavior of HPAM and polysaccharides in porous media. The polymers were found to be satisfactory in some laboratory experiments and unsatisfactory in others. Also, according to Lake (1989), HPAM is inexpensive per unit amount than polysaccharides, however, when compared on a unit amount of mobility reduction, particularly at high salinities, the costs become close enough. Thus, both types of polymers have advantages and disadvantages. This means that a preferred polymer for a given field application is site-specific, and the selection and screening of polymers for EOR is a very important task and should be done very carefully (Saavedra et al., 2002; Levitt and Pope, 2008; Pandey et al., 2008).

Laboratory investigation of polymers used in EOR operations generally covers the following types of laboratory tests:

- Viscometric tests
- Filterability tests
- Stability tests
- Retention tests
- Porous media tests

Viscometric tests are carried out to determine the effect of shear rate, temperature, salinity, hardness, pH, and polymer concentration on the viscosity of polymer solutions.

Filterability tests are carried out to measure variations in polymer solution filterability due to undissolved solids, which can be affected by one of the following factors:

- Quality of the mix water used for preparing a polymer solution
- Quality and compatibility of a polymer
- Bacterial degradation
- Shearing conditions during polymer mixing.

Stability tests are performed to assess the resistance of a polymer solution to biological, mechanical and chemical degradation.

- Chemical degradation is the breakdown of polymer molecules, either through short-term attack by contaminants, such as oxygen, or through longer term attack of the molecular backbone by a process such as hydrolysis.
- Mechanical degradation is the breakdown of polymer molecules as a result of high mechanical stresses resulting in an irreversible loss of viscosity and resistance factor. Mechanical degradation typically occurs in the high

flow rate region of the reservoir close to the well as well as in polymer handling equipment and etc.

- Biological degradation is the breakdown of polymer molecules by bacteria. Both synthetic polymers and biopolymers are subject to biological degradation, which occurs during storage in polymer handling equipment or in a reservoir. However, biopolymers are more sensitive to this type of degradation compared to synthetic polymers (Sorbie, 1991).

To achieve the desired efficiency of polymer flooding, polymer solutions should be able to maintain their properties under the reservoir conditions for many years. One of these properties is a long-term thermal stability of polymer solutions at elevated temperatures that are expected in a reservoir. Therefore, thermal stability tests should also be included in the laboratory evaluation of polymer flood projects.

Polymer adsorption/retention data are among the most critical in terms of their impact on the recovery efficiency. Therefore, retention tests are carried out on both types of polymers to measure the adsorption effects.

Mechanisms of the polymer retention process that tends to reduce efficiency of polymer flooding can be grouped into three categories:

- Polymer adsorption refers to the interaction between the polymer molecules and the solid surface—as mediated by the solvent

(Sorbie, 1991). It is the main mechanism of polymer retention in porous media in most practical applications.

- Mechanical entrapment occurs when larger polymer molecules become lodged in narrow flow channels (Dominguez and Willhite, 1976).
- Hydrodynamic retention is the polymer retention mechanism that increases the total level of retention when the fluid rate is increased. However, it is not a large contributor to the overall levels of polymer retention in porous media (Sorbie, 1991), and can be neglected in most practical situations.

More attention should be given to the polymer adsorption, since it is the main mechanism of polymer retention in porous media.

Polymer adsorption in porous media depends on the following:

- Polymer type and properties of polymer molecules (HPAM or xanthan, molecular weight, hydrodynamic size, charge density)
- Solvent conditions (pH, salinity, hardness, temperature)
- Surface chemistry of the adsorbing substrate (silica sand, clay, sandstone, carbonate).

Adsorption is commonly measured as the surface excess  $\Gamma_s$  (mass of polymer per unit surface area of solid):

$$\Gamma_s = \frac{V\Delta C}{A} \left( \frac{\text{mass}}{\text{area}} \right) \quad 2-5$$

where:

V is the volume of polymer solution

A is the total surface area

$\Delta C = C_1 - C_2$  is the difference between the initial concentration and bulk solution concentration when the adsorption has reached equilibrium.

There are 4 types of methods for determining polymer retention during the polymer solution flow through porous media (API RP 63: Recommended Practices for Evaluation of Polymers Used in Enhanced Oil Recovery Operations, 1990):

- Large slug retention method
- Multiple slug retention method
- Recirculation method
- Static method.

Each method has its advantages and disadvantages; therefore, it is important to select the method most appropriate and possible to perform.

Last but not least, porous media tests are carried out to evaluate the resistance factor and the residual resistance factor of polymer solutions in porous media. The tests require pressure and flow rate measurements under steady state conditions.

### **2.3 Rheological Properties of Aqueous Polymer Solutions**

#### **2.3.1 Shear Viscosity**

Shear viscosity of a fluid can be defined as its resistance to shear forces during flow. Some fluids like water or oil show the same viscosity at any flow rate and their behavior can be described by the following simple relationship, in accordance with the Newton's law of viscosity:

$$\tau = \mu \dot{\gamma} \quad 2-6$$

where:

$\tau$  is the shear stress

$\dot{\gamma}$  is the rate of strain (shear rate)

$\mu$  is the Newtonian viscosity.

Fluids, for which the relation between the shear stress and the rate of strain (shear rate) can be described by Eq. 2-6 are called Newtonian fluids.

Unlike Newtonian fluids, polymer solutions are usually characterized by a shear-dependent viscosity function, i.e. the relation between the shear stress and the shear rate is nonlinear. Therefore, such fluids are called non-Newtonian fluids.

### 2.3.2 Normal Stress Difference

Normal stresses that may arise during a simple shear flow of fluids are important parameters that can be used as the characteristics of the fluids. This phenomenon of the normal stress effect is known as the Weissenberg effect named after an Austrian physicist Karl Weissenberg (Vinogradov and Malkin, 1980):

$$\sigma = \sigma_{11} - \sigma_{22} \quad 2-7$$

$$\sigma' = \sigma_{22} - \sigma_{33} \quad 2-8$$

The above quantities  $\sigma$  and  $\sigma'$  are called the first and second normal stress differences. The parameters are related to the elasticity of fluids, and, therefore, are considered good indicators of elastic properties of fluids.

Thus, during the flow of Newtonian fluids  $\sigma$  and  $\sigma'$  are equal to zero. However, normal forces during the flow of non-Newtonian fluids, like polymer solutions,

can be very high, i.e. fluids with  $\sigma$  and  $\sigma'$  parameters different from zero flow differently from Newtonian fluids.

### 2.3.3 Extensional Viscosity

The shear viscosity of a fluid is a measure of the fluid resistance to shear forces. Similarly, extensional or elongational viscosity of a fluid can be defined as the measure of the fluid resistance to extensional stresses:

$$\eta_e = \frac{\sigma_n}{\dot{\epsilon}} \quad 2-9$$

where:

$\eta_e$  is the extensional viscosity

$\sigma_n$  is the normal stress ( $\sigma_{11} - \sigma_{33}$ )

$\dot{\epsilon}$  is the extensional rate.

Extensional viscosity can be measured using special rheometers called extensional rheometers that apply extensional stress.

For a Newtonian fluid, the elongational viscosity is constant and is three times the shear viscosity (Jones et al., 1987). However, the elongational viscosity of non-Newtonian fluids is dependent on the strain rate. It is clear from Eq. 2-9 that

polymer solutions exhibiting higher normal stresses have higher extensional viscosity.

Fig. 2-4 presents the results of extensional viscosity measurements of the test fluid M1 made by James and Chandler (1990) in a converging channel rheometer. The measurements were carried out at 24°C at three tap locations (2, 3 and 4). It is clear from the figure that the extensional viscosity of the fluid increases with increasing strain rates. The figure also shows that the extensional viscosity strongly depends on the tap location, i.e. strain.

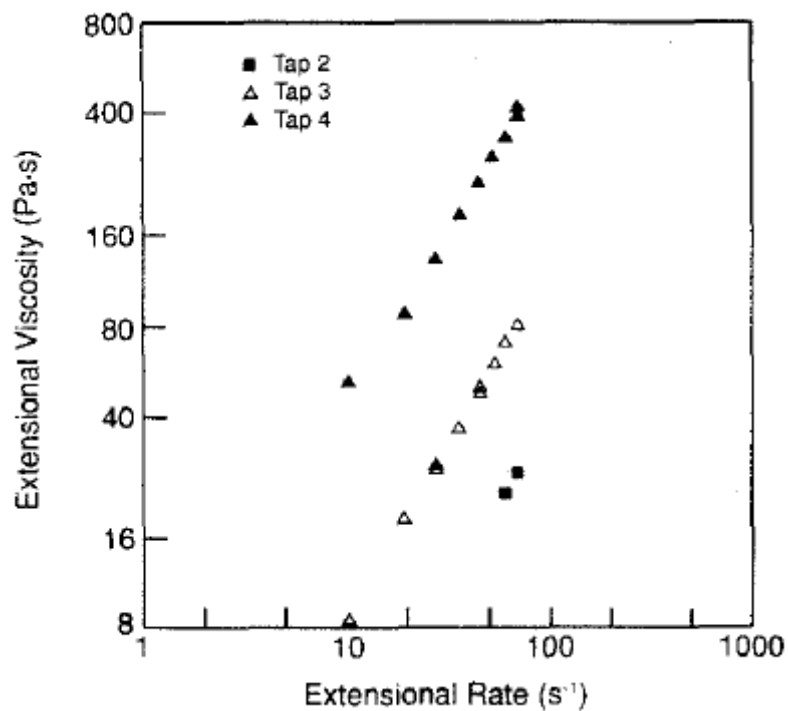


**Fig. 2-4—Extensional Viscosity of M1 as a Function of Strain Rate and Axial Location (James and Chandler, 1990)**

### 2.3.4 Trouton Ratio

The relation between extensional and shear flow properties of a fluid can be described by the Trouton ratio (Petrie, 2006), which is given by:

$$T_R = \frac{\eta_e}{\eta} \quad 2-10$$

The following relation was suggested by Jones et al. (1987):

$$T_R = \frac{\eta_e(\dot{\epsilon})}{\eta(\sqrt{3}\dot{\epsilon})} \quad 2-11$$

Thus, the Trouton ratio can be defined as the ratio of the extensional viscosity over the shear viscosity measured at a shear rate of  $\sqrt{3}$  times the extensional strain rate (Chan, 2007).

Since the Trouton ratio is defined as the ratio of extensional viscosity to shear viscosity, it can be an effective parameter in studying viscoelastic properties of fluids. For Newtonian fluids, the Trouton ratio is equal to 3. However, the Trouton ratio can be much higher for non-Newtonian fluids due to the elastic properties of the fluids.

Fig. 2-5 compares the Trouton ratio values by Chan (2007) for casein (solid square), waxy maize starch (open circle) and a purely viscous fluid (dash line).

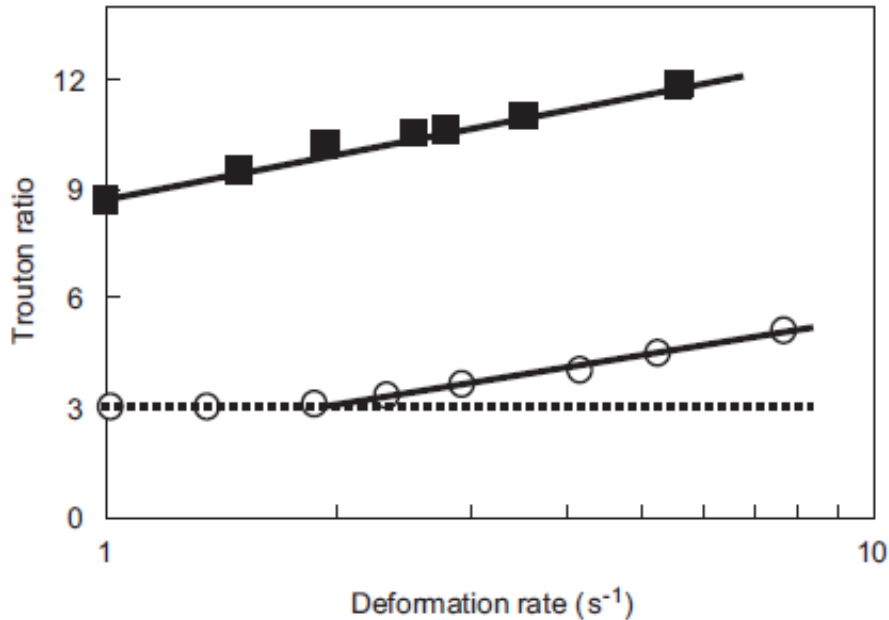


**Fig. 2-5—Trouton Ratio of 20.0% w/w Casein and 35.0% w/w Waxy Maize Starch as a Function of Extensional Strain Rate at 25°C Compared to Purely Viscous Fluid (Chan, 2007)**

Fig. 2-5 shows that the Trouton ratio for the casein system increased with increasing deformation rates. Also, the ratio was much higher than 3. This indicated that the casein system exhibited viscoelastic properties. The Trouton ratio for the starch system was close to 3 at low strain rates. However, the ratio started to increase linearly when the strain rate exceeded 2 1/s. This suggests that the starch system showed purely viscous behavior at low deformation rates; however, both biopolymers exhibited elastic properties at higher strain rates.

## 2.4 Effect of Weight Average Molecular Weight and Molecular Weight Distribution on Rheological Properties of Polymer Solutions

It is widely accepted in the literature that molecular parameters such as molecular weight averages and MWD strongly influence rheological properties of polymer solutions (Ferry, 1980; Pinaud, 1987).

### 2.4.1 Weight Average Molecular Weight

The following expression can be used to describe the relation of zero-shear viscosity  $\mu_o$  of a polymer solution to its weight average molecular weight (Pinaud, 1987):

$$\mu_o \approx M_w^\beta \quad 2-12$$

where:

$M_w$  is the weight average molecular weight

$\beta$  is the experimentally established constant close to 3.4.

With addition of the constant K, which depends on the polymer type and temperature, the expression in Eq. 2-12 can be given as follows (Ferry, 1980):

$$\mu_o = KM_w^\beta \quad 2-13$$

Dehghanpour (2008) studied viscoelastic properties of polymeric fluids using various blends of PEO. Based on the relation of the zero shear viscosity and the weight average molecular weight as given by Eq. 2-13, he prepared various polymer blends with similar weight average molecular weights, which showed similar shear viscosity behavior. He suggested the following equation to determine the weight average molecular weight of the polymer blends:

$$M_{w,B} = \prod_{i=1}^n M_{w,i}^{\omega_i} \quad 2-14$$

where:

$M_{w,B}$  is the weight average molecular weight of a blend consisting of n polymer grades

$M_{w,i}$  is the weight average molecular weight of polymer grade i

$\omega_i$  is the weight fraction of polymer grade i.

Also, it should be noted that the weight average molecular weight of polymer solutions influences their viscoelastic properties (Pinaud, 1987).

Pinaud (1987) studied viscoelastic properties of poly(ethylene terephthalate), polyamide and poly(dimethyl siloxane) polymer melts and deduced the following relation of the weight average molecular weight to the first normal stress difference related to elasticity of polymer solutions:

$$P_{11} - P_{22} \approx M_w^{6.8} \dot{\gamma}^2 / (1 + b \dot{\gamma}^\alpha)^2 \quad 2-15$$

where:

$P_{11} - P_{22}$  is the first normal stress difference.

Parameters  $\alpha$  and  $b$  can be determined by steady-shear analysis. They characterize the slope of the power-law region and the onset of non-Newtonian behavior, respectively.

#### **2.4.2 Molecular Weight Distribution**

The width of MWD is also reflected in the properties of polymeric fluids (Dehghanpour, 2008). Therefore, the determination of MWD can give essential information on the polymer properties.

The polymer MWD is usually described by the polydispersity index I defined by:

$$I = \frac{M_w}{M_n} \quad 2-16$$

where:

$M_w$  is weight average molecular weight

$M_n$  is number average molecular weight.

Dehghanpour (2008) used the polydispersity index to estimate the MWD of polymer blends mixed from various grades of PEO. The difference in polydispersity indices (i.e. difference in MWD) gave a difference in viscoelastic properties of the polymer blends.

Dehghanpour (2008) suggested the following equation for the polydispersity indices of the polymer blends:

$$I = \left( \sum_{i=1}^n \omega_i M_{w,i} \right) \left( \sum_{i=1}^n \frac{\omega_i}{M_{w,i}} \right) \quad 2-17$$

It should be noted here that the polydispersity index cannot be an absolute measure of MWD. Rogošić et al. (1996) reported that there have been some objections in the literature to confront the common misinterpretation of the polydispersity index as an absolute measure of MWD. They showed that the

higher polydispersity index indeed implies the wider MWD; however, the reverse is not true.

Since the higher polydispersity index implies the wider MWD, the polydispersity index was used as a measure of MWD of the polymer solutions used in this experimental study.

## **2.5 Rheological Behavior of Polymer Solutions in Porous Media**

### **2.5.1 Rheological Models Describing the Rheological Behavior of Polymer Solutions**

#### **2.5.1.1 Power-Law Model**

Polymer solutions are generally pseudoplastic or shear thinning, i.e. the viscosity of polymer solutions decreases with increasing shear rates. This applies to solutions of both types of polymers – xanthan and polyacrylamide.

However, the flow of biopolymers in porous media differs from that of polyacrylamides. Solutions of biopolymers show Newtonian behavior at sufficiently low flow rates, then the flow changes from Newtonian to shear thinning at increasing flow rates. The behavior of polyacrylamide is even more complex: it changes from Newtonian flow via shear thinning into shear thickening (or dilatant, i.e. viscosity increases with increasing shear rates) beyond a certain critical flow rate.

Schematic representation of such flow behavior is illustrated in Fig. 2-6:

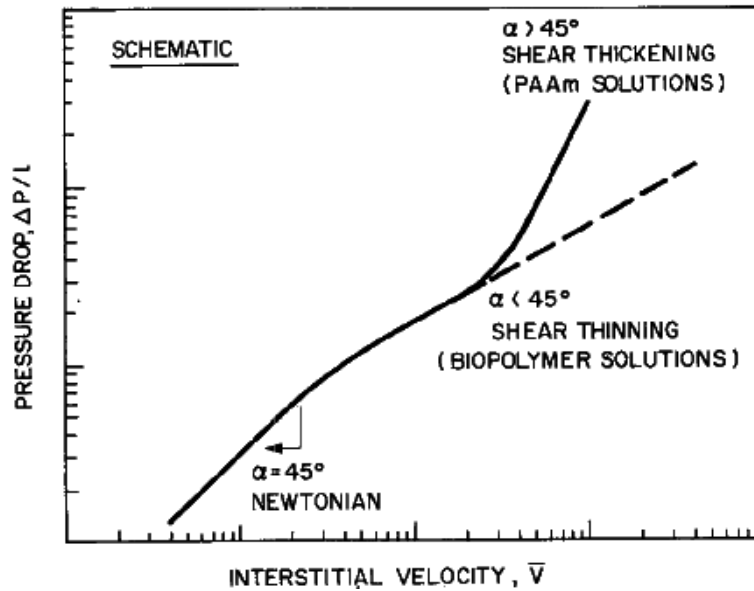


**Fig. 2-6—Schematic Presentation of the Flow Behavior of Polymer Solutions (Heemskerk et al., 1984)**

One of the non-Newtonian models commonly used to describe the rheological behavior of polymer solutions is the power-law or Ostwald-de Waele mathematical model given by:

$$\tau = K\dot{\gamma}^n \tag{2-18}$$

where:

$\tau$  is the shear stress

$K$  is the consistency index

$\dot{\gamma}$  is the shear rate

$n$  is the power-law or flow behavior index.

Then the apparent viscosity  $\eta$  is given by:

$$\eta = K\dot{\gamma}^{n-1} \quad 2-19$$

The power-law constants ( $K$ ,  $n$ ) can be determined by taking the logarithm of Eq. 2-19:

$$\log \eta = \log K + (n-1)\log \dot{\gamma} \quad 2-20$$

It should be noted here, that for shear thinning fluids, the power-law index  $n$  is lower than 1, for shear thickening fluids, it is higher than 1, while the parameter equals 1 for Newtonian fluids.

#### **2.5.1.2 Carreau Model**

While the power-law model accurately reflects polymer solution behavior within a certain range of shear rates, it is not quite satisfactory at high and very low shear rates.

Instead, the Carreau model is found to give better results for these shear regimes (Carreau et al., 1979; Bird et al., 1987):

$$\frac{\eta - \eta_{\infty}}{\eta_0 - \eta_{\infty}} = \left[ 1 + (\lambda \dot{\gamma})^2 \right]^{(n-1)/2} \quad 2-21$$

where:

$\eta$  is the viscosity at the shear rate  $\dot{\gamma}$

$\eta_0$  is the zero shear rate Newtonian viscosity

$\eta_{\infty}$  is the high shear rate Newtonian viscosity

$(n-1)$  is the slope of the power-law portion of the data

$\lambda$  is the time constant.

The Carreau model gives a good fit to viscometry data over a wide range of shear rates; however, the disadvantage of the model is that it requires four parameters as opposed to two in the power-law model.

The Carreau model is compared with the power-law model in Fig. 2-7:

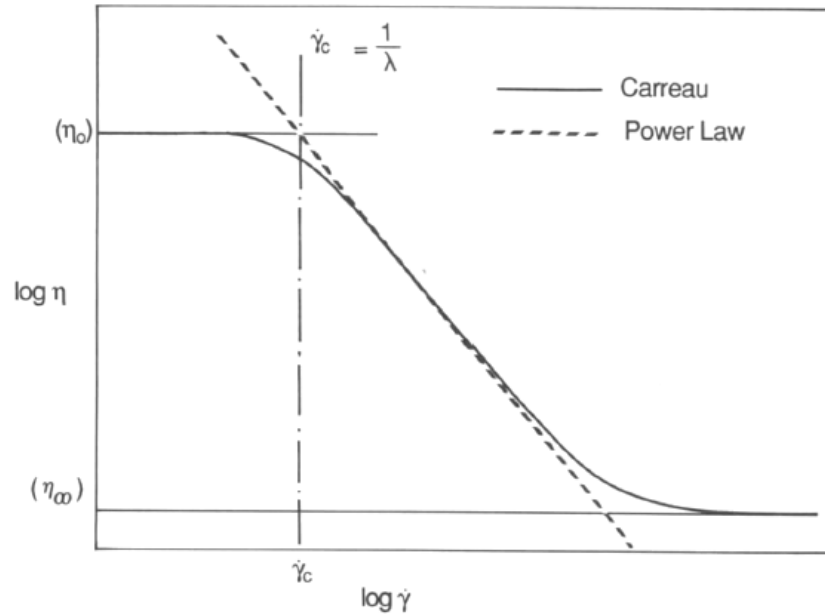


**Fig.2-7—Comparison of the Carreau and Power-Law Models (Sorbie, 1991)**

### 2.5.2 Viscoelastic Models for Polymer Flow in Porous Media

The flow of viscoelastic polymer solutions in porous media has been studied extensively by many authors. Numerous attempts have been taken to quantify viscoelastic effects of polymer solutions. Some of the models proposed to describe the viscoelastic flow in porous media will be described herein.

Heemskerk et al. (1984) provided practical information on the critical flow rate representing an onset point for the change of the flow of polyacrylamide solutions from shear-thinning into shear-thickening. Laboratory investigations of the polymer solutions determined the effect of various factors on the onset of shear-thickening.

The results by Heemskerk et al. (1984) are summarized in Fig. 2-8.

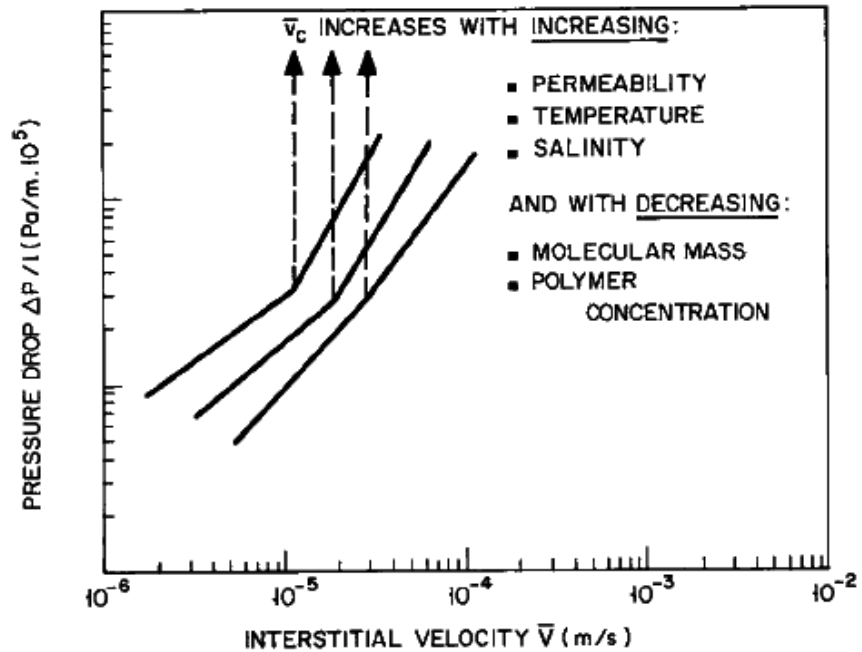


**Fig. 2-8—Effect of the Main Practical Parameters on the Core Flow (Heemskerk et al., 1984)**

Fig. 2-8 illustrates the effect of permeability, temperature, salinity, molecular weight, and concentration of polymer solutions on the onset of shear thickening based on the core flow experiment results for polyacrylamide solutions. Thus, the critical flow rate increases with increasing permeability, temperature, salinity of brine in which a polyacrylamide solution was prepared, and with decreasing molecular weight and polymer concentration.

Heemskerk et al. (1984) suggested that the Deborah number should be used to give a first rough estimate of the critical flow rate, which represents the onset of shear-thickening behavior:

$$D_e = \dot{\epsilon} \cdot \tau_f \quad 2-22$$

where:

$D_e$  is the Deborah number

$\dot{\epsilon}$  is the stretching rate

$\tau_f$  is the fluid relaxation time.

The stretching rate was approximated as follows:

$$\dot{\epsilon} = \frac{\bar{v}}{\bar{D}_p / 2} \quad 2-23$$

where:

$\bar{v}$  is the average interstitial velocity

$\bar{D}_p$  is the average grain diameter.

However, it was noted that the Deborah number can only give a rough estimate due to inadequacy of calculating the stretching rate.

The core flow behavior of viscoelastic polyacrylamide solutions can be described using the critical flow rate and two power-law exponents  $n_1$  and  $n_2$  (Fig. 2-9). Details on the quantification of viscoelastic effects are given by Heemskerk et al. (1984).

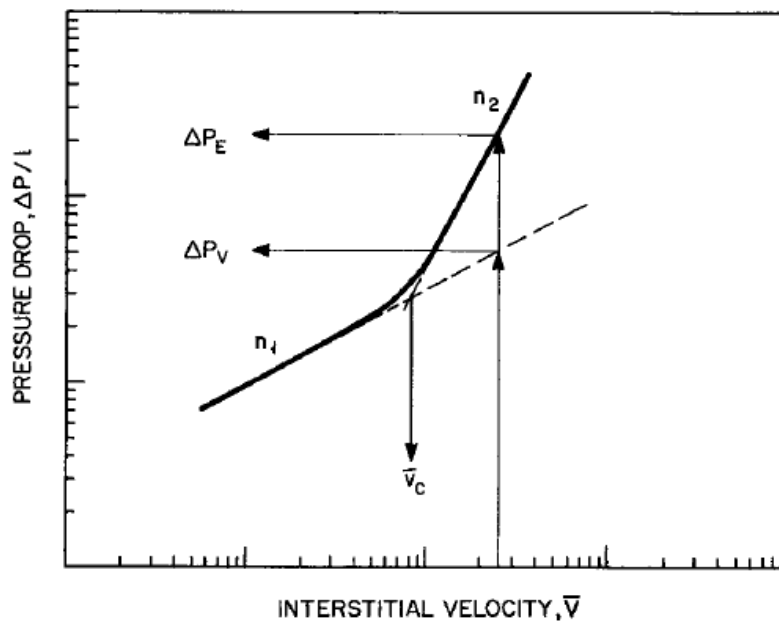


**Fig. 2-9—Overview of Parameters for the Description of the Core Flow of Polyacrylamide Solutions (Heemskerk et al., 1984)**

Ranjbar et al. (1992) suggested a model that also describes the flow of viscoelastic polymer solutions through porous media. The model applied the Maxwell Fluid approach, which assumes that viscoelastic fluid behaves as an element composed of elastic and viscous components during uniaxial strain.

The suggested model was based on the observation that after decreasing the injection rate, the pressure difference does not adjust to the new injection rate instantaneously, but follows a time dependent exponential function as indicated in Fig. 2-10.

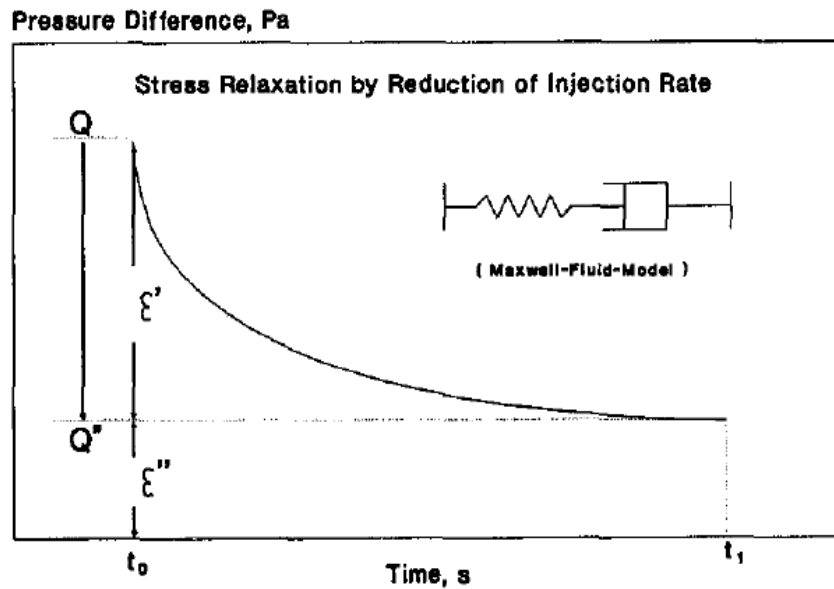


**Fig. 2-10—Relation Between Pressure Difference and Time for Viscoelastic Fluids (Ranjbar et al., 1992)**

They suggested that the model index  $E'$  is the parameter, which should be used for the quantification of viscoelastic effects of polymer solutions in porous media.

$$\Delta P_t = P' + P'' \cdot e^{-\frac{t}{E'}} \quad 2-24$$

where:

$\Delta P_t$  is the pressure difference

$P'$  is the pressure after reducing the injection rate

$P''$  is the pressure by which the original pressure was reduced.

The index  $E'$ , which has a dimension of time, is a function of the relaxation time and the fourth power of the ratio of the effective pore radius, caused by the different orientation of polymer molecules, before and after decreasing the injection rate.

Garrouch (1999) presented another viscoelastic model, which accounted for the polymer solution viscosity, by using an average porous media power-law constant, and for the polymer solution elasticity, by using the longest relaxation time.

$$N_v = \alpha \left( \frac{\Delta P}{L} \right)^\beta \quad 2-25$$

where:

$N_v$  is the viscosity number

$\alpha$  is an intercept of a log-log plot of  $N_v$  vs. pressure gradient

$\beta$  is a slope of a log-log plot of  $N_v$  vs. pressure gradient.

$N_v$  is a parameter used to characterize viscoelastic properties of polymer solutions in porous media (Wreath et al., 1990). It is given by:

$$N_v = \frac{\sqrt{k\phi}}{\theta_{f_1} u^{\bar{n}-1}} \quad 2-26$$

where:

$\theta_{f_1}$  is the longest relaxation time

$u$  is the fluid velocity.

Also of note is the apparent viscosity model suggested by Delshad et al. (2008), which accounts for shear-thinning as well as shear-thickening behavior of polymer solutions in porous media for a wide range of flow velocities.

The suggested apparent viscosity model consists of the shear-viscosity dominant part and the elongational-viscosity dominant part.

The model is given by:

$$\mu = \mu_\infty + (\mu_p^0 - \mu_\infty) \left[ 1 + (\lambda \gamma_{eff})^\alpha \right]^{(n-1)/\alpha} + \mu_{max} \left[ 1 - \exp\left(-(\lambda_2 \tau_r \gamma_{eff})^{n_2-1}\right) \right] \quad 2-27$$

where:

$\mu_p^0$  and  $\mu_\infty$  are the limiting Newtonian viscosities at the low and high shear limits, respectively

$\gamma_{eff}$  is the effective shear rate

$\lambda, n, \mu_{max}, \lambda_2, \alpha, n_2$  are empirical constants.

The first part of the right-hand side of the Eq. 2-27 is the shear-viscosity dominant part (shear thinning regime), while the second part is the elongational-viscosity dominant part (shear thickening regime).

## **2.6 Viscoelasticity of Polymer Solutions in Polymer Flooding Operations**

### **2.6.1 Mobilization of Oil in Polymer Flooding**

The flow of viscoelastic fluids in porous media is distinctively different from the Newtonian flow. It is known that, unlike Newtonian fluids, polymer solutions are characterized by expansion and contraction phenomena when flowing through porous media. The polymer molecules continuously stretch and recoil in porous media when flowing through the pores. These phenomena, observed in the viscoelastic flow, result in the improved sweep efficiency, as illustrated in Fig. 2-11.

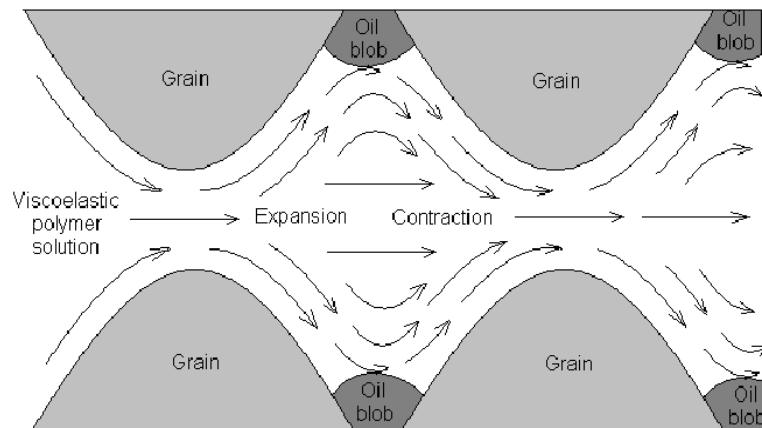


**Fig. 2-11—Schematic of Viscoelastic Flow in Porous Media**

As can be seen from the figure, polymer solution penetrates as far as possible into the reservoir pores and efficiently displaces oil, thus improving the reservoir sweep efficiency. This results in higher oil recovery and lower residual oil saturation.

Fig. 2-12 and Fig. 2-13 compare the mobilization of oil droplet by a Newtonian fluid and a viscoelastic polymer solution in oil wet and water wet systems, respectively.

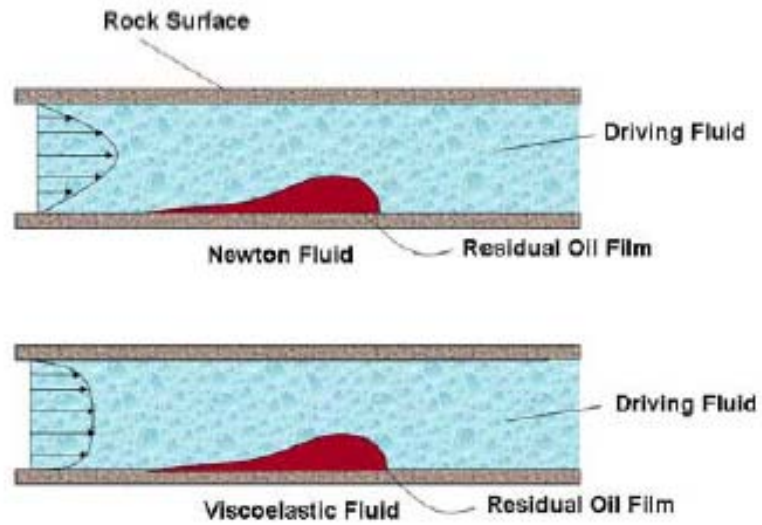


Fig. 2-12—Forces Acting on Residual Oil Film in Oil Wet Systems (Wang et al., 2007; Jiang et al., 2008)

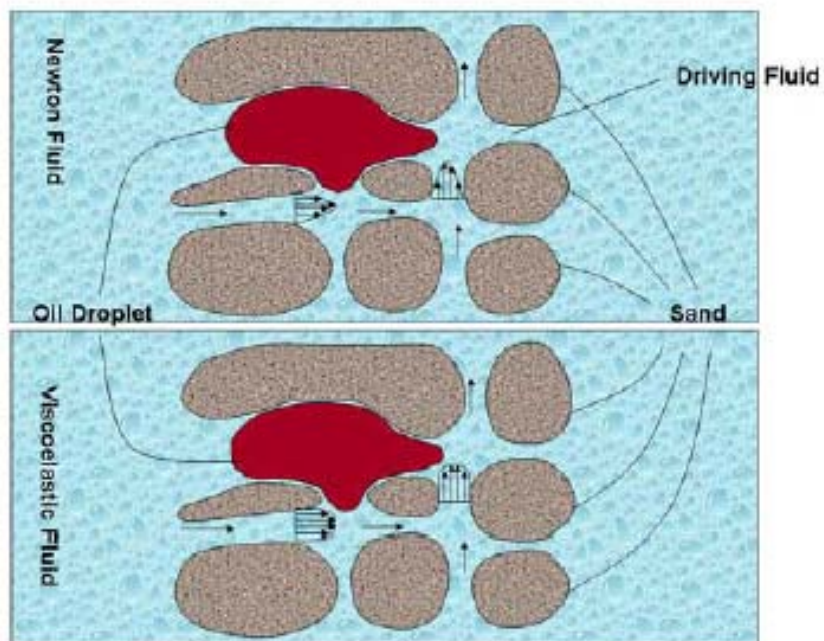


Fig. 2-13—Forces Acting on Residual Oil Droplet in Water Wet Systems (Wang et al., 2007)

As the above figures show, the flow of viscoelastic fluids differs markedly from that of Newtonian fluids. The viscoelastic flood front is more uniform compared to that of Newtonian fluid, which has a more protruding form. Thus, viscoelastic polymer solution behaves like an “expanding piston”, reaching out farther into the pore “corners” and sweeping oil more efficiently than Newtonian fluids.

### **2.6.2 Effect of Viscoelasticity of Polymer Solutions on the Displacement Efficiency**

A number of authors have presented laboratory results showing the effect of viscoelasticity on the displacement efficiency in polymer flooding operations. The increase in the oil recovery was attributed mainly to elastic properties of the injected polymeric fluids.

Wang et al. (2000) indicated that incremental oil recovery can be increased due to elastic properties of polymer solutions. They reported that the incremental oil recovery of 13% OIIP was achieved in Daqing oil field located in the north of China. The authors claimed that this magnitude of the incremental oil recovery cannot be explained by the viscous effects of the injected polymer solutions.

Identical results of core flood tests with viscoelastic polymer solutions were reported later by Wang et al. (2001). They reported that elastic properties of the injected fluids substantially increased the displacement efficiency.

Fig. 2-14 compares the effect of water and polymer solution on the mobilization of residual oil in “dead ends”.

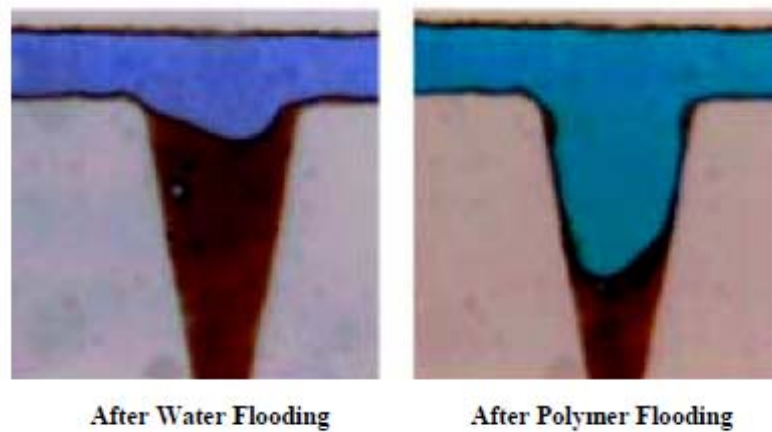


**Fig. 2-14—Residual Oil in “Dead Ends” After Waterflooding and Polymer Flooding (Wang et al., 2001)**

It is clear from Fig. 2-14 that a polymer solution mobilized oil trapped in “dead ends” more efficiently compared to water.

Fig. 2-15 shows how residual oil in films is mobilized by a polymer solution.

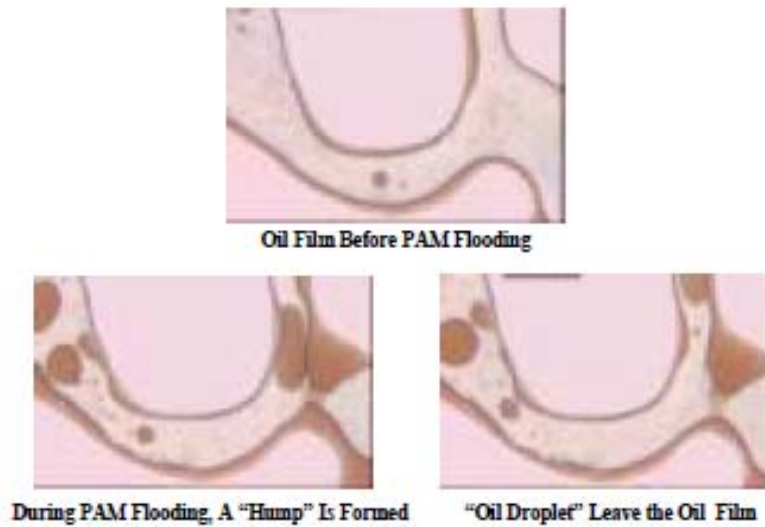


**Fig. 2-15—Mobilization of Residual Oil in Films (Wang et al., 2001)**

The effect of viscoelastic properties of polymer solutions was also studied by Xia et al. (2004) and Wang et al. (2007), who, in agreement with the previously-mentioned studies, attributed the increase in oil recovery to elastic properties of polymer solutions. More recent studies by Jiang et al. (2008) and Wang et al. (2010) also discuss the influence of viscoelasticity on the displacement efficiency. The authors suggested a field-proven polymer flooding method using high concentration viscoelastic polymer solution, which could result in considerably higher incremental oil recovery compared to waterflooding and conventional polymer flooding. They reported that the increase in oil recovery was achieved due to high elasticity of the polymer solution, which resulted in the improved displacement efficiency, as well as to high viscosity, which, in its turn, led to the more efficient volumetric sweep.

## **CHAPTER 3**

### **EXPERIMENTAL PROGRAM**

---

Experimental program consisted of the following parts:

1. Preparation of aqueous polymer solutions:
  - a) PEO solutions with identical shear viscosity behavior (i.e. similar weight average molecular weight) and different elastic properties (i.e. different MWD): PEO Samples 1 and 2
  - b) HPAM solutions with identical shear viscosity behavior (i.e. similar weight average molecular weight) and different elastic properties (i.e. different MWD): HPAM Samples 1 and 2 and HPAM Samples 3 and 4
  - c) Xanthan gum solution characterized by very weak elastic properties.
2. Rheological measurements of viscous and elastic properties of the polymer solutions.
3. Polymer flooding experiments using the polymer solutions to investigate the individual effect of elasticity on the sweep efficiency.

### 3.1 Materials Used in the Experimental Study

Three types of polymers were used in this experimental study: PEO, HPAM and xanthan gum.

#### *Polyethylene Oxide*

The PEO polymers included three grades of POLYOX™ non-ionic water-soluble resins (WSR) with molecular weights ranging from  $0.2 \times 10^6$  to approximately  $8 \times 10^6$ . The polymers were supplied at no cost by Dow Chemical Company in the form of free flowing white to off-white granular powder with a slightly ammoniacal odor.

**Table 3-1** shows approximate weight average molecular weights of the PEO grades used to prepare the polymer solutions:

<b>TABLE 3-1—PEO GRADES WITH VARIOUS WEIGHT AVERAGE MOLECULAR WEIGHT VALUES</b>	
<u>PEO Grade</u>	<u>Weight Average Molecular Weight</u>
WSR-308	8,000,000
WSR-1105	900,000
WSR N-80	200,000

***Partially Hydrolyzed Polyacrylamide***

The HPAM polymers used in this study included four polymer grades supplied at no cost by SNF S.A.S: FLOPAAM™ S (solid) series and AB series. The FLOPAAM™ polymers are anionic water-soluble polymers supplied in the form of odor-free white granular solids with molecular weights ranging from  $0.5 \times 10^6$  to  $20 \times 10^6$ . The degree of hydrolysis of the HPAM polymers is 25-30 mole %.

**Table 3-2** lists weight average molecular weights of the HPAM grades:

<b>TABLE 3-2—HPAM GRADES WITH VARIOUS WEIGHT AVERAGE MOLECULAR WEIGHT VALUES</b>	
<u>HPAM Grade</u>	<u>Weight Average Molecular Weight</u>
3630 S	20,000,000
3330 S	8,000,000
3130 S	2,000,000
AB 005V	500,000

### *Xanthan Gum*

Xanthan gum characterized by low elasticity was also used in the experimental study. The xanthan gum used in the studies was Barazan D Plus™. Barazan D Plus™ is a yellow to white powdered, dispersant-added biopolymer with a molecular weight of  $2 \times 10^6$ .

### *Porous Media*

SPHERIGLASS® A-GLASS 3000 solid glass spheres supplied by Potters Industries Inc. were used as porous media material. The glass beads had a particle size distribution of 30-50 microns. The specific gravity of the glass beads as specified by the manufacturer was equal to 2.5.

The mineral oil used in the experiments was supplied by Fisher Scientific. It had a viscosity of 33.5 cSt @ 40°C and a specific gravity of 0.83 @ 15.6°C. The API gravity of the oil was 39 °API.

## **3.2 Preparation of Polymer Solutions**

### **3.2.1 Procedure for the Preparation of Polymer Solutions**

All polymer solutions were prepared by directly adding a given polymer to deionized water. To ensure that optimum solution properties were obtained, the

polymers were mixed in strict accordance with the recommended procedures provided by the polymer manufacturers.

### ***PEO Solutions***

Separating individual resin particles from each other during the first seconds of stirring is the most important step in dissolving the PEO polymers; therefore, vigorous stirring was applied for the initial dispersion of the powder by use of a Hamilton Beach overhead mixer. This helped to avoid the agglomeration of partially dissolved polymer particles and the formation of gels. The polymers were not added to water too rapidly so as to avoid lumping of the powder. It was not added slowly either; this would prevent proper dissolution of the powder because of the solution thickening before adding the rest of the powder. Also, high-speed agitation of dissolved PEO solutions was avoided, since the polymers can rapidly degrade at high shear.

Two PEO solutions were prepared: PEO Samples 1 and 2. PEO Sample 1 consisted of one polymer grade and PEO Sample 2 consisted of three polymer grades. When preparing the PEO solution consisting of 3 polymer grades, powders were added into water one after another starting with the PEO grade of higher molecular weight. The PEO grade with the lowest molecular weight was added last.

The PEO solutions were mixed directly at the desired polymer concentrations. After dissolution, the mixed polymer solutions were stored at room temperature for up to 24 hours until complete hydration of the solutions was achieved followed by rheology testing and core flood experiments.

PEO Samples 1 and 2 were prepared at concentrations of 1.25 and 1 wt%, respectively.

### ***HPAM Solutions***

Two groups of HPAM solutions were prepared: HPAM Samples 1 and 2 and HPAM Samples 3 and 4. HPAM Sample 1 and 3 consisted of one polymer grade and HPAM Samples 2 and 4 consisted of three polymer grades.

The HPAM solutions consisting of one polymer grade (HPAM Samples 1 and 3) were first prepared in a stock solution. The stock solution was mixed using the Hamilton Beach overhead mixer. After complete hydration of the solutions (up to 24 hours), the stock solutions were diluted to the desired concentrations and mixed using a magnetic stirrer at 60 rpm for additional 15 minutes. The diluted solutions were prepared the day the solutions were used for rheology testing and core flood experiments.

The HPAM solutions consisting of three polymer grade (HPAM Samples 2 and 4) were mixed directly at the desired polymer concentrations. When preparing the HPAM solutions consisting of 3 polymer grades, powders were added into water

one after another starting with the polymer grade of higher molecular weight. The HPAM grade with the lowest molecular weight was added last.

Both HPAM Samples 1 and 2 were prepared at a concentration of 0.09 wt%. HPAM Samples 3 and 4 were mixed at concentrations of 0.09 and 0.1 wt%, respectively.

### ***Xanthan Gum Solution***

The xanthan gum solution was first prepared as a stock solution. The stock solution was mixed for 5 minutes using the Hamilton Beach overhead mixer. It was stored overnight and then diluted to a desired concentration by additional mixing with a magnetic stirrer. The diluted solution was mixed at 60 rpm for 15 minutes. The diluted solution was prepared the day it was used for rheology tests and core flood experiments.

The xanthan gum solution was prepared at a concentration of 0.1 wt%.

### **3.2.2 Preparation of Polymer Solutions with Identical Shear Viscosity but Different Elastic Properties**

The mixing rule suggested by Dehghanpour (2008) was applied to prepare polymer solutions with identical shear viscosity behavior but different elastic characteristics.

Two PEO solutions (PEO Samples 1 and 2) with identical shear behavior (i.e. identical weight average molecular weight) but different elastic properties (i.e. different MWD) were prepared for the experimental study.

Four HPAM solutions were prepared for the experimental study. HPAM Samples 1 and 2 had identical shear viscosities (i.e. identical weight average molecular weight) and different elastic characteristics (i.e. different MWD). Similarly, HPAM Samples 3 and 4 exhibited identical shear viscosity behavior (i.e. identical weight average molecular weight) but different elasticity (i.e. different MWD). However, the weight average molecular weight of HPAM Samples 3 and 4 was lower than that of HPAM Samples 1 and 2 as discussed in Chapter 5.

The compositions of the polymer blends, which yielded polymer solutions with identical shear viscosity and different elastic characteristics, were determined on the basis of the estimated weight average molecular weights and MWD of the solutions.

Weight average molecular weights of the blends were calculated by using Eq.2-14. Thus, the weight average molecular weight values for PEO Sample 2, HPAM Samples 2 and 4 were estimated as the product of a sequence of  $M_w^0$  terms of three polymer grades mixed to prepare the polymer blends. The polydispersity index was used as a measure of MWD. Polydispersity values of the polymer blends were calculated using Eq. 2-17.

The compositions of the polymer solutions, their weight average molecular weights and polydispersity indices are given in respective chapters.

Detailed explanation of the rule for mixing the polymer solutions, with identical shear viscosity but different elastic characteristics, can be found elsewhere (Dehghanpour, 2008).

### **3.3 Rheological Characterization of Polymer Solutions**

The CVOR150 Peltier Bohlin rheometer equipped with the cone and plate measuring system (Fig. 3-1) was used to rheologically characterize the polymer solutions.

Samples were placed in a 0.15mm gap between a rotating upper cone with a 4° angle and a diameter of 40mm, and a fixed lower plate with a diameter of 60mm.



**Fig. 3-1—Rotational Rheometer Used for Rheological Characterization of Polymer Solutions**

Three types of rheological measurements were conducted: viscometry tests, oscillation tests and creep/recovery tests. Oscillation and creep/recovery tests were conducted on the tested samples to determine the linear viscoelastic behavior of the samples in addition to viscometry tests, which studied the samples' non-linear properties, namely shear viscosity and normal force values. Thus, elastic properties were investigated at two different deformational modes. Oscillation and

creep/recovery tests were performed primarily to support the viscometry test results.

All measurements were carried out at laboratory room temperature. At least two replicates of each test were performed on the samples to ensure the repeatability of the test results.

### 3.3.1 Viscometry Tests

The viscometry test studies the viscosity and flow of tested samples as a function of shear, time or temperature.

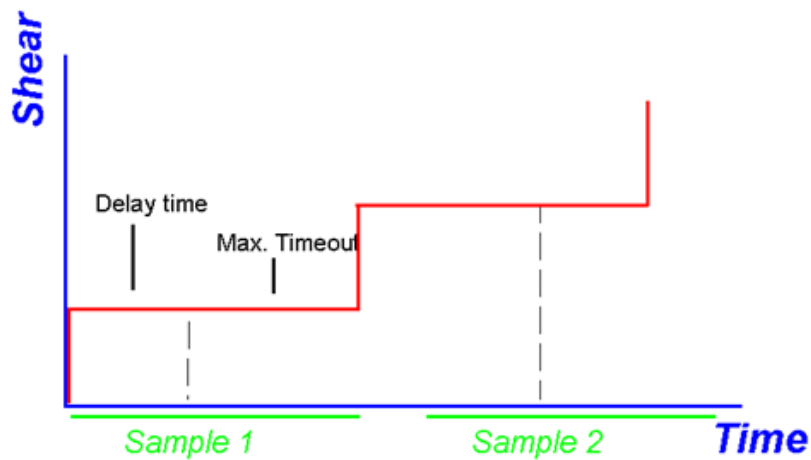


**Fig. 3-2—Viscometry Test (Bohlin Instruments, 2003)**

The viscometry test procedure is illustrated in Fig. 3-2. The test consists of the delay and the integration intervals. The shear is applied for the delay time; the

average value of shear stress (or shear rate if stress is applied) is measured during the integration time and the viscosity is then calculated.

In this study, flow and viscosity of the polymer solutions were measured at shear rates ranging from 1 to 100 1/s.

Since it is the relationship of shear stress to shear rate that is strictly related to flow, the flow characteristics of the tested samples were presented by plotting shear stress vs. shear rate. Shear viscosity was also plotted using the viscometry test results.

The viscometry tests also measured the normal force values related to the elasticity of the tested samples.

### **3.3.2 Oscillation Tests**

The oscillation test measures viscoelastic properties of materials, which can be studied as a function time, temperature or frequency. Two types of the oscillation test were used in this study.

#### **3.3.2.1 Amplitude Sweep**

The amplitude sweep test is performed to define the region of linear viscoelastic response (LVR) of tested samples. Materials exhibit linear viscoelastic behavior, when strain and rate of strain are infinitesimal and, therefore, the ratio of stress to

strain is independent of the stress magnitude, but is a function of time (or frequency) only.

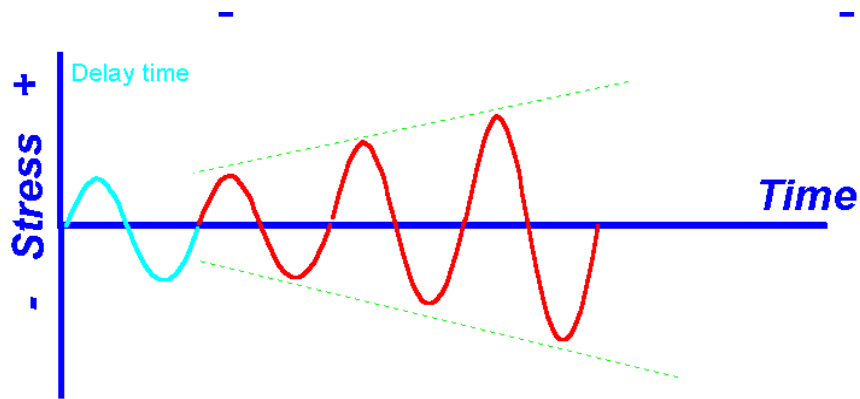


**Fig. 3-3—Amplitude Sweep Test (Bohlin Instruments, 2003)**

As illustrated in Fig. 3-3, in the amplitude sweep test, test samples are oscillated at a fixed frequency with slowly increasing amplitude (strain or stress). The measured viscoelasticity values remain constant within the LVR. When the applied stress becomes too great, the induced strain will start to break the elastic structure of tested samples. Thus, strains below that point should be used to work within LVR.

Results of amplitude sweep tests are used for subsequent tests, i.e. the LVR region is determined and a stress value falling within the LVR is selected, which is consequently used in other rheological tests.

### 3.3.2.2 Frequency Sweep

The frequency sweep test measures viscoelastic properties of tested materials as a function of frequency.

The test is graphically presented in Fig. 3-4.

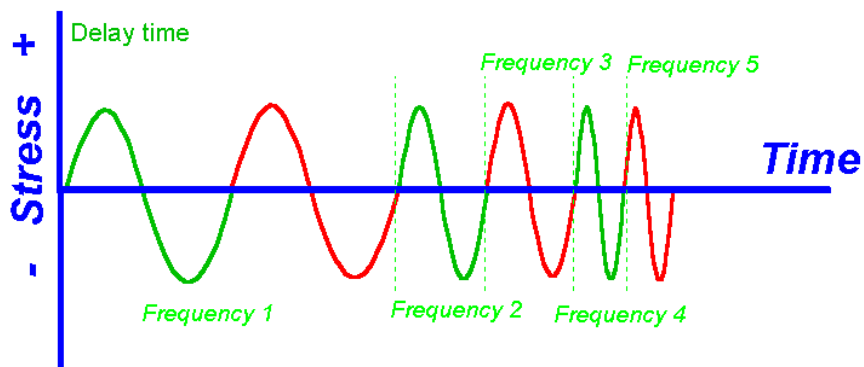


**Fig. 3-4—Frequency Sweep Test (Bohlin Instruments, 2003)**

During the test, a varying frequency is applied on tested samples with a constant value of stress. The test consists of the delay and sampling intervals: frequency is applied during the delay time and the phase shift  $\delta$  between the stress and the strain as well as the complex modulus  $G^*$  is measured during the sampling interval. Other viscoelastic functions, including the elastic modulus  $G'$  and the viscous modulus  $G''$ , are then calculated.

The complex modulus is obtained from the ratio of the stress amplitude to the strain amplitude. It constitutes the sum of the elastic component  $G'$  and the viscous component  $G''$ .

The complex modulus is given by:

$$G^* = G' + i \times G'' \quad 3-1$$

The elastic modulus  $G'$  is usually referred to as the storage modulus to describe the elastic storage of energy, because strain is recoverable in elastic materials. The viscous modulus  $G''$  is referred to as loss modulus to describe the viscous dissipation or loss of energy due to permanent deformation in flow.

The parameter  $G'$  and  $G''$  are given as (Shaw and MacKnight, 2005):

$$G' = G^* \cos \delta \quad 3-2$$

$$G'' = G^* \sin \delta \quad 3-3$$

### **3.3.3 Creep/Recovery Tests**

The creep/recovery tests are carried out to study the creep and recovery compliance of materials as a function of time. Creep is the tendency of a solid material to slowly move or deform permanently under the influence of stresses.

Fig. 3-5 illustrates the creep/recovery test process.

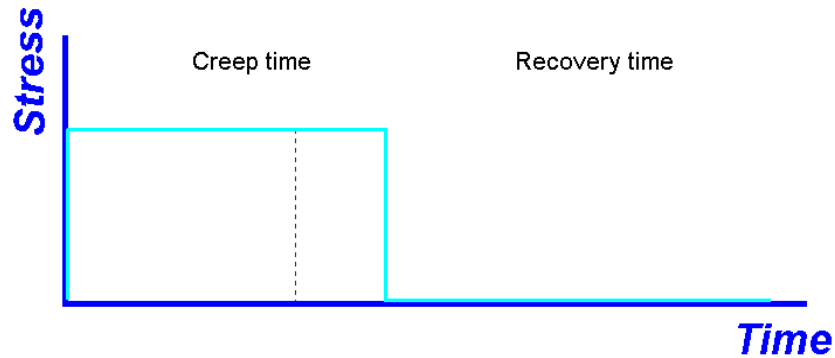


**Fig. 3-5—Creep/Recovery Tests (Bohlin Instruments, 2003)**

As shown in Fig. 3-5, the creep test involves the application of a constant stress on the test samples and the measurement of the resultant strain (displacement) from the time the stress was applied. The recovery test follows the creep test to study the recovery response (recoil properties) of the polymer solutions after the removal of the constant stress.

### **3.4 Polymer Flooding Experiments**

#### **3.4.1 Experimental Set-Up for Polymer Flooding Experiments**

The experimental set-up for the polymer flooding experiments consisted of the following components: radial core holder; syringe pump for saturating the core holder with mineral oil; positive displacement pump for injecting polymeric fluids into the core holder; polymer solution reservoir; graduated cylinders for collecting

effluent samples; data logger for monitoring pressure measurements through a pressure transducer, and a personal computer to which pressure readings were transferred.

Fig. 3-6 illustrates a schematic diagram of the experimental set-up used for the polymer flooding experiments within the scope of this study.

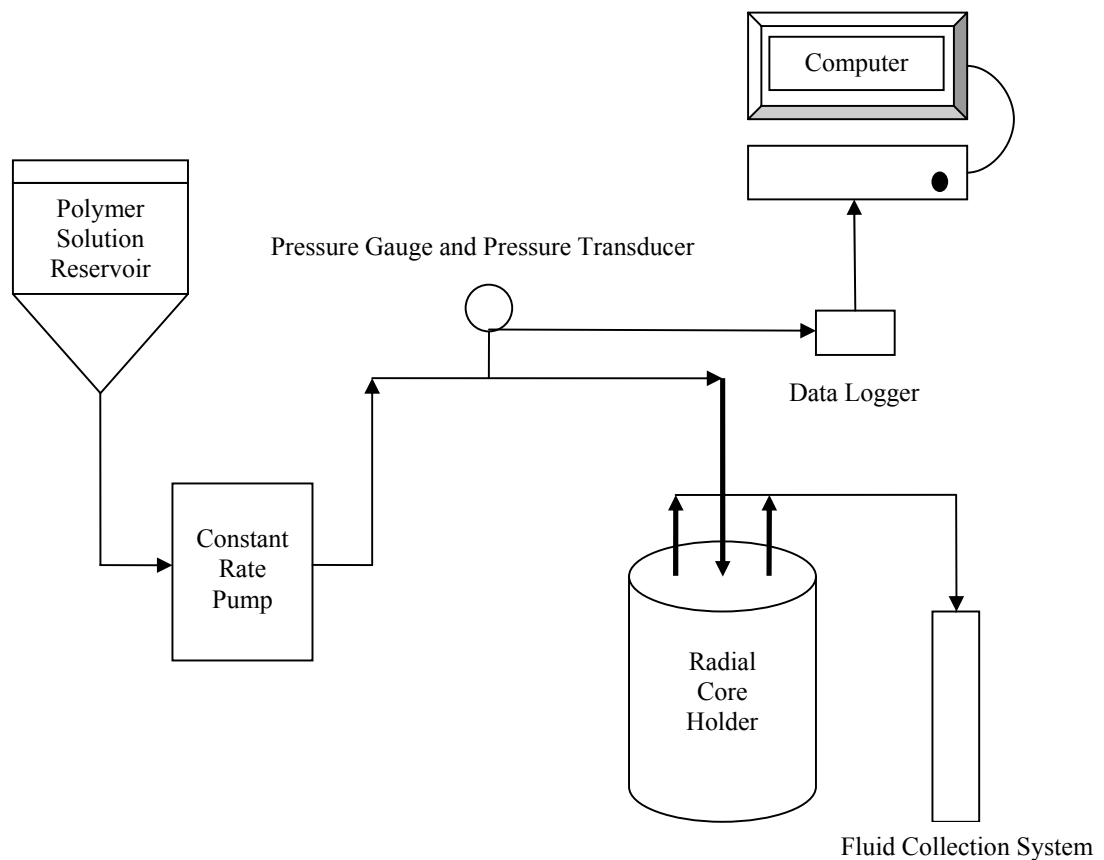


**Fig. 3-6—Schematic Diagram of the Experimental Set-up**

### 3.4.1.1 Radial Core Holder

The polymer flooding experiments were conducted using a special core holder designed to simulate radial flow, which allowed to conduct flooding experiments in more realistic wellbore conditions.

The radial core holder (Fig. 3-7) with an internal diameter of 98 mm and a height of 191 mm (perforated height of 145 mm) had one injection line and two production lines. Injection was done through the injector located at the center of the cell and fluid was produced through the producers located at the periphery. The radius of the injection line was 7 mm and the radius of both production lines was 3.6 mm. The injector and the two producers were encased with a screen with an opening size of approximately 10 microns.



**Fig. 3-7—Radial Core Holder**

### 3.4.1.2 Syringe Pump for Saturating the Core Holder with Mineral Oil

The Isco LC-5000 syringe pump was used for saturation of the core holder with mineral oil. The pump with a maximum pressure of 3700 psi (25.5MPa) has a 500-ml capacity and flow rate range of 0.1 up to 400 ml/hr. The pump operates in a constant flow mode.

The picture of the syringe pump used for saturating the core holder with oil is given in Fig. 3-8.

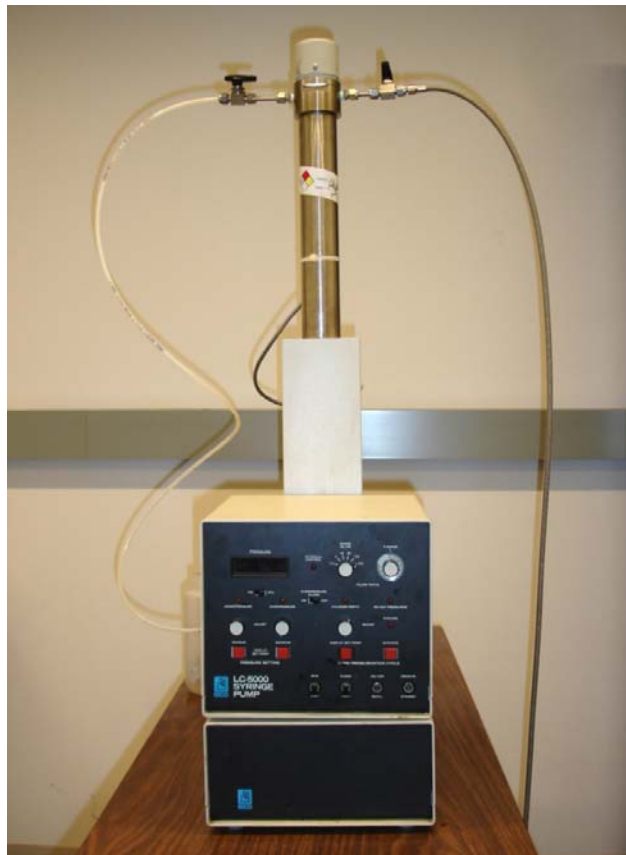


**Fig. 3-8—Syringe Pump Used to Saturate the Core Holder with Mineral Oil.**

### **3.4.1.3 Positive Displacement Pump for Injecting Polymer Solutions**

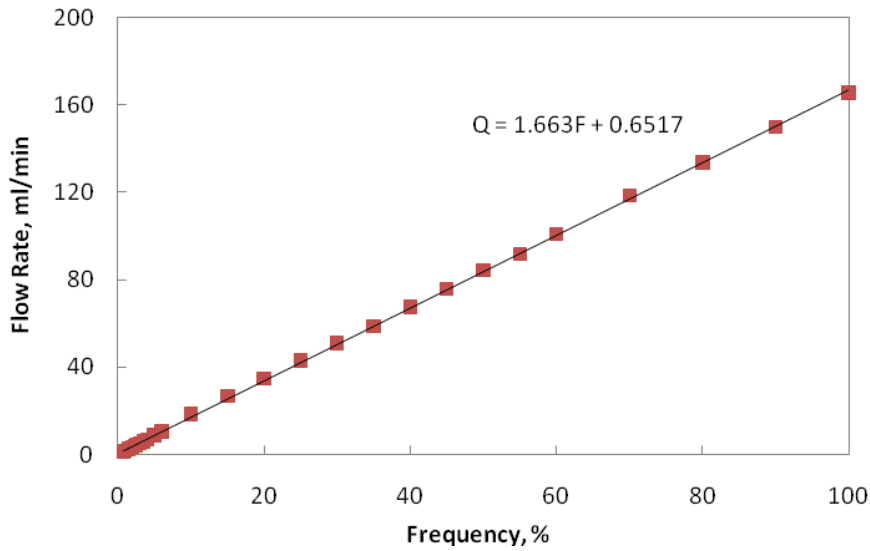
A positive displacement pump with the variable frequency drive control was used to inject polymer solutions into the core holder. The frequency drive used was the AC Tech MC1000 Series drive with efficiency over 97% throughout the speed range.

Fig. 3-9 presents a picture of the pump used for injecting the polymer solutions into the core holder.



**Fig. 3-9—Positive Displacement Pump with the Variable Frequency Drive Used to Inject Polymer Solutions into the Core Holder**

The frequency of the pump was set using the variable frequency drive. Each frequency corresponded to a specific flow rate; therefore a calibration curve for the pump flow rate was constructed as shown in Fig. 3-10.



**Fig. 3-10—Calibration Curve for Positive Displacement Pump Flow Rate**

#### **3.4.1.4 Data Acquisition System**

The data acquisition system used in the experimental study consisted of two parts: hardware and software. The hardware part included a transducer, which measured pressure data in the injection system, and the OWL 400 DC Voltage data logger (Fig. 3-11), which monitored pressure readings through the transducer. The data logger recorded DC voltage at a fixed interval and transferred the readings to a personal computer for analysis with the ACR TrendReader software.

The ACR TrendReader software converted voltage signals to pressure values in psi and the pressure data were then analyzed. Pressure data were recorded every eight seconds.



**Fig. 3-11—Data Logger**

### **3.4.2 Experimental Procedure**

#### **3.4.2.1 Core Holder Packing Procedure**

The core holder was packed with dry spherical glass beads with the use of a mechanical vibrator operated by air pressure. The mechanical vibrator was pressed onto the cell walls while dry glass beads were poured into the core holder. Vibration continued until the entire granular material dispersed evenly and packed closely in the core holder. When no more glass beads could be loaded, the loading was stopped and the core holder was then saturated with mineral oil.

### **3.4.2.2 Porosity Measurement**

The pore volume of the porous medium was measured using the direct method by subtracting the volume of glass beads in the core holder from the bulk volume, i.e. the volume of the core holder. Therefore, the weight of the glass beads loaded into the core holder was recorded and the volume of the material was determined accurately for each experiment. A specific gravity of 2.5 as specified by the glass beads manufacturer was used in the calculations.

### **3.4.2.3 Absolute Permeability Measurement**

The absolute permeability of the porous medium was measured using the radial core holder. Water was used as the flowing medium in the permeability measurements. It was injected through an injection line into the core holder initially packed with glass beads and saturated with water, and was produced through two production lines at the periphery. The injection pressure was measured with a pressure transducer, which recorded pressure readings every eight seconds. The pressure at the external boundary, i.e. at the outlet, was atmospheric. Therefore, the injection pressure data were taken as the pressure drop values.

The stabilized pressure drop data were obtained for different flow rates and the pressure drop-flow rate profile was plotted as shown in Fig. 3-12.

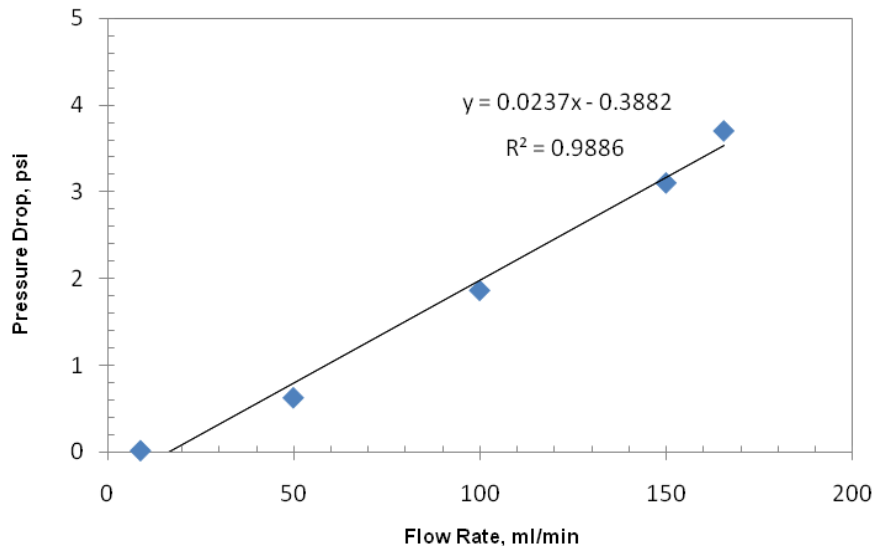


**Fig. 3-12—Pressure Drop vs. Flow Rate Profile for Water Injection**

The absolute permeability of the porous medium was calculated using Darcy's Law for radial steady-state flow given by:

$$Q = \frac{2\pi kh(P_e - P_w)}{\mu \ln r_e / r_w} \quad 3-4$$

where:

Q is the flow rate of water

k is the absolute permeability of the porous medium

$h$  is the height of the core

$\mu$  is the dynamic viscosity of water, which equals 0.00089 Pa.s at 25°C

$r_e$  is the radius at the external boundary

$P_e$  is the pressure at the external boundary

$r_w$  is the radius of the wellbore

$P_w$  is the pressure at the wellbore.

Using the slope of the pressure drop vs. flow rate line, the absolute permeability of the porous medium is given as:

$$k = \frac{\mu}{2\pi hm} \ln \frac{r_w}{r_e} = \frac{0.00089 Pa.s \times \ln \frac{0.69 cm}{4.9 cm}}{2 \times 3.14 \times 19.1 cm \times 0.0237 \frac{psi}{ml / min}} = 0.15 Darcy = 150 mD$$

3-5

#### 3.4.2.4 Flow Rate Determination

A flow rate was estimated that would induce the shear rates, at which the polymer solutions with different elastic properties would exhibit identical shear viscosity when flowing through the porous media.

The shear viscosity vs. shear rate profiles of the polymer solutions showed a range of shear rates at which the samples exhibited identical shear viscosity behavior (PEO Samples 1 and 2; HPAM Samples 1 and 2; HPAM Samples 3 and 4).

The minimum shear rate of 10 1/s and a maximum shear rate of 100 1/s were selected as the desired shear rates at the core outer wall and at the wellbore, respectively. These two values of shear rate were taken into account when calculating the flow rate for the polymer flooding experiments. Procedure for the calculation of the desired experimental flow rate is explained below.

The following expression can be used to estimate shear rates in the core (Christopher and Middleman, 1965):

$$\dot{\gamma} = \frac{3n+1}{4n} \cdot \frac{4Q}{A[8k\phi]^{1/2}} \quad 3-6$$

where:

$\dot{\gamma}$  is effective shear rate, 1/s

$(3n+1)/4n$  is non-Newtonian correction for Power-Law fluids or Rabinowitsch correction factor

Q is flow rate, cm<sup>3</sup>/sec

A is cross sectional area of the core, cm<sup>2</sup>

k is permeability, cm<sup>2</sup>

$\phi$  is porosity.

Additionally, Chauveteau (1982) suggested a material constant  $\alpha$  equal to 1.7 for glass beads to be adopted when estimating the average shear rate during the porous media flow of non-Newtonian fluids. It is also of note that at very low flow rates the non-Newtonian correction factor can be omitted, which will cause no serious loss in accuracy.

Therefore, the desired flow rate was calculated as:

$$Q = \frac{A[8k\phi]^{1/2} \dot{\gamma}}{4\alpha} \quad 3-7$$

A flow rate of 4 ml/min was estimated to give the shear rates in the core that fall within the above-mentioned shear rate range.

The boundaries of the equivalent shear rate envelope are presented as an example in Fig. 3-13. The figure shows that the shear viscosity vs. shear rate behavior of PEO Samples 1 and 2 were identical within the expected range of shear rates in the core at a flow rate of 4 ml/min.

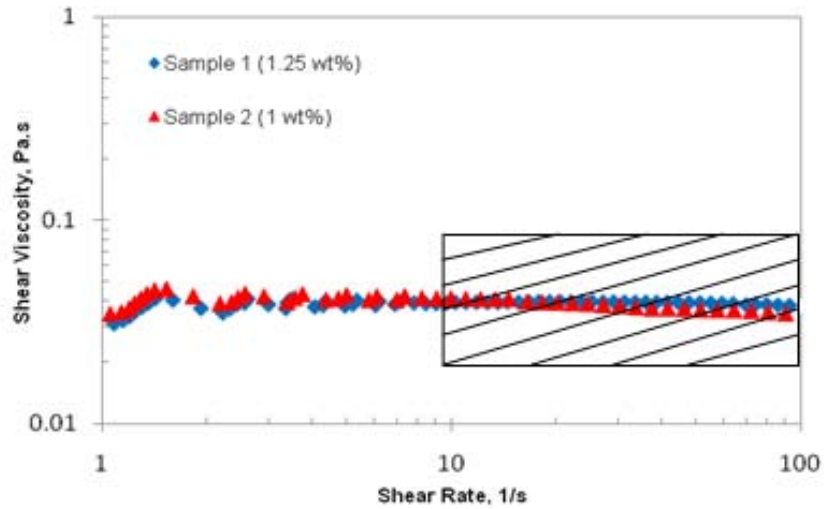


**Fig. 3-13—Shear Rate Envelope for the Polymer Flooding Experiments**

Moreover, the selected flow rate was expected to induce shear rates (14 to 100 1/s) within the core sample that are comparable to field applications (Gleasure and Phillips, 1990; API RP 63: Recommended Practices for Evaluation of Polymers Used in Enhanced Oil Recovery Operations, 1990).

### 3.4.2.5 Flooding Procedure

After the core holder was packed with dry glass beads and saturated with mineral oil, the core flood experiments started. The oil was displaced with the polymer solutions at a flow rate of 4 ml/min, which was selected as explained above.

The solutions were prepared according to the mixing procedure discussed earlier and were injected into the radial core by using a constant rate pump. Pressure was monitored throughout the experiments. The effluent fluid samples were collected

from the radial core, and the resulting oil recovery was recorded accurately. Shear viscosity of the produced polymer solution was measured at the end of the polymer flooding experiments to determine the loss of polymer from solution due to shear degradation and polymer retention onto solid surfaces (polymer adsorption or mechanical trapping within porous media).

Each polymer flooding experiment continued for 1.8-1.9 PV until the oil produced was too low and water cut increased up to 90% or higher.

# CHAPTER 4

## EXPERIMENTAL RESULTS AND DISCUSSION (POLYETHYLENE OXIDE)

---

In this chapter the results of the rheological tests carried out on PEO blends with identical shear viscosity behavior and different elastic characteristics are discussed. Also, the results of polymer flooding experiments using the blends are given and the individual effect of elasticity on the microscopic sweep efficiency is investigated.

### 4.1 Weight Average Molecular Weight and Polydispersity Indices of PEO Solutions

PEO Sample 1 was prepared from WSR-1105, while PEO Sample 2 consisted of three PEO grades: WSR-308, WSR-1105, and WSR N-80. Table 4-1 shows mass fractions of the PEO blend components.

<b>TABLE 4-1—COMPOSITION OF PEO SAMPLES 1 AND 2</b>			
<u>PEO Solution</u>	<u>Weight Percentage of Polymer Solution Components</u>		
	WSR N-80	WSR-1105	WSR-308
PEO Sample 1	0	100	0
PEO Sample 2	25	50	25

The compositions of the PEO blends, which yielded polymer solutions with identical shear viscosity and different elastic characteristics, were determined on the basis of the estimated weight average molecular weights and MWD of the solutions.

<b>TABLE 4-2—WEIGHT AVERAGE MOLECULAR WEIGHT AND POLYDISPERSITY OF PEO SAMPLES 1 AND 2</b>		
<u>PEO Solution</u>	<u>Weight Average Molecular Weight</u>	<u>Polydispersity Index</u>
PEO Sample 1	900,000	1
PEO Sample 2	1,000,000	4.6

As can be seen from Table 4-2, the weight average molecular weights of PEO Samples 1 and 2 were very close to each other. The MWD of the PEO blends, however, differed significantly as indicated by the variance of their polydispersity values.

The similar weight average molecular weights and a significant difference in polydispersity indices of the PEO solutions yielded identical shear viscosity behavior and different elastic characteristics of the samples.

## **4.2 Rheological Characterization of PEO Solutions**

A full-scale rheological characterization of PEO blends was performed to measure viscous and elastic properties of the solutions. Three types of rheological measurements were conducted: viscometry tests, oscillation tests and creep/recovery tests.

### **4.2.1 Viscometry Test Results**

The viscometry tests studied the shear viscosity and flow of the polymer solutions as a function of shear. Shear stress vs. shear rate as well as shear viscosity vs. shear rate profiles for PEO Samples 1 and 2 were generated using the test results. The viscometry tests also measured normal force values for both samples as a function of shear rate. The viscosity behavior of the solutions as well as the normal force values were measured at shear rates from 1 to 100 1/s.

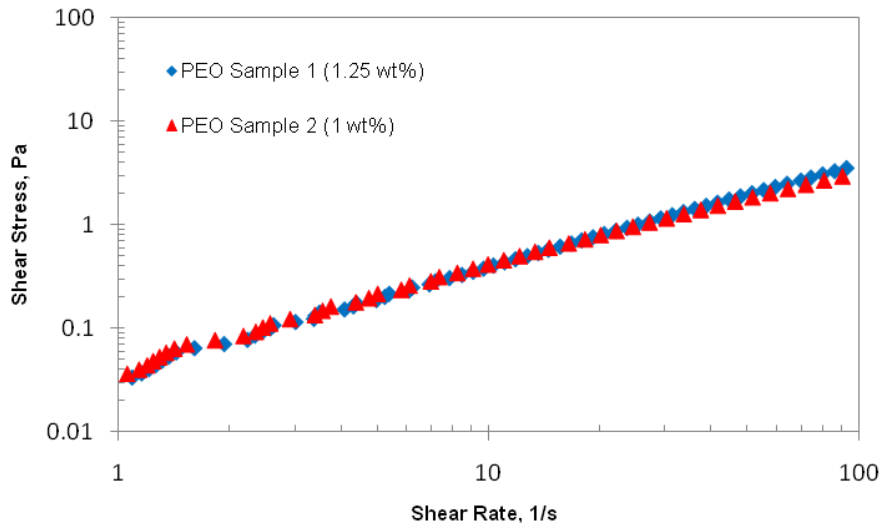


**Fig. 4-1—Shear Stress vs. Shear Rate Profiles for PEO Samples 1 and 2**

The rheological behavior of the samples can be characterized by the power-law model. As shown in Fig. 4-1, the shear stress vs. shear rate profiles of PEO Samples 1 and 2 were identical at a range of shear rates from 1 to 100 1/s. The consistency index,  $K$ , and power-law index,  $n$ , for PEO Samples 1 and 2 are listed in Table 4-3.

<b>TABLE 4-3—POWER-LAW PARAMETERS FOR PEO SAMPLES 1 AND 2</b>		
<u>PEO Solution</u>	<u>Consistency Index <math>K</math>, Pa.s<sup>n</sup></u>	<u>Power-Law Index <math>n</math></u>
PEO Sample 1	0.04	1.00
PEO Sample 2	0.05	0.96

The identical values of the samples' rheological parameters are indicative of their similar shear viscosity behavior. This can be explained by similar weight average molecular weights of the solutions as shown in Table 4-2.

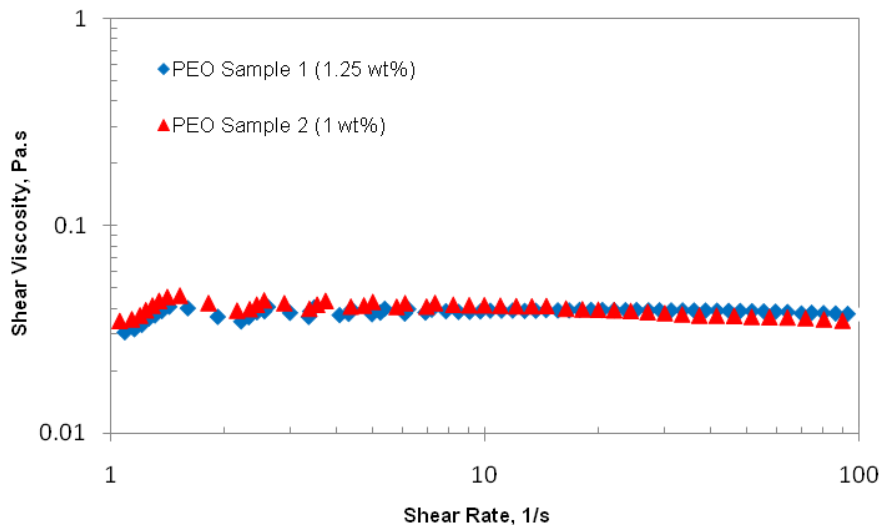


**Fig. 4-2—Shear Viscosity vs. Shear Rate for PEO Samples 1 and 2**

Fig. 4-2 compares shear viscosities of PEO Samples 1 and 2 as a function of shear rate. As can be seen from the figure, shear viscosities of the samples differed slightly only at very low shear rates, but the PEO solutions exhibited almost identical viscosity behavior at shear rates up to 100 1/s.

Normal force values of the samples were also measured under steady shear conditions as a function of shear rate. The values for PEO Samples 1 and 2 are compared in Fig. 4-3.

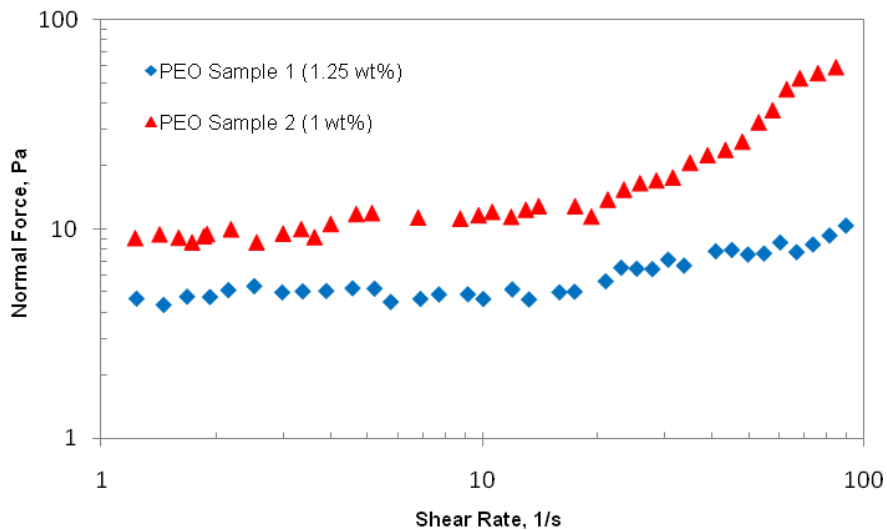


**Fig. 4-3—Normal Force vs. Shear Rate for PEO Samples 1 and 2**

Fig. 4-3 presents the normal force values related to the elasticity of the PEO blends. As expected, PEO Sample 2, characterized by higher elasticity, exhibited higher normal forces compared to PEO Sample 1. PEO Sample 1 with less elastic properties, correspondingly, exhibited lower normal force values. Since the difference in normal forces gives a good indication of the difference in elastic properties, it may be concluded that PEO Sample 2 had a more elastic structure than PEO Sample 1.

## 4.2.2 Oscillation Test Results

The oscillation tests measured viscoelastic properties of the PEO solutions. Two modes of the test were carried out: amplitude sweep and frequency sweep.

### 4.2.2.1 Amplitude Sweep Results

The amplitude sweep tests were performed to define the LVR regions of PEO Samples 1 and 2. The tests were performed on the PEO solutions at a frequency of 0.01 Hz for stress values ranging from 0.006 to 0.5 Pa.

The LVR regions of PEO Samples 1 and 2 were determined from the amplitude sweep results as shown in Fig. 4-4.

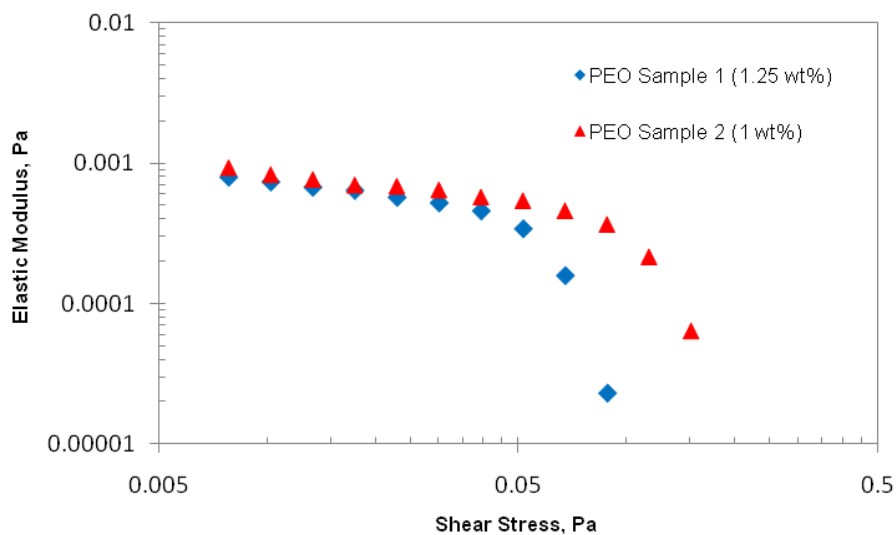


**Fig. 4-4—Elastic Modulus vs. Shear Stress for PEO Samples 1 and 2**

Fig. 4-4 shows that there was no obvious stress dependence of the elastic moduli of PEO Samples 1 and 2 for a range of shear stresses up to about 0.03 Pa and 0.05 Pa, respectively. At a stress of 0.03 Pa (and correspondingly 0.05 Pa) the elastic moduli of the samples started to decrease markedly with increasing shear stress amplitude. This rapid decrease of the elastic moduli indicated the limit of the samples' linear region, i.e. the transition from the linear to non-linear viscoelastic region. Based on the test results, a shear stress of 0.006 Pa falling within the LVR regions of both PEO Samples 1 and 2 was selected for the subsequent tests.

Although the amplitude sweep tests were performed on PEO Samples 1 and 2 primarily to determine their LVR regions, they also provided some information on the samples' structure. Fig. 4-4 shows that shear stresses higher than 0.03 Pa caused the induced strain to breakdown the structure of PEO Sample 1. The induced strain became too high for PEO Sample 2 at shear stresses higher than 0.05 Pa. Thus, the measured value of elasticity decreased earlier at lower shear stress values for PEO Sample 1 as compared to PEO Sample 2. This can be explained by the more elastic structure of the latter.

#### **5.2.2.1 Frequency Sweep Results**

After the LVR regions of PEO Samples 1 and 2 were determined, the frequency sweep tests were carried out, which consisted in applying a varying frequency on the samples with a constant value of shear stress that falls within the LVR regions of the solutions.

The frequency sweep tests were carried out on PEO Samples 1 and 2 at a range of frequencies from 0.01 to 2 Hz with a fixed shear stress of 0.006 Pa. For the mentioned frequency range, the rheometer was able to make accurate measurements of the tested samples' properties. A stress of 0.006 Pa was used in the frequency sweep to eliminate the risk of the test samples being oscillated outside the samples' linear region.

The frequency sweep results for PEO Samples 1 and 2 are presented in Fig. 4-5 and Fig. 4-6 as a function of angular frequency. Fig. 4-5 shows the viscous moduli of the PEO solutions. Fig. 4-6 compares the elastic moduli of the samples as a function of angular frequency.

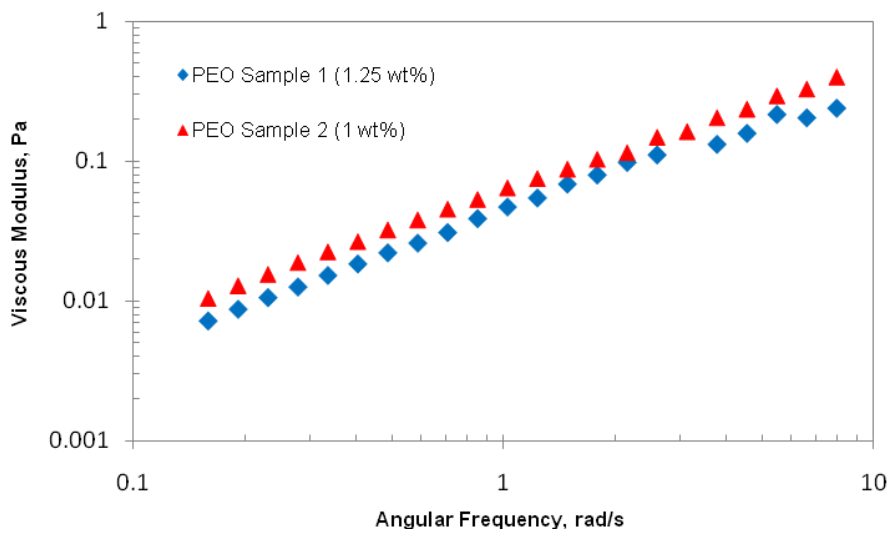


**Fig. 4-5—Viscous Modulus vs. Angular Frequency for PEO Samples 1 and 2**

Measurements of the viscous modulus values at a varying frequency showed that both samples had identical viscous moduli as shown in Fig. 4-5. The similar viscous moduli indicated that PEO Samples 1 and 2 had similar viscous characteristics. This is in support of the identical shear viscosity vs. shear rate curves of the polymer solutions as shown in Fig. 4-2.

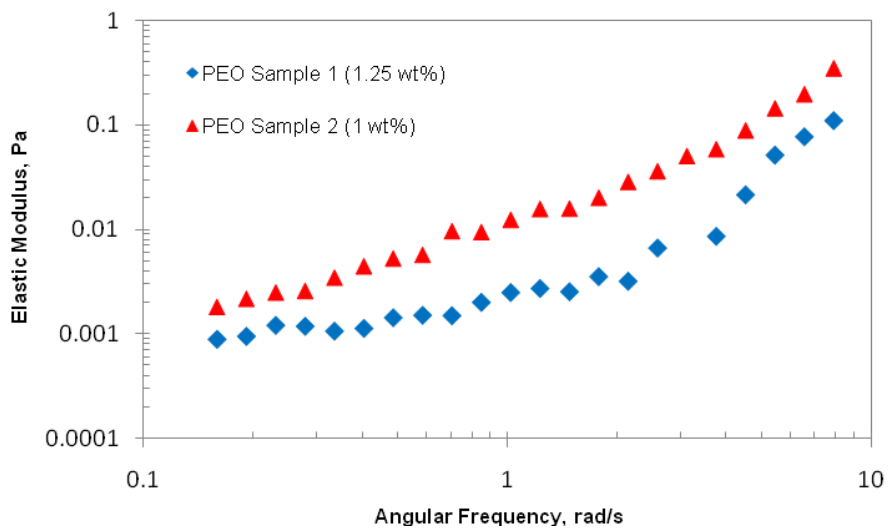


**Fig. 4-6— Elastic Modulus vs. Angular Frequency for PEO Samples 1 and 2**

It is clear from the elastic modulus vs. angular frequency profiles of the PEO solutions (Fig. 4-6) that the elastic moduli of PEO Sample 2 were higher than those of PEO Sample 1. The higher elastic moduli of PEO Sample 2 indicated its higher elastic properties, which can be explained by the different polydispersity indices of the solutions. Since elastic modulus values can give a good indication of samples' elasticity, it can be concluded that PEO Sample 2 was more elastic

than PEO Sample 1. Again, these results support the normal force measurements for PEO Samples 1 and 2 as discussed earlier.

#### 4.2.3 Creep/Recovery Test Results

The creep/recovery tests were performed on PEO Samples 1 and 2 to study the creep and recovery compliance of the solutions as a function of time.

A stress of 0.006 Pa, which falls within the LVR regions of the polymer solutions, was applied during the creep test. The stress was applied for 100 s in the creep test and the recovery properties were monitored for 100 s in the recovery test.

The creep and recovery curves for PEO Samples 1 and 2 are given in Fig. 4-7.

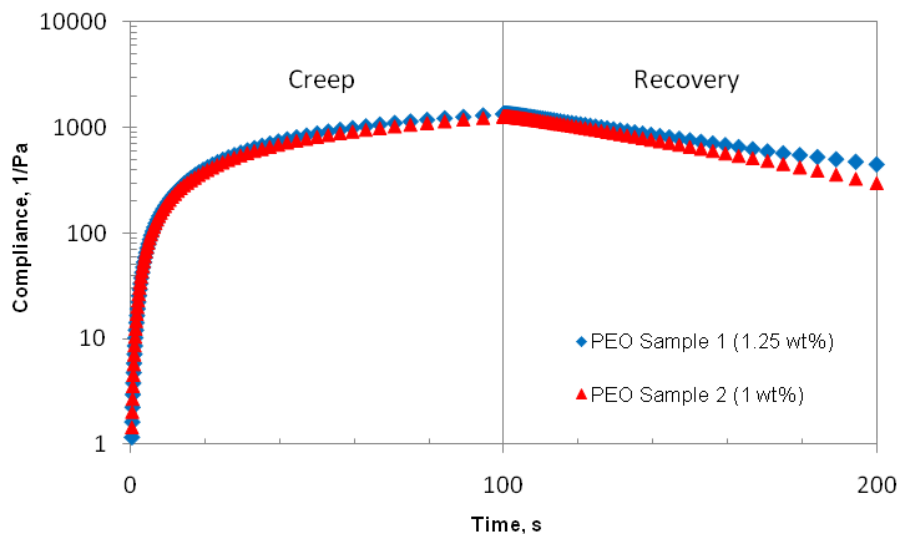


**Fig. 4-7— Creep and Recovery Compliance vs. Time for PEO Samples 1 and 2**

The comparison of the creep curves in Fig. 4-7 shows that PEO Samples 1 and 2 exhibited almost identical creep behavior with the measured creep compliance of PEO Sample 2 only slightly lower than that of PEO Sample 1.

The difference in recovery response of PEO Samples 1 and 2 was more pronounced than the samples' creep response. The recovery curves of the polymer solutions in Fig. 4-7 indicated that PEO Sample 2 exhibited slightly greater recovery than PEO Sample 1 after the constant stress was removed. Correspondingly, PEO Sample 1 exhibited less recovery, which suggested that PEO Sample 2 had stronger recoil properties, and, therefore, it was more elastic in nature as compared to PEO Sample 1.

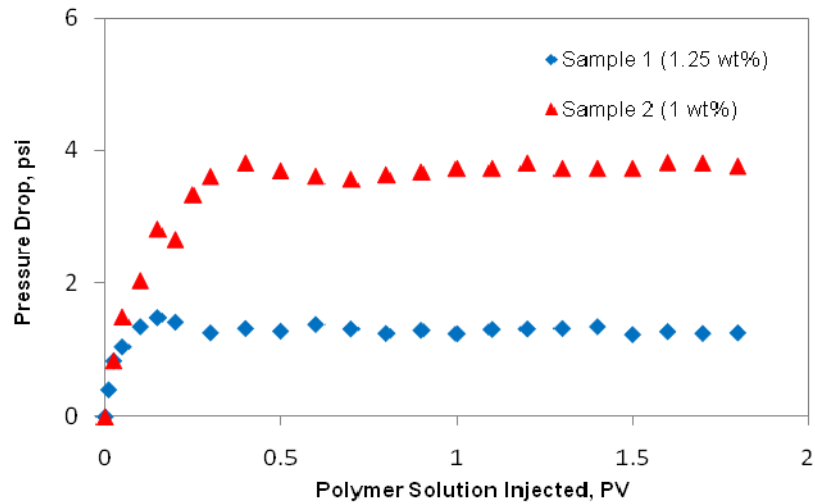
### **4.3 Polymer Flooding Experiments with PEO Solutions**

Polymer flooding experiments were carried out with two PEO solutions, which had identical shear viscosity but considerably different elasticity. The oil recovery was compared to see the effect of elastic properties of the injected fluids on the displacement efficiency.

#### **4.3.1 Pressure Drop During Polymer Flooding Experiments**

Pressure drop readings were recorded during each polymer flooding experiment.

The recorded pressure response data for PEO Samples 1 and 2 are compared in Fig. 4-8.



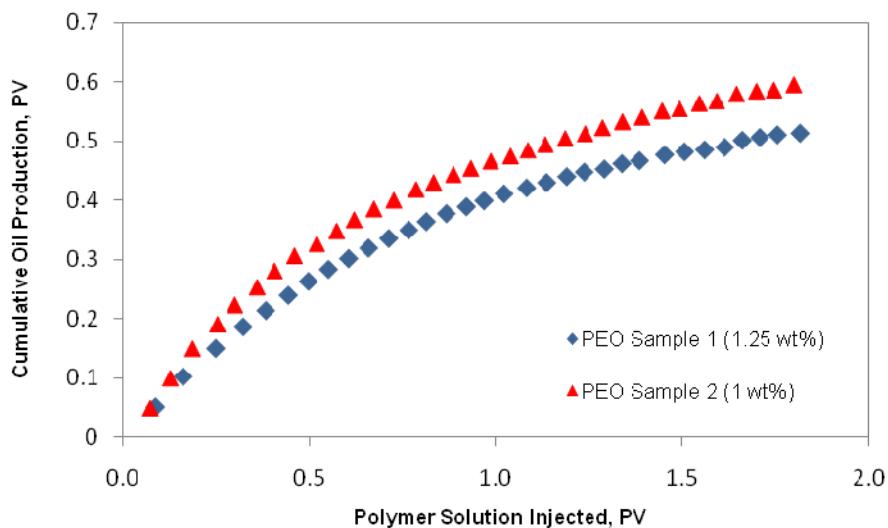
**Fig. 4-8—Pressure Drop During Injection of PEO Samples 1 and 2**

Fig. 4-8 comparing pressure response vs. PV of polymer solution injected for PEO Samples 1 and 2 shows a noticeable difference in the pressure drop response during the flooding experiments. Higher pressure drop was observed when flooding the core with the more elastic PEO Sample 2. Correspondingly, the pressure drop was lower during the flooding experiment with PEO Sample 1. It is clear that the difference in the pressure response indicates the difference in the elastic properties of the polymer solutions, and higher pressure drops are indicative of higher elasticity of the injected solution. Again, the pressure drop results supported the results of rheological measurements carried out on PEO

Samples 1 and 2, which indicated that PEO Sample 2 was more elastic than the other.

#### 4.3.2 Oil Displacement Results

Fig. 4-9 shows the cumulative oil recovery as a function of PV of the injected polymer solution for PEO Samples 1 and 2.



**Fig. 4-9—Cumulative Oil Recovery vs. Polymer Solution Injected for PEO Samples 1 and 2**

As can be seen from Fig. 4-9, PEO Sample 2 characterized by higher elasticity than PEO Sample 1 gave higher oil recovery throughout the entire polymer flooding experiment. This means that oil was recovered earlier at lower water cuts when flooding the core with PEO Sample 2.

Fig. 4-10 presents the breakthrough recovery as well as total oil recovery obtained by injecting the PEO blends into the core.

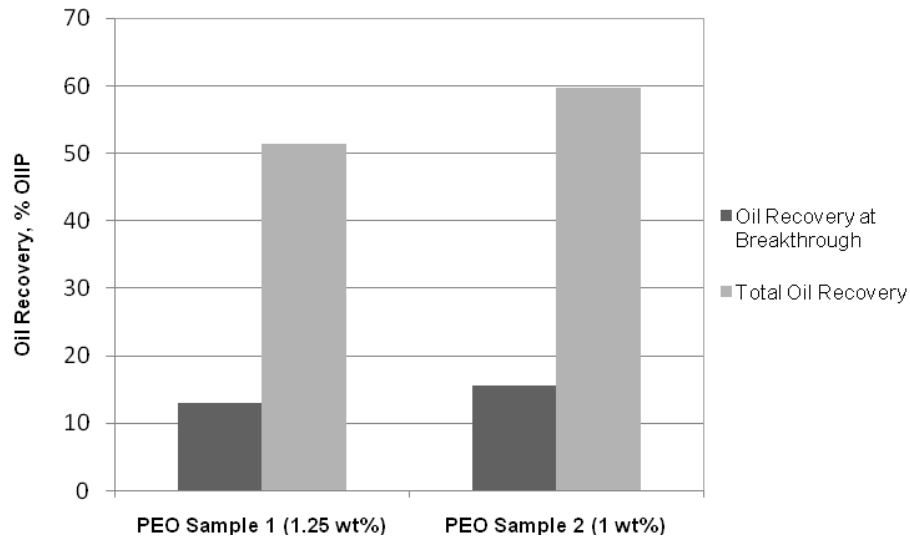


**Fig. 4-10—Breakthrough Recovery and Total Oil Recovery for PEO Samples 1 and 2**

Fig. 4-10 also clearly shows that there is a significant difference in oil recovery between the two PEO blends with identical shear viscosity behavior and different elastic characteristics. The total oil recovered by injecting PEO Sample 2 amounted to 59.7% of OIIP. Injection of PEO Sample 1 into the core resulted in the total oil recovery of 51.5% of OIIP.

It is important to note that two replicates of the polymer flooding experiment were conducted with PEO Sample 1. The total oil recovery was estimated at 51.5%, 53.9% and 50.7% for the flooding experiment with PEO Sample 1 and the two

replicates of the experiment, respectively. Thus, the total oil recovery obtained by injecting PEO Sample 1 averaged 52% of OIIP.

Also of note is the difference in the breakthrough times of the PEO blends. Fig. 4-10 shows that the breakthrough time was observed later when injecting PEO Sample 2 into the core. Injection of PEO Sample 1 resulted in earlier breakthrough of the polymer solution and consequently lower oil recovery at the breakthrough time. The oil recovered before breakthrough when injecting more elastic PEO Sample 2 was estimated to be 16.7% higher than that of PEO Sample 1.

#### **4.3.3 Effluent Viscometry Results**

Effluent fluid samples were collected at the end of the polymer flooding experiments.

Shear viscosity vs. shear rate profiles of the produced effluent samples are given in Fig. 4-11.

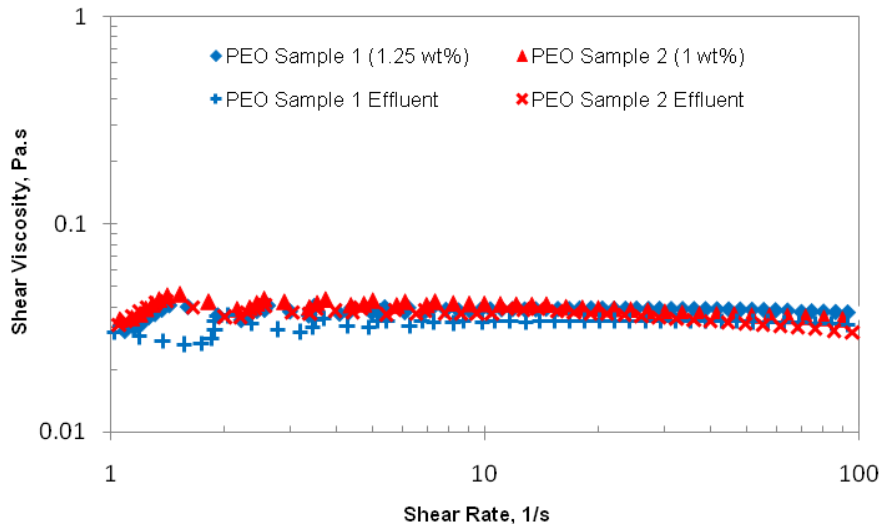


**Fig. 4-11—Shear Viscosity vs. Shear Rate for Effluent Fluids of PEO Samples 1 and 2**

Fig. 4-11 shows that there was only a slight difference in the shear viscosity values of PEO Samples 1 and 2 before and after injection. This means that there was no significant loss of polymer from solution due to its flow in the porous media. It can be concluded that there was no substantial polymer adsorption or mechanical trapping of polymer within the porous media. Also, the shear rates expected in the core during the polymer flooding experiments did not result in considerable shear degradation of the polymer solution, which can be explained by the shear viscosity behavior of the PEO Samples 1 and 2 within the shear rate range (Fig. 4-2).

#### **4.3.4 Summary of Experimental Results**

Table 4-4 shows a comparison of the primary experimental data for the polymer flooding tests carried out with PEO Samples 1 and 2. The table includes input as well as output experimental data for both polymer solutions.

The comparison of input experimental data for both PEO Samples 1 and 2 listed in Table 4-4 shows that polymer flooding experiments were carried out under identical conditions, the only variable being the elastic properties of the solutions. However, output data for the polymer flooding experiments with PEO Samples 1 and 2 were distinctly different, as outlined in the summary table.

<b>TABLE 4-4—SUMMARY TABLE OF EXPERIMENTAL DATA FOR POLYMER FLOODING EXPERIMENTS WITH PEO SAMPLES 1 AND 2</b>		
<u>Polymer Flooding Parameter</u>	<u>PEO Sample 1</u>	<u>PEO Sample 2</u>
<b>INPUT DATA</b>		
Core Porosity, %	42.7	43
Core Absolute Permeability, mD	150	150
Flow Rate, ml/min	4	4
Equivalent Shear Rate Range, 1/s	10-100	10-100
Polymer Solution Injected, PV	1.8	1.8
Polymer Solution Injection Time, hrs	4.5	4.5
<b>OUTPUT DATA</b>		
Breakthrough Time, hrs	0.50	0.52
Polymer Solution Injected at Breakthrough, PV	0.20	0.21
Oil Recovery at Breakthrough, % OIIP	13.0	15.6
Total Polymer Solution Production, PV	1.134	1.127
Residual Oil Saturation, PV	0.49	0.40
Total Oil Recovery, % OIIP	51.5	59.7

## CHAPTER 5

### EXPERIMENTAL RESULTS AND DISCUSSION (PARTIALLY HYDROLYZED POLYACRYLAMIDE)

---

In this chapter the results of the rheological tests carried out on HPAM blends with identical shear viscosity behavior and different elastic characteristics are discussed. Also, the results of polymer flooding experiments are given and the individual effect of elasticity on the microscopic sweep efficiency is investigated.

#### 5.1 Weight Average Molecular Weight and Polydispersity Indices of HPAM Solutions

HPAM Sample 1 was prepared from one grade of HPAM (3330 S), while HPAM Sample 2 was mixed from three HPAM grades (3130 S, 3330 S and 3630 S) as shown in Table 5-1.

<b>TABLE 5-1—COMPOSITION OF HPAM SAMPLES 1 AND 2</b>			
<u>HPAM Solution</u>	<u>Weight Percentage of Polymer Solution Components</u>		
	3130 S	3330 S	3630 S
HPAM Sample 1	0	100	0
HPAM Sample 2	30	25	45

The weight average molecular weight and polydispersity indices of HPAM Samples 1 and 2 were estimated using Eq. 2-14 and Eq. 2-17, respectively. Table 5-2 shows that the estimated weight average molecular weight of HPAM Sample 2 consisting of 3130 S (30%), 3330 S (25%) and 3630 S (45%) was equal to the weight average molecular weight of HPAM Sample 1 consisting of only one HPAM grade. The polydispersity indices of HPAM Samples 1 and 2 were 1 and 2.4, respectively.

<b>TABLE 5-2—WEIGHT AVERAGE MOLECULAR WEIGHT AND POLYDISPERSITY OF HPAM SAMPLES 1 AND 2</b>		
<u>HPAM Solution</u>	<u>Weight Average Molecular Weight</u>	<u>Polydispersity Index</u>
HPAM Sample 1	8,000,000	1
HPAM Sample 2	8,000,000	2.4

HPAM Sample 3 and 4 were mixed accordingly to yield polymer solutions with identical shear viscosity behavior but different elastic characteristics as discussed in Chapter 3 earlier.

Table 5-3 presents the composition of HPAM Samples 3 and 4.

<b>TABLE 5-3—COMPOSITION OF HPAM SAMPLES 3 AND 4</b>			
<u>HPAM Solution</u>	<u>Weight Percentage of Polymer Solution Components</u>		
	AB 005V	3130 S	3630 S
HPAM Sample 3	0	100	0
HPAM Sample 4	40	35	25

Table 5-4 compares the estimated weight average molecular weight and polydispersity index values for HPAM Samples 3 and 4.

<b>TABLE 5-4—WEIGHT AVERAGE MOLECULAR WEIGHT AND POLYDISPERSITY OF HPAM SAMPLES 3 AND 4</b>		
<u>HPAM Solution</u>	<u>Weight Average Molecular Weight</u>	<u>Polydispersity Index</u>
HPAM Sample 3	2,000,000	1
HPAM Sample 4	2,000,000	5.8

## **5.2 Rheological Characterization of HPAM Solutions**

A full-scale rheological characterization of HPAM blends was performed to measure viscous and elastic properties of the solutions. Three types of rheological

measurements were conducted: viscometry tests, oscillation tests and creep/recovery tests.

### 5.2.1 Viscometry Test Results

The viscometry tests studied the shear viscosity and flow of the HPAM solutions (HPAM Sample 1 and 2 and HPAM Sample 3 and 4) as a function of shear.

The tests also measured the normal force values for the solutions as a function of shear rate. The viscosity behaviors as well as the normal force values were measured at shear rates from 1 to 100 1/s.

Shear stress vs. shear rate profiles for HPAM Samples 1 and 2 and HPAM Sample 3 and 4 generated using the viscometry test results are given in Fig. 5-1 and Fig. 5-2, respectively.

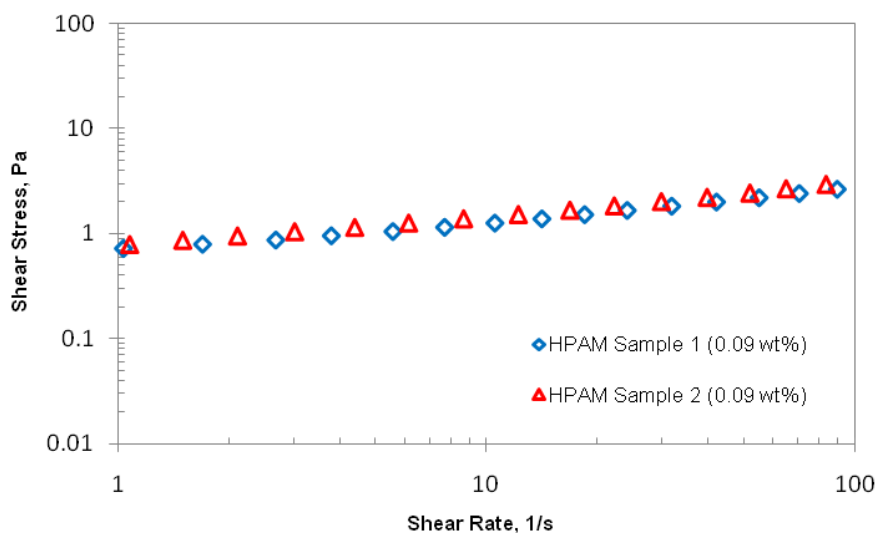


**Fig. 5-1—Shear Stress vs. Shear Rate Profiles for HPAM Samples 1 and 2**

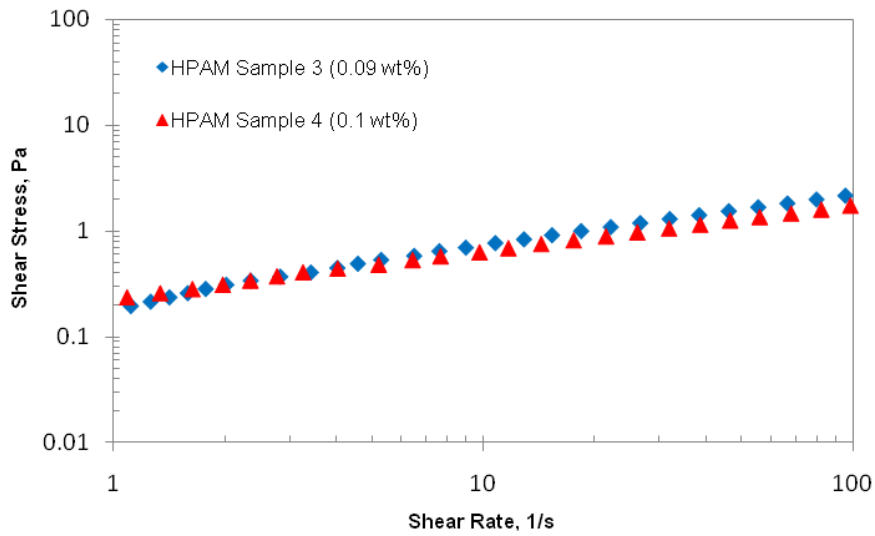


**Fig. 5-2—Shear Stress vs. Shear Rate Profiles for HPAM Samples 3 and 4**

As shown in Fig. 5-1 and Fig. 5-2, the shear stress vs. shear rate profiles of HPAM Samples 1 and 2 and HPAM Samples 3 and 4 were identical at a range of shear rates from 1 to 100 1/s.

Also, the shear stress vs. shear rate values of the HPAM solutions shown in the figures indicate that the rheological behavior of the samples can be characterized by the power-law model within the covered range of shear rates.

The consistency index, K, and power-law index, n, for HPAM Samples 1 and 2 are listed in Table 5-5.

<b>TABLE 5-5—POWER-LAW PARAMETERS FOR HPAM SAMPLES 1 AND 2</b>		
<u>HPAM Solution</u>	<u>Consistency Index K, Pa.s<sup>n</sup></u>	<u>Power-Law Index n</u>
HPAM Sample 1	0.65	0.30
HPAM Sample 2	0.69	0.33

The rheological parameters for HPAM Samples 3 and 4 are given in Table 5-6.

<b>TABLE 5-6—POWER-LAW PARAMETERS FOR HPAM SAMPLES 3 AND 4</b>		
<u>HPAM Solution</u>	<u>Consistency Index K, Pa.s<sup>n</sup></u>	<u>Power-Law Index n</u>
HPAM Sample 3	0.21	0.52
HPAM Sample 4	0.24	0.45

The identical values of the samples' rheological parameters are indicative of their similar shear viscosity behavior. This can be explained by similar weight average molecular weights of the solutions.

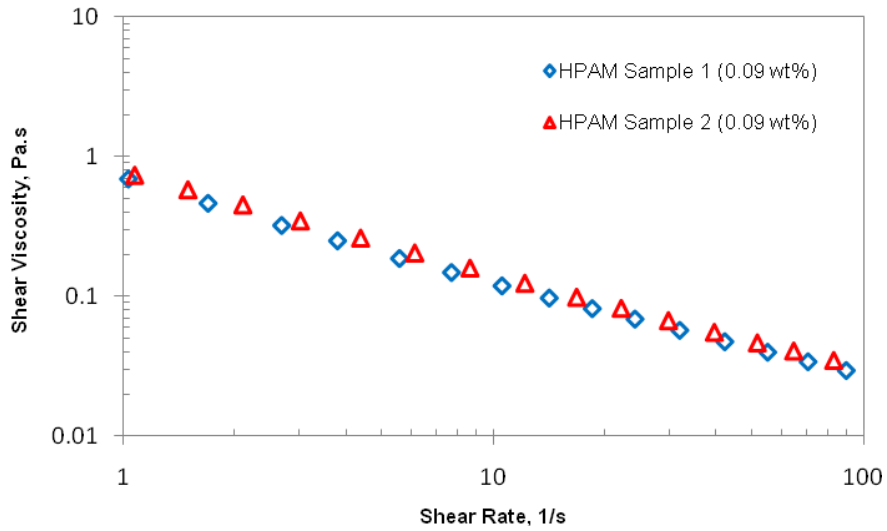


**Fig. 5-3—Shear Viscosity vs. Shear Rate Profiles for HPAM Samples 1 and 2**

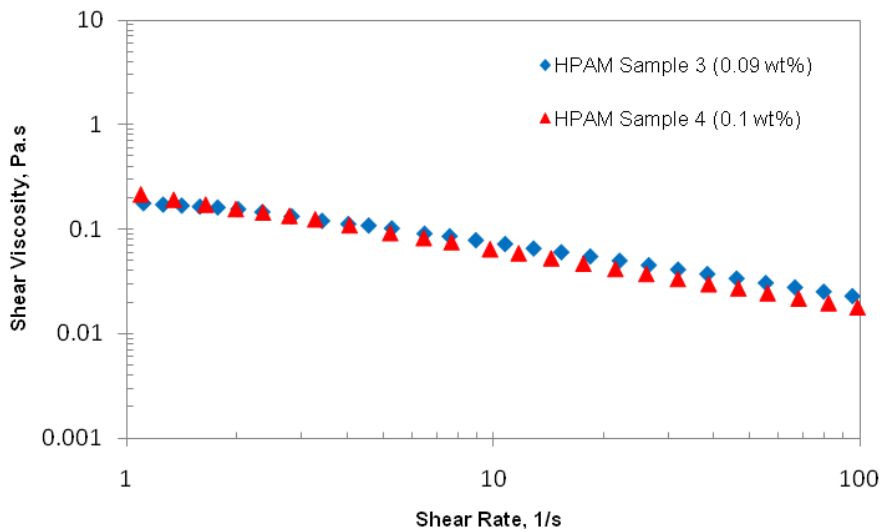


**Fig. 5-4—Shear Viscosity vs. Shear Rate Profiles for HPAM Samples 3 and 4**

As can be seen from Fig. 5-3 and Fig. 5-4, shear viscosities of the HPAM samples exhibited almost identical viscosity behavior at shear rates from 1 to 100 1/s.

Normal force values of the HPAM samples were also measured as a function of shear rate. The normal force values for HPAM Samples 1 and 2 are compared in Fig. 5-5. Fig. 5-6 compares the normal force values for HPAM Samples 3 and 4.

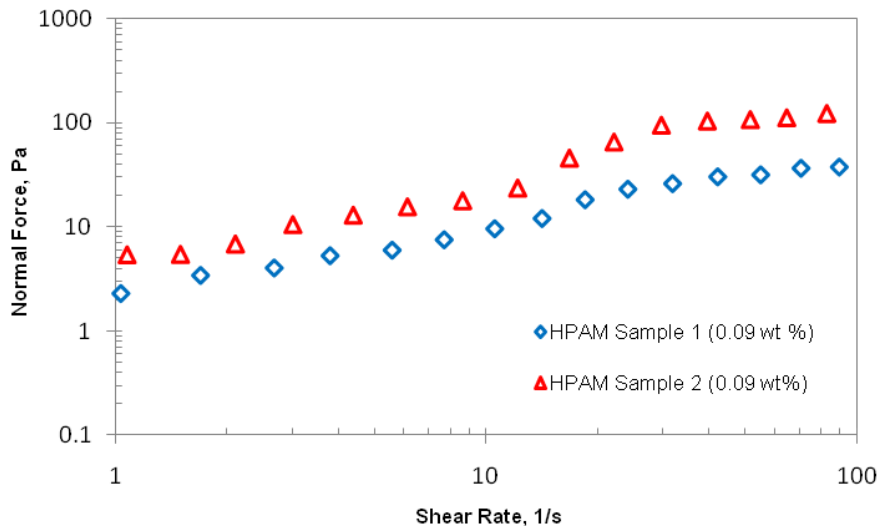


**Fig. 5-5—Normal Force vs. Shear Rate for HPAM Samples 1 and 2**

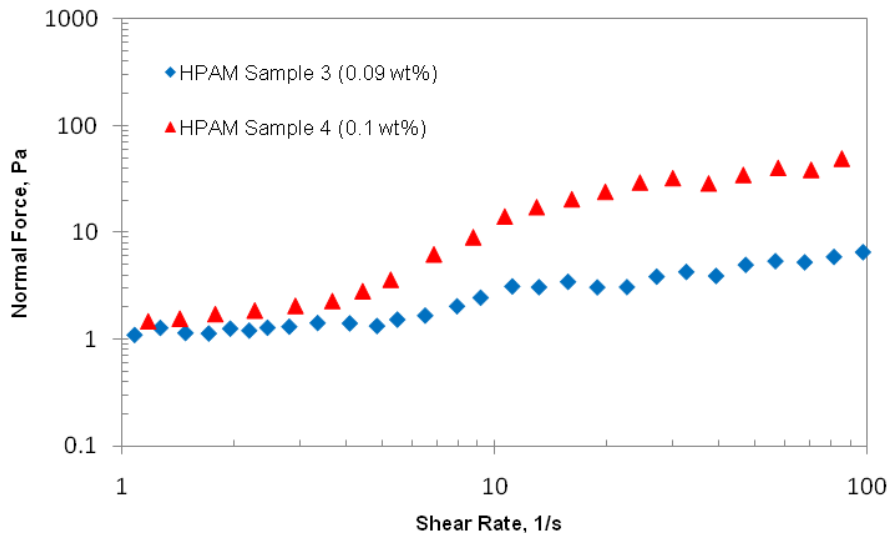


**Fig. 5-6—Normal Force vs. Shear Rate for HPAM Samples 3 and 4**

As expected, HPAM Samples 2 and 4, characterized by higher elasticity exhibited higher normal forces compared to HPAM Samples 1 and 3, respectively. Since the difference in normal forces gives a good indication of the difference in elastic properties, it may be concluded that HPAM Sample 2 had a more elastic structure than HPAM Sample 1. Correspondingly, HPAM Sample 4 was found to be more elastic than HPAM Sample 3. It should be noted here, that the difference between the normal forces of HPAM Sample 1 and 2 was not significant, while HPAM Sample 4 exhibited considerably higher normal forces compared to HPAM Sample 3. This can be explained by a significant difference in the polydispersity indices of HPAM Samples 3 and 4 as compared to HPAM Samples 1 and 2. For instance, at a shear rate of 20 1/s, the normal force values were approximately 20 Pa and 40 Pa for HPAM Samples 1 and 2, while the normal force values for HPAM Samples 3 and 4 were 3 Pa and 25 Pa.

### **5.2.2 Oscillation Test Results**

The oscillation tests measured viscoelastic properties of the HPAM solutions. Two modes of the oscillation tests were carried out: amplitude sweep and frequency sweep.

### 5.2.2.1 Amplitude Sweep Results

The amplitude sweep tests were performed to define the LVR regions of the HPAM solutions. The tests were performed on the polymer solutions at a frequency of 0.1 Hz for stress values ranging from 0.006 to 5 Pa.

The LVR regions of HPAM Samples 1 and 2 were determined from the amplitude sweep results as shown in Fig. 5-7.

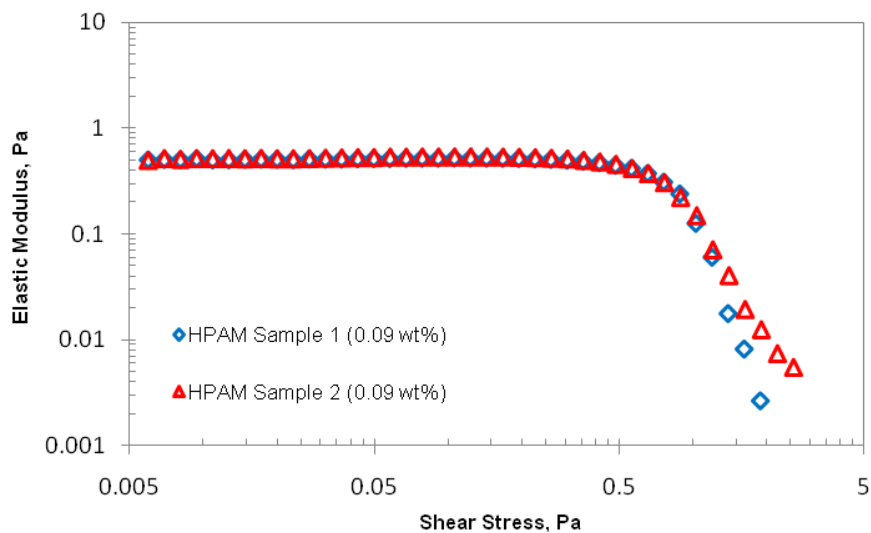


**Fig. 5-7—Elastic Modulus vs. Shear Stress for HPAM Samples 1 and 2**

As shown in Fig. 5-7, there was no obvious stress dependence of elastic moduli of HPAM Samples 1 and 2 for a range of shear stresses up to 0.5 Pa. The elastic moduli of the samples started to decrease sharply at stresses higher than 0.5 Pa. This rapid decrease of the elastic moduli indicated the transition of the samples' linear viscoelastic behavior to non-linear. Based on the amplitude sweep results

presented in Fig. 5-7, a shear stress of 0.015 Pa was selected for the subsequent tests as it falls within the LVR regions of both HPAM Samples 1 and 2.

It should also be noted that the amplitude sweep tests not only determined the samples' LVR regions, but they also indicated that the elastic structure of the HPAM Samples 1 and 2 were identical. It can be explained by the difference in the polydispersity indices of the samples (polydispersity indices of 1 and 2.4, respectively), which was not high enough to ensure noticeably different elastic behavior. This can also be seen in Fig. 5-5, which showed only fairly modest difference in the normal force values for HPAM Samples 1 and 2.

The LVR regions of HPAM Samples 3 and 4 were determined from the amplitude sweep results as presented in Fig. 5-8.

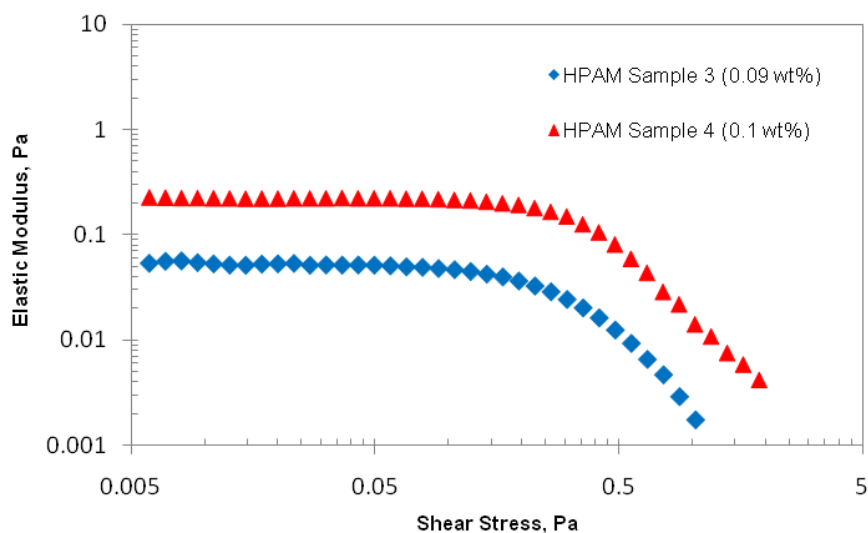


**Fig. 5-8—Elastic Modulus vs. Shear Stress for HPAM Samples 3 and 4**

Fig. 5-8 shows that the elastic moduli of HPAM Samples 3 and 4 were constant for shear rates up to about 0.08 Pa and 0.1 Pa, respectively, with further rapid decrease in the elastic moduli. Thus, the samples' LVR was determined and a shear stress of 0.015 Pa, that falls within the samples' LVR regions, was selected for the subsequent tests.

Although the amplitude sweep tests were performed on HPAM Samples 3 and 4 primarily to determine their LVR regions, some useful information on the samples' elastic properties was also obtained. Fig. 5-8 shows that the elastic modulus values of HPAM Sample 4 were considerably higher than those of HPAM Sample 3. Also, shear stresses higher than 0.08 Pa caused the induced strain to breakdown the structure of HPAM Sample 3, which lead to sharp decrease in the measured values of elasticity. However, the resultant strain became too high for HPAM Sample 4 only at shear stresses higher than 0.1 Pa. Thus, the measured value of elasticity decreased at slightly lower shear stress values for HPAM Sample 3 compared to HPAM Sample 4. This can be explained by more elastic structure of HPAM Sample 4, as indicated by the significant difference between the polydispersity indices of the samples, which amounted to 1 and 5.8 for HPAM Samples 3 and 4, respectively.

### 5.2.2.2 Frequency Sweep Results

The frequency sweep tests were carried out on the HPAM solutions at a range of frequencies from 0.01 to 1 Hz, while the stress was kept constant at 0.015 Pa, which was found to be within the LVR regions of the solutions. The frequency sweep tests provided viscous and elastic modulus data for the HPAM solutions as a function of frequency.

Fig. 5-9 and Fig. 5-10 compare the viscous moduli of HPAM Samples 1 and 2 and HPAM Samples 3 and 4, respectively.

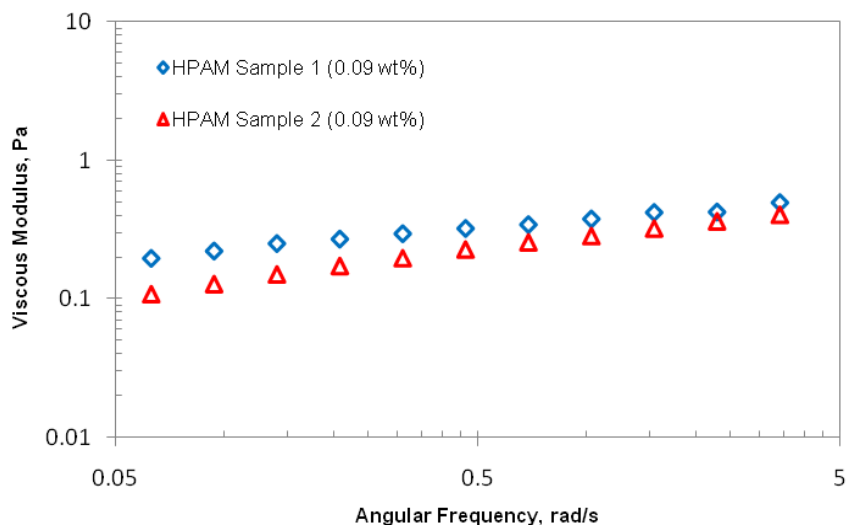


**Fig. 5-9—Viscous Modulus vs. Angular Frequency for HPAM Samples 1 and 2**

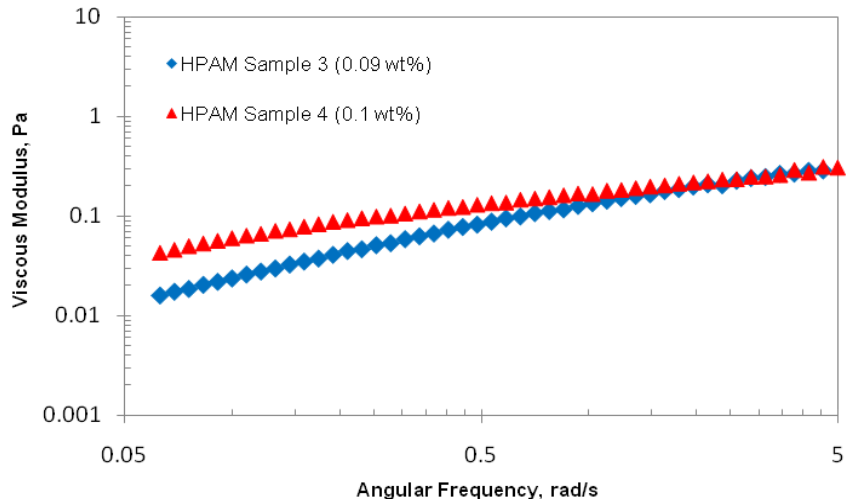


**Fig. 5-10—Viscous Modulus vs. Angular Frequency for HPAM Samples 3 and 4**

Fig. 5-9 and Fig. 5-10 show the measured values of viscous modulus as a function of angular frequency. The measurements showed that the viscous moduli of HPAM Sample 1 and 2 were very close to each other. The viscous modulus values of HPAM Sample 3 are slightly lower than those of HPAM Sample 4 at angular frequencies between 0.05-0.5 rad/s. At angular frequencies between 0.5 to 5 rad/s, however, HPAM Samples 3 and 4 had identical viscous moduli as indicated in Fig. 5-10. This can be explained by the samples' similar viscous characteristics as determined by the viscometry test results.

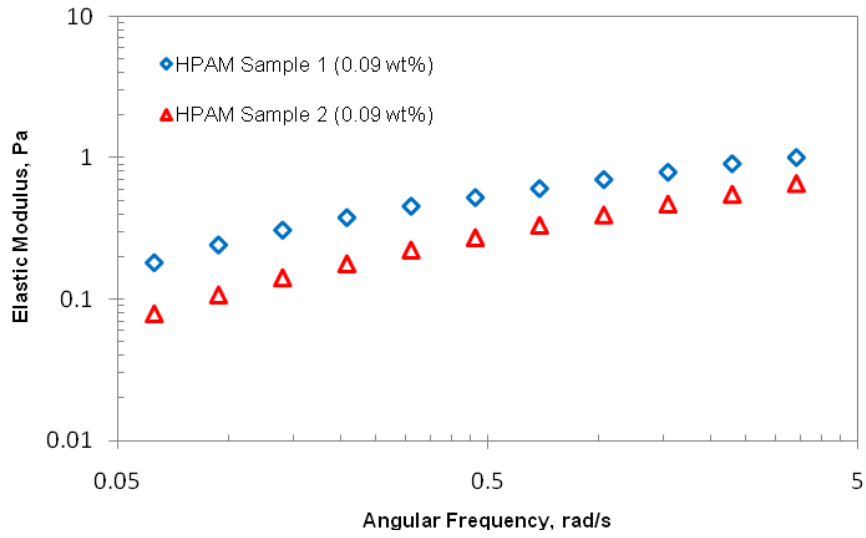


**Fig. 5-11—Elastic Modulus vs. Angular Frequency for HPAM Samples 1 and 2**

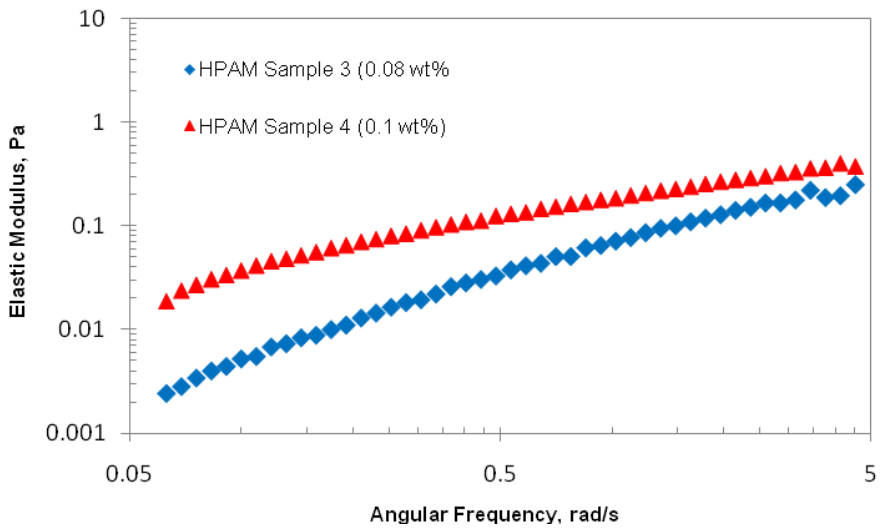


**Fig. 5-12—Elastic Modulus vs. Angular Frequency for HPAM Samples 3 and 4**

The elastic modulus values for HPAM Sample 2 (Fig. 5-11) were slightly lower than those of HPAM Sample 1. This suggested that HPAM Sample 1 was more elastic than HPAM Sample 2, which contradicts the normal force measurements, which indicated that HPAM Sample 2 was more elastic than HPAM Sample 1. The slight difference in the elastic moduli might be explained by the close values of the polydispersity indices (i.e. elastic properties) of HPAM Samples 1 and 2.

It is clear from the elastic modulus vs. angular frequency curves of HPAM Sample 3 and 4 (Fig. 5-12) that the elastic modulus values of HPAM Sample 4 were higher than those of HPAM Sample 3. The higher elastic moduli of HPAM Sample 4 indicated its higher elastic properties, which can be explained by the wider MWD of the solution as indicated by its higher polydispersity index.

### **5.2.3 Creep/Recovery Test Results**

The creep/recovery tests were performed on the HPAM solutions to measure the creep and recovery compliance of the solutions as a function of time.

A stress of 0.02 Pa, which falls within the LVR regions of the polymer solutions, was applied for 100 s during the creep test. The recovery test followed the creep test for another 100 s.

The creep and recovery compliance values of HPAM Samples 1 and 2 are given in Fig. 5-13.

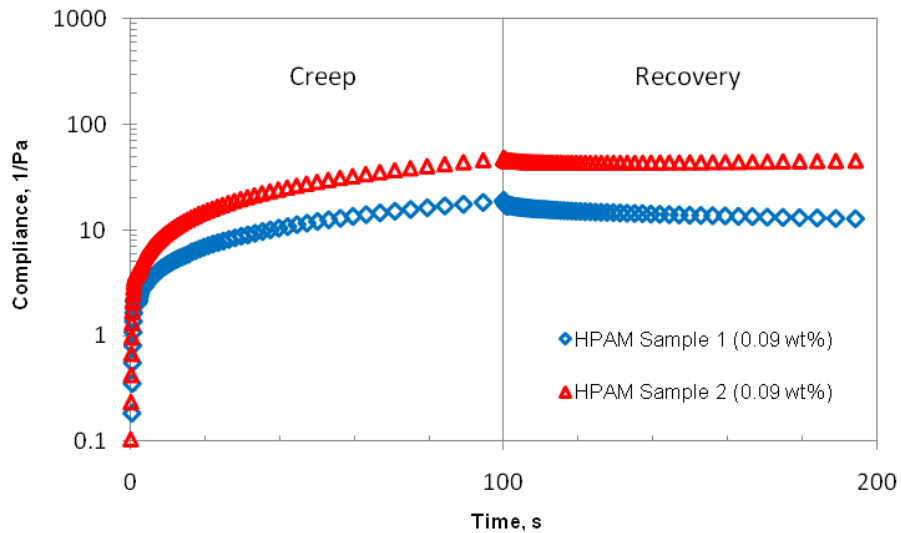


**Fig. 5-13— Creep and Recovery Compliance vs. Time for HPAM Samples 1 and 2**

The higher compliance values for HPAM Sample 2 (Fig. 5-13) indicated that HPAM Sample 1 is more resistant than HPAM Sample 2, which contradicts the normal force measurements. Thus, the results of the creep and recovery tests were inconclusive. More data and measurements are required.

Also, both samples showed very little recovery, which could be explained by the low value of the applied stress, which was not sufficient to deform the samples considerably. Since only slight deformation occurred, there was very little recovery after the stress was removed.

The creep and recovery compliance of HPAM Samples 3 and 4 is compared in Fig. 5-14.

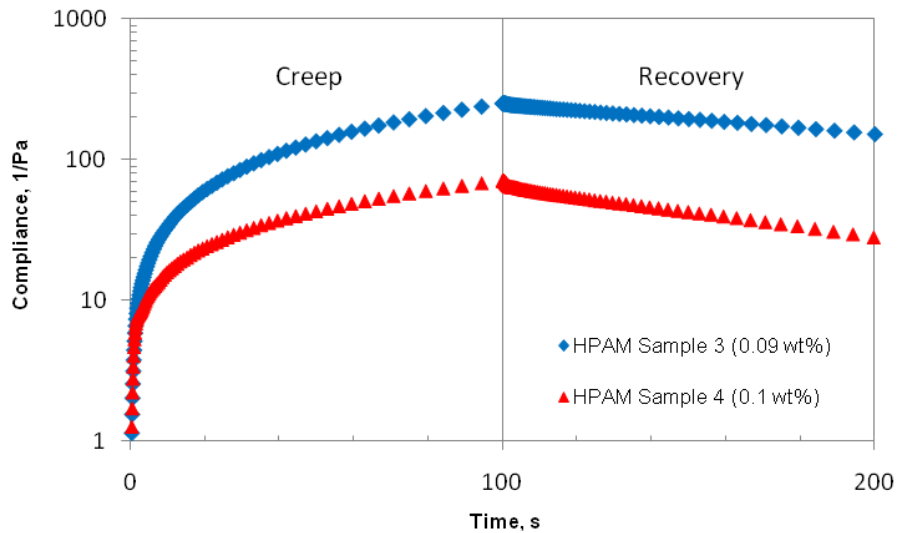


**Fig. 5-14— Creep and Recovery Compliance vs. Time for HPAM Samples 3 and 4**

The creep/recovery test results presented in Fig. 5-14 showed that HPAM Samples 3 and 4 had different creep and recovery behavior when a stress of 0.02 Pa was applied for 100 s and subsequently removed to measure the resultant strain during the recovery phase of 100 s.

It is clear from the figure that the measured values of creep compliance of HPAM Sample 3 are higher than those of HPAM Sample 4. The lower creep compliance of HPAM Sample 4 indicated that the sample was more creep resistant and, consequently, more elastic in nature than HPAM Sample 3.

Also, there was observed some difference in the samples' response to the removal of the constant stress. HPAM Sample 4 showed more recovery after the constant stress was removed compared to HPAM Sample 3, which indicated stronger recoil properties of HPAM Sample 4. However, both samples showed little recovery. This can be explained by the low value of the applied stress, which did not deform the samples substantially during the application of the stress. Nevertheless, based on the creep and recovery curves of the samples, it can be concluded that HPAM Sample 4 was more elastic compared to HPAM Sample 3.

### **5.3 Polymer Flooding Experiments with HPAM Solutions**

Polymer flooding experiments were carried out with HPAM solutions with identical shear viscosity but different elastic characteristics to investigate the individual effect of elasticity on the displacement efficiency isolated from the shear viscosity effect.

#### **5.3.1 Pressure Drop During Polymer Flooding Experiments**

The pressure drop readings were recorded during polymer flooding experiments. The recorded pressure response data for HPAM Samples 3 and 4 are presented in Fig. 5-15.

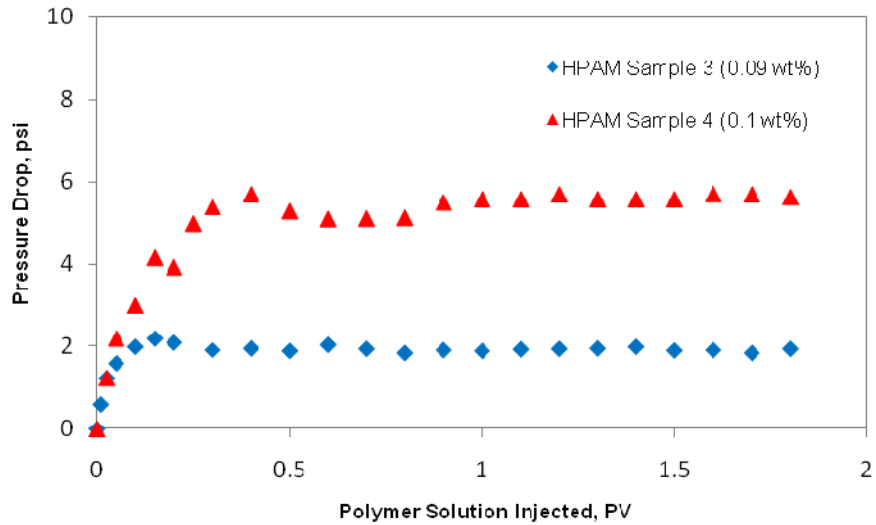
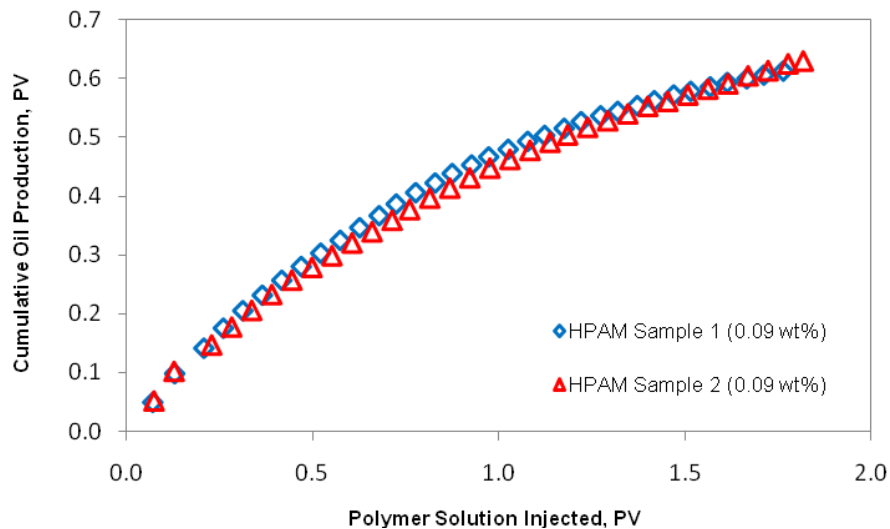


**Fig. 5-15—Pressure Drop During Injection of HPAM Samples 3 and 4**

Fig. 5-15 compares pressure response vs. PV of polymer solution injected for HPAM Samples 3 and 4. As is clear from the figure, there was observed a noticeable difference in the pressure drop during the flooding experiments with HPAM Samples 3 and 4. The higher pressure drop was observed when flooding the core with the more elastic HPAM solution—HPAM Sample 4. The pressure drop was lower during the flooding experiment with HPAM Sample 3. The higher pressure drop indicated that HPAM Sample 4 had higher elasticity compared to HPAM Sample 3, which supported the results of the rheological measurements discussed earlier in this chapter.

### 5.3.2 Oil Displacement Results

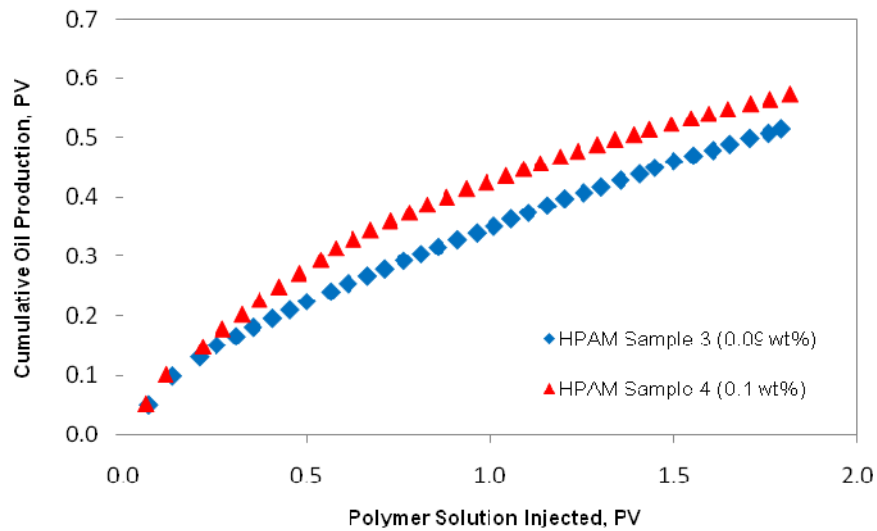
Fig. 5-16 shows the polymer flooding results for HPAM Samples 1 and 2.



**Fig. 5-16—Cumulative Oil Recovery vs. Polymer Solution Injected for HPAM Samples 1 and 2**

It is clear from Fig. 5-16, that the oil recovery obtained by injection of HPAM Samples 1 and 2 was almost identical. This can be explained by the fact that the estimated polydispersity indices of the polymer solutions did not differ considerably as opposed to the polydispersity indices of PEO Samples 1 and 2 and HPAM Samples 3 and 4. The polydispersity indices of 1 and 2.4 gave the moderate difference in the elastic properties of HPAM Samples 1 and 2, as indicated by results of the conducted rheological tests.

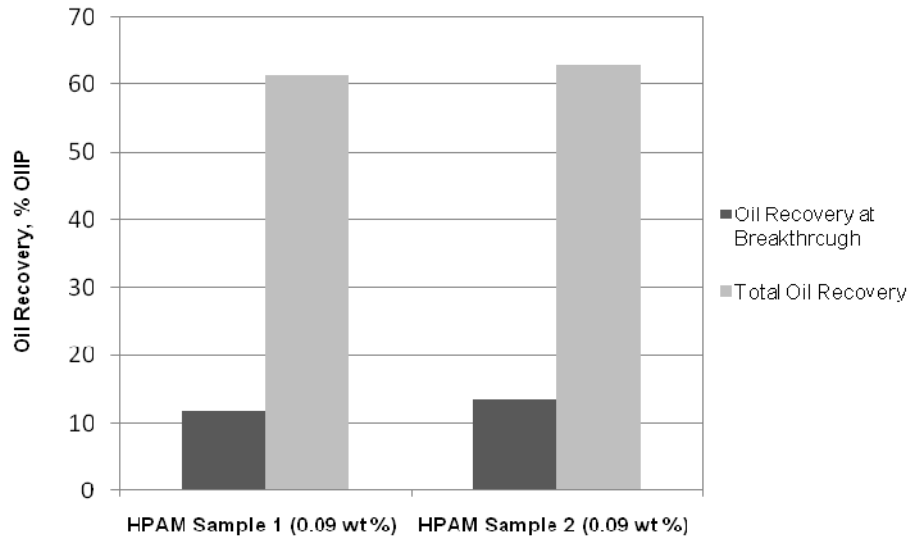
Fig. 5-17 shows the cumulative oil recovery as a function of PV of the injected polymer solution for HPAM Samples 3 and 4.



**Fig. 5-17—Cumulative Oil Recovery vs. Polymer Solution Injected for HPAM Samples 3 and 4**

Fig. 5-17 shows that HPAM Sample 4 characterized by higher elasticity than HPAM Sample 3 gave higher oil recovery throughout the entire polymer flooding experiment. This suggests that oil was recovered earlier at lower water cuts when injecting HPAM Sample 4 into the core to displace oil.

Fig. 5-18 compares the breakthrough recovery and total oil recovery by HPAM Samples 1 and 2.



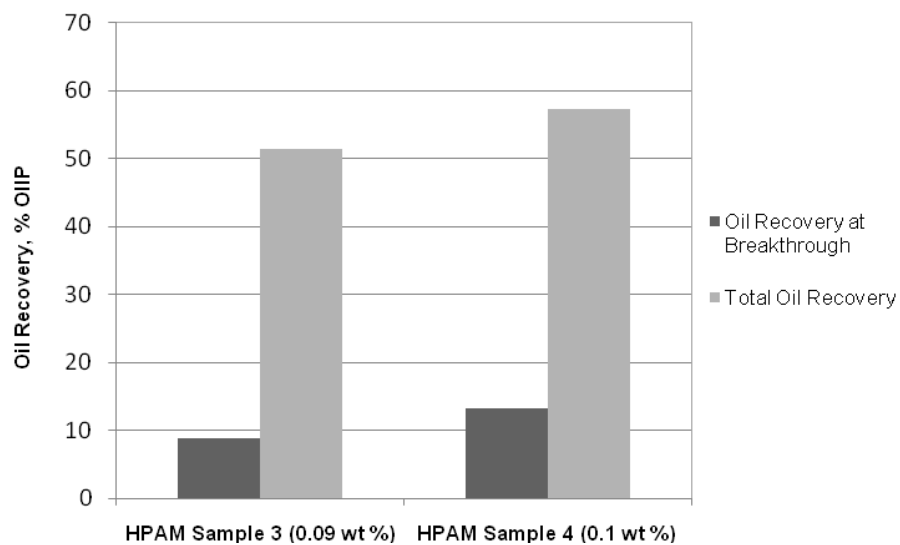
**Fig. 5-18—Breakthrough Recovery and Total Oil Recovery for HPAM Samples 1 and 2**

Fig. 5-18 shows that there was only a slight difference in the oil recovery between HPAM Samples 1 and 2. The total oil recovery obtained by flooding HPAM Sample 1 amounted to 61.3% OIIP, while HPAM Sample 2 gave 62.9% OIIP.

As expected, polymer solution breakthrough was recorded later with HPAM Sample 2 compared to less elastic HPAM Sample 1. The oil recovered before the breakthrough time for HPAM Sample 2 was 11.4% higher than that of HPAM Sample 1.

The slight difference in the polymer flooding results for HPAM Samples 1 and 2 can be explained by the moderate difference in the normal force values of the HPAM samples as shown in Fig. 5-5.

Fig. 5-19 below presents the breakthrough recovery as well as the total oil recovery obtained by injecting HPAM Samples 3 and 4.



**Fig. 5-19—Breakthrough Recovery and Total Oil Recovery for HPAM Samples 3 and 4**

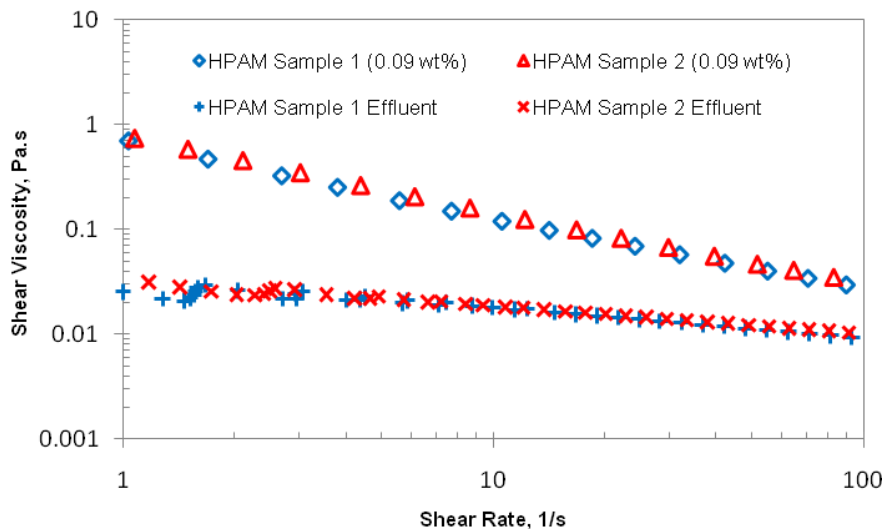
Fig. 5-19 shows that there was a significant difference in the oil recovery between the HPAM blends with identical shear viscosity behavior and different elastic characteristics. The total oil recovered by injecting HPAM Samples 3 amounted to 51.3%. The total oil recovery by more elastic HPAM Sample 4 reached as high as 57.3% of OIIP.

Fig. 5-19 also shows that the breakthrough time was observed later with HPAM Sample 4. Injection of HPAM Sample 3 resulted in earlier breakthrough of the polymer solution. The oil recovered before breakthrough when injecting more elastic HPAM Sample 4 was 33.8% higher than that of HPAM Sample 3.

### 5.3.3 Effluent Viscometry Results

Effluent fluid samples were collected at the end of the polymer flooding experiments and the viscometry tests were performed.

Shear viscosity vs. shear rate profiles of the produced effluent samples are given in Fig. 5-20 and Fig. 5-21.



**Fig. 5-20—Shear Viscosity vs. Shear Rate for Effluent Fluids of HPAM Samples 1 and 2**

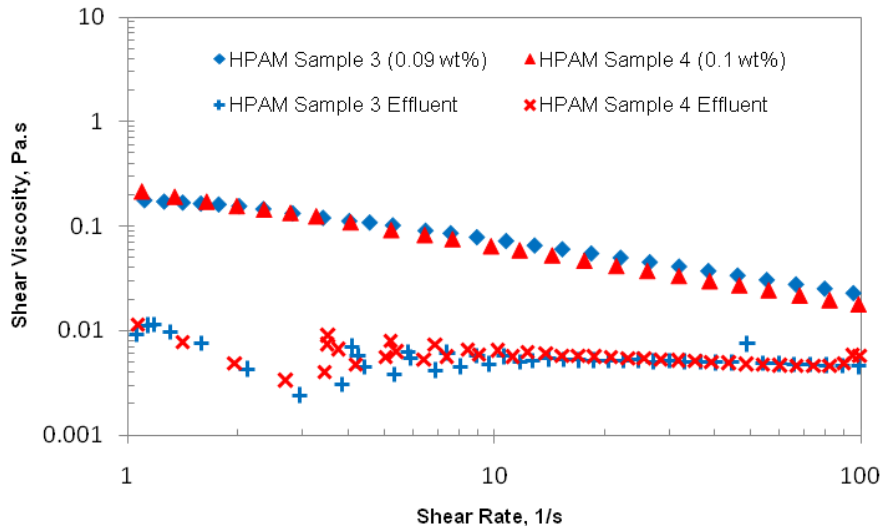


**Fig. 5-21—Shear Viscosity vs. Shear Rate for Effluent Fluids of HPAM Samples 3 and 4**

Fig. 5-20 and Fig. 5-21 show that there was a considerable difference in the shear viscosity values of the HPAM samples before and after injection into the core. It is clear from the figures that there was significant loss of polymer from solution due to its flow in the porous media. The loss of viscosity of the HPAM solutions indicated considerable mechanical degradation of the polymer solutions due to shear, which can be explained by the shear thinning behavior of the samples. Also, there might have occurred some adsorption or mechanical trapping of polymer in the porous media, which also led to the decrease in the shear viscosities of the polymer solutions.

#### **5.3.4 Summary of Experimental Results**

Table 5-7 compares the major experimental data for the polymer flooding experiments carried out with HPAM Samples 1 and 2.

Table 5-8 compares the major experimental data for the polymer flooding experiments with HPAM Samples 3 and 4.

The comparison of input experimental data for the HPAM samples shows that the polymer flooding experiments were carried out under identical conditions. All the parameters were kept identical except for the elastic properties of the solutions. Therefore, the increase in the resultant oil recovery for HPAM Samples 2 and 4 can be attributed to elastic properties of the solutions, which were found to be stronger compared to HPAM Sample 1 and 3.

<b>TABLE 5-7—SUMMARY TABLE OF EXPERIMENTAL DATA FOR POLYMER FLOODING EXPERIMENTS WITH HPAM SAMPLES 1 AND 2</b>		
<u>Polymer Flooding Parameter</u>	<u>HPAM Sample 1</u>	<u>HPAM Sample 2</u>
<b>INPUT DATA</b>		
Core Porosity, %	43.9	43.0
Core Absolute Permeability, mD	150	150
Flow Rate, ml/min	4	4
Equivalent Shear Rate Range, 1/s	10-100	10-100
Polymer Solution Injected, PV	1.8	1.8
Polymer Solution Injection Time, hrs	4.5	4.5
<b>OUTPUT DATA</b>		
Breakthrough Time, hrs	0.38	0.42
Polymer Solution Injected at Breakthrough, PV	0.15	0.17
Oil Recovery at Breakthrough, % OIIP	11.8	13.4
Total Polymer Solution Production, PV	1.05	1.03
Residual Oil Saturation, PV	0.39	0.33
Total Oil Recovery, % OIIP	61.3	62.9

<b>TABLE 5-8—SUMMARY TABLE OF EXPERIMENTAL DATA FOR POLYMER FLOODING EXPERIMENTS WITH HPAM SAMPLES 3 AND 4</b>		
<u>Polymer Flooding Parameter</u>	<u>HPAM Sample 3</u>	<u>HPAM Sample 4</u>
<b>INPUT DATA</b>		
Core Porosity, %	43.2	42.7
Core Absolute Permeability, mD	150	150
Flow Rate, ml/min	4	4
Equivalent Shear Rate Range, 1/s	10-100	10-100
Polymer Solution Injected, PV	1.8	1.8
Polymer Solution Injection Time, hrs	4.5	4.5
<b>OUTPUT DATA</b>		
Breakthrough Time, hrs	0.28	0.38
Polymer Solution Injected at Breakthrough, PV	0.11	0.16
Oil Recovery at Breakthrough, % OIIP	8.8	13.3
Total Polymer Solution Production, PV	1.24	1.17
Residual Oil Saturation, PV	0.49	0.43
Total Oil Recovery, % OIIP	51.3	57.3

## **CHAPTER 6**

### **EXPERIMENTAL RESULTS AND DISCUSSION (XANTHAN GUM)**

---

This chapter presents the experimental data for an aqueous solution of xanthan gum, generally known to have low elasticity. The data include the results of the viscometry tests and the polymer flooding experiment conducted in the radial core holder using the polymer solution.

#### **6.1 Rheological Characterization of Xanthan Gum Solution**

The viscometry tests have been carried out on the xanthan gum samples.

##### **6.1.1 Viscometry Test Results**

The viscometry tests studied the shear viscosity and flow of the xanthan gum solution at shear rates from 1 to 100 1/s. The tests also measured the normal force values.

The concentration of the xanthan gum solution was selected to give the shear viscosity values comparable to other solutions used in the experimental study. More details will be given in Chapter 7.

The shear stress vs. shear rate profile for the xanthan gum solution is given in Fig. 6-1.

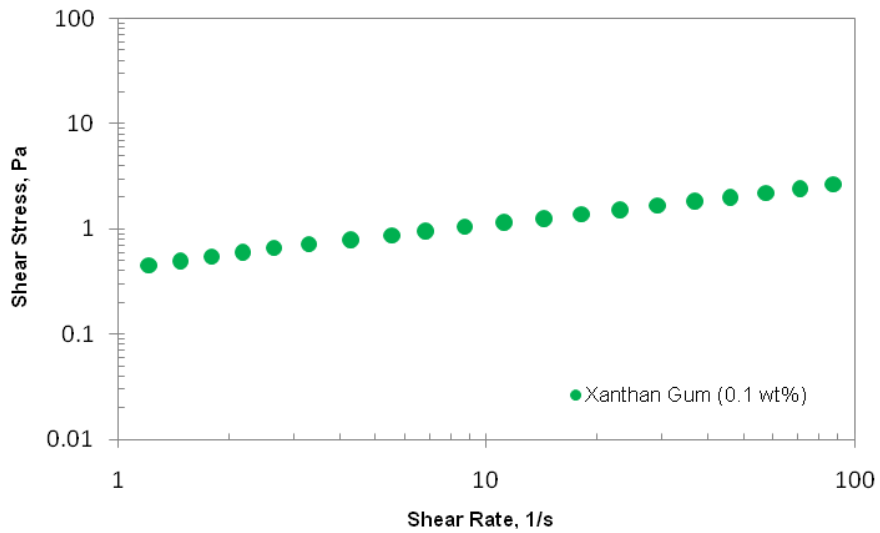


**Fig. 6-1—Shear Stress vs. Shear Rate Profile for the Xanthan Gum Solution**

Table 6-1 indicates the consistency index, K, and power-law index, n, for the xanthan gum solution.

<b>TABLE 6-1—POWER-LAW PARAMETERS FOR XANTHAN GUM SOLUTION</b>		
<u>Polymer Solution</u>	<u>Consistency Index K, Pa.s<sup>n</sup></u>	<u>Power-Law Index n</u>
Xanthan Gum	0.43	0.41

The shear viscosity values for the xanthan gum solution are given in Fig. 6-2.

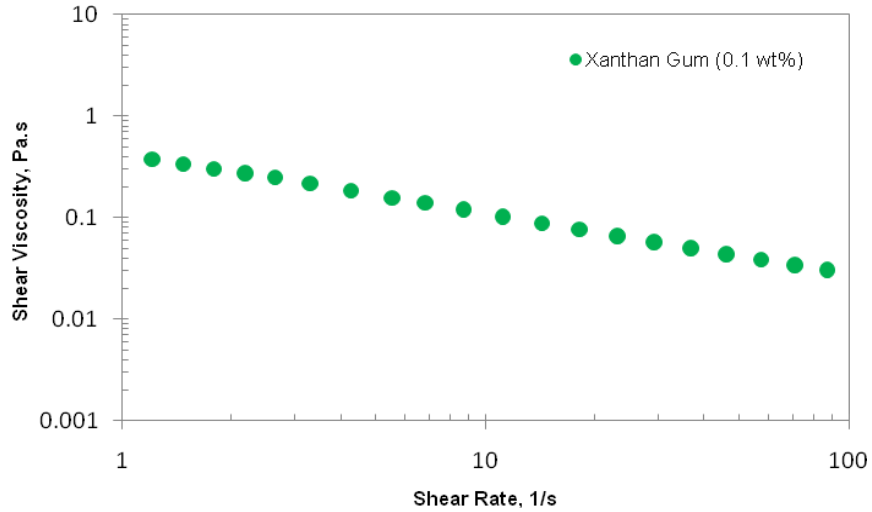


**Fig. 6-2—Shear Viscosity vs. Shear Rate for the Xanthan Gum Solution**

Normal force values of the solution were also measured in the viscometry test.

The results are presented in Fig. 6-3.

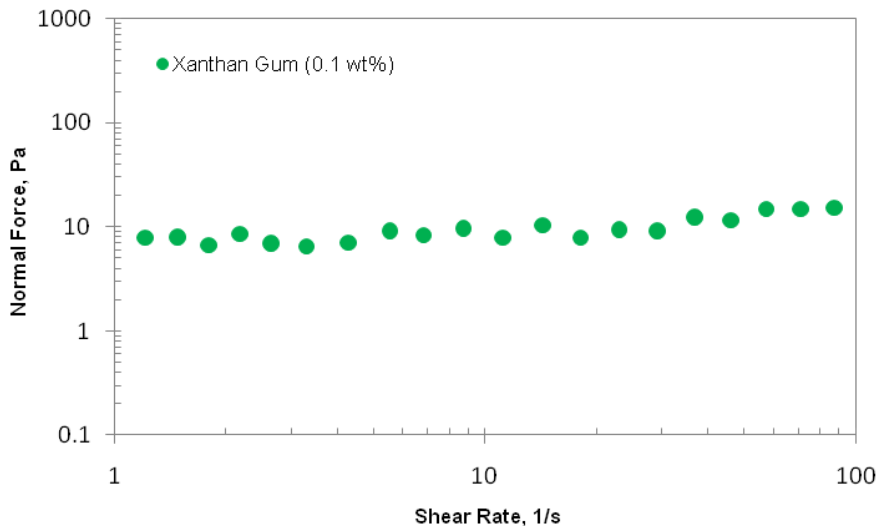
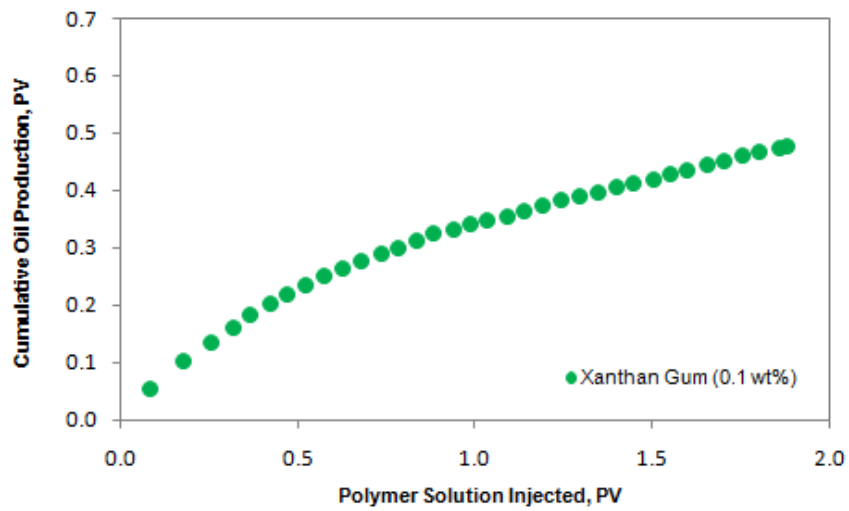


**Fig. 6-3—Normal Force vs. Shear Rate for the Xanthan Gum Solution**

## 6.2 Polymer Flooding Experiments with Xanthan Gum Solution

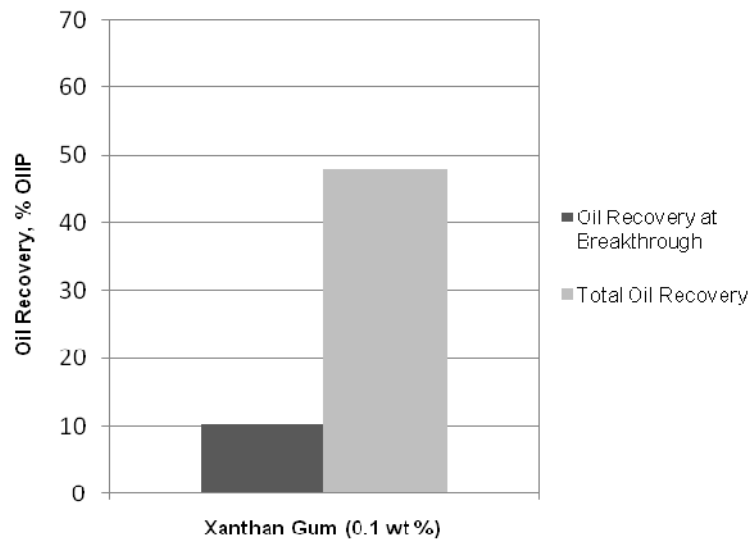
### 6.2.1 Oil Displacement Results

Fig. 6-4 shows the polymer flooding results for the xanthan gum solution.



**Fig. 6-4—Cumulative Oil Recovery vs. Polymer Solution Injected for the Xanthan Gum Solution**

Fig. 6-5 shows the breakthrough recovery and total oil recovery obtained when injecting the xanthan gum solution into the core.



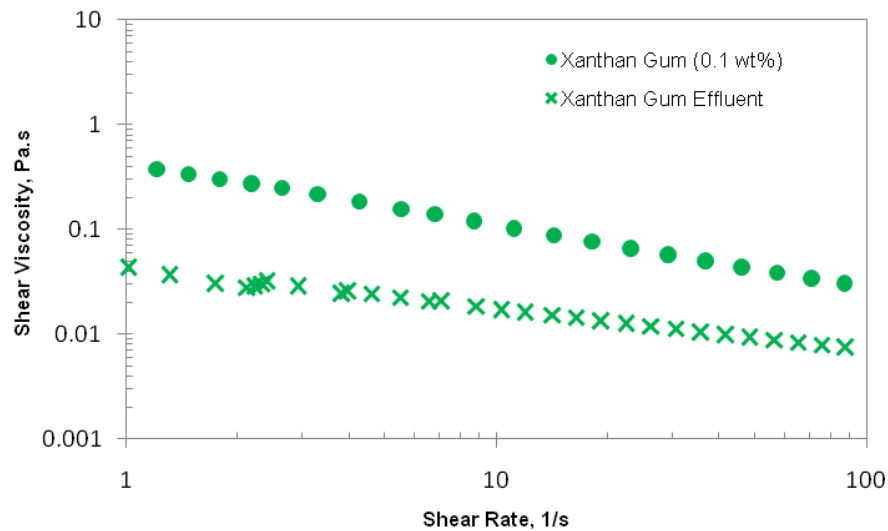
**Fig. 6-5—Breakthrough Recovery and Total Oil Recovery for the Xanthan Gum Solution**

Fig. 6-5 shows that the total oil recovery obtained by flooding the xanthan gum solution was estimated at 47.8% OIIP. Breakthrough of the polymer solution was recorded early; therefore the oil recovered before the breakthrough time was only 10.3% of OIIP.

The comparison of the xanthan gum oil recovery data with other polymer solutions used in the experimental study is given in Chapter 7.

## 6.2.2 Effluent Viscometry Results

Effluent fluid samples were collected at the end of the polymer flooding experiment and the viscometry test was performed.



**Fig. 6-6—Shear Viscosity vs. Shear Rate for Effluent Fluids of the Xanthan Gum Solution**

It is clear from Fig. 6-6 that there was a loss of polymer during the flow of the xanthan gum solution in the core due to the shear degradation. The observed shear degradation, which led to the decrease in the shear viscosity of the solution, can be explained by the shear thinning behavior of the sample as shown in Fig. 6-2.

### **6.2.3 Summary of Experimental Results**

Table 6-2 lists the major experimental data for the polymer flooding experiment carried out with xanthan gum characterized by very weak elastic properties.

<b>TABLE 6-2—SUMMARY TABLE OF EXPERIMENTAL DATA FOR POLYMER FLOODING EXPERIMENT WITH XANTHAN GUM SOLUTION</b>	
<u>Polymer Flooding Parameter</u>	<u>Xanthan Gum Solution</u>
<b>INPUT DATA</b>	
Core Porosity, %	41.2
Core Absolute Permeability, mD	150
Flow Rate, ml/min	4
Equivalent Shear Rate Range, 1/s	10-100
Polymer Solution Injected, PV	1.9
Polymer Solution Injection Time, hrs	4.5
<b>OUTPUT DATA</b>	
Breakthrough Time, hrs	0.42
Polymer Solution Injected at Breakthrough, PV	0.17
Oil Recovery at Breakthrough, % OIIP	10.3
Total Polymer Solution Production, PV	1.32
Residual Oil Saturation, PV	0.52
Total Oil Recovery, % OIIP	47.8

## **CHAPTER 7**

### **COMPARISON OF EXPERIMENTAL DATA FOR PEO, HPAM AND XANTHAN GUM SOLUTIONS**

---

#### **7.1 Comparison of Experimental Results for Xanthan Gum Solution and HPAM Samples 1 and 2**

##### **7.1.1 Comparison of Viscometry Test Results**

According to the viscometry test results of xanthan gum and HPAM Samples 1 and 2, the polymer solutions had very similar identical shear behavior:

- Shear thinning behavior
  
- Identical values of shear viscosity within the range of the expected shear rates (from 10 to 100 1/s).

The shear stress vs. shear rate profile of the xanthan gum solution is compared with the viscometry test results of HPAM Samples 1 and 2 in Fig. 7-1.

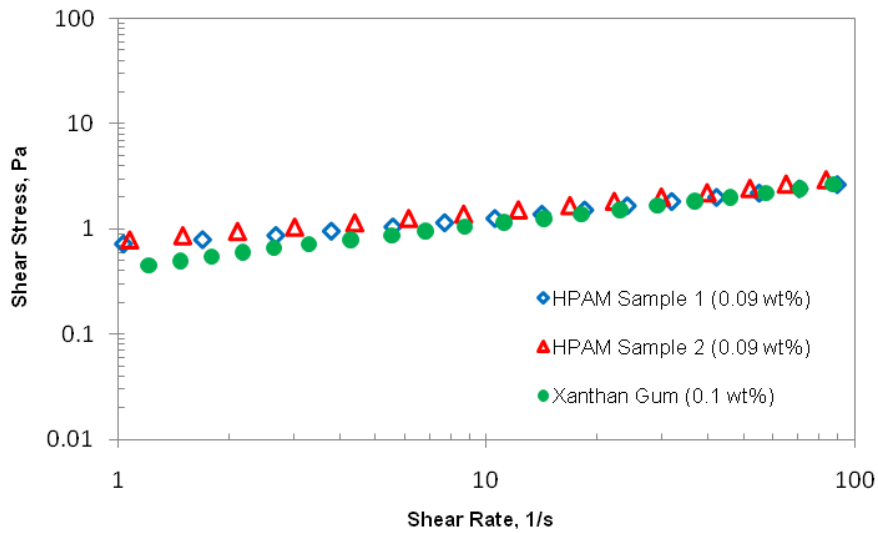


**Fig. 7-1—Shear Stress vs. Shear Rate Profile for the Xanthan Gum Solution Compared to HPAM Samples 1 and 2**

As shown in Fig. 7-1, the flow curve of the xanthan gum solution is identical to that of HPAM Samples 1 and 2 at a range of shear rates from 10 to 100 1/s.

Fig. 7-2 shows that the shear viscosity of the xanthan gum solution is comparable to that of HPAM Samples 1 and 2.

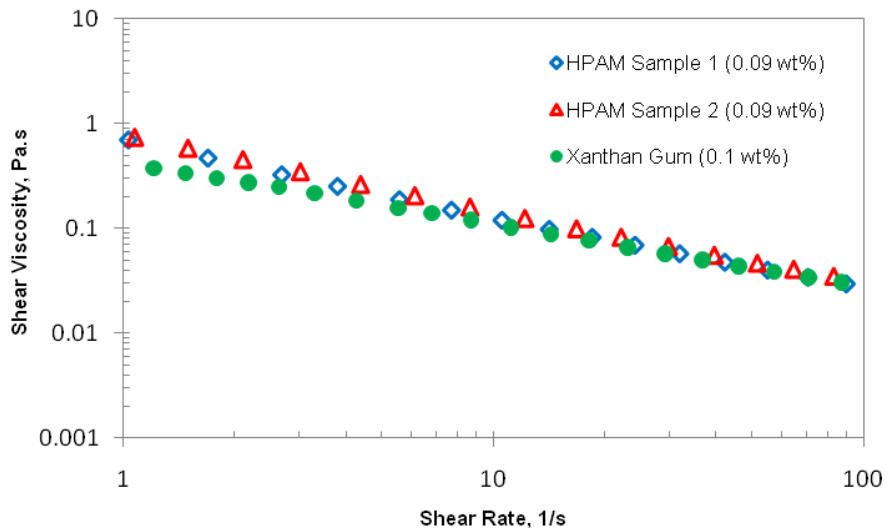


**Fig. 7-2—Shear Viscosity vs. Shear Rate Profile for the Xanthan Gum Solution Compared to HPAM Samples 1 and 2**

However, the normal force values of the xanthan gum solution were lower than those of HPAM Samples 1 and 2.

The normal force values of the solutions are compared in Fig. 7-3.

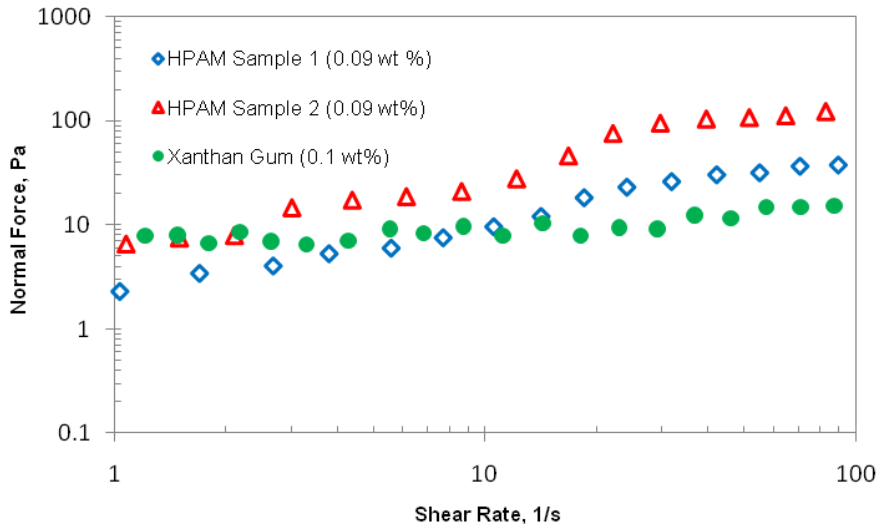


**Fig. 7-3—Normal Force vs. Shear Rate for the Xanthan Gum Solution as Compared to HPAM Samples 1 and 2**

As expected, the xanthan gum solution characterized by low elasticity exhibited lower normal forces compared to HPAM Samples 1 and 2. Since the difference in normal forces gave a good indication of the difference in elastic properties, it may be concluded that HPAM Samples 1 and 2 had stronger elastic properties than the xanthan gum solution.

### 7.1.2 Comparison of Polymer Flooding Results

Fig. 7-4 compares the results of polymer flooding experiments with the xanthan gum solution and the HPAM Samples 1 and 2, which exhibited very similar shear viscosity behavior as given in Fig. 7-1 and Fig. 7-2.

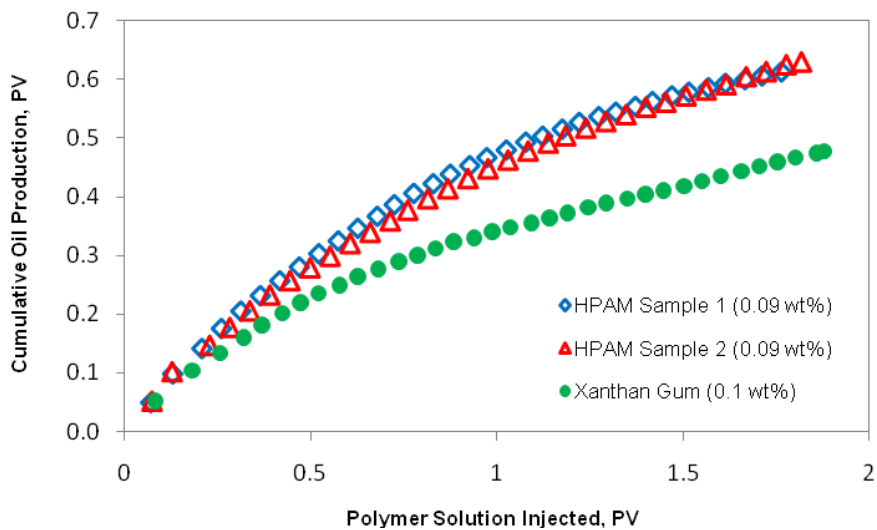


**Fig. 7-4—Cumulative Oil Recovery vs. Polymer Solution Injected for the Xanthan Gum Solution and HPAM Samples 1 and 2**

Fig. 7-4 clearly shows that the xanthan gum solution and HPAM Samples 1 and 2 gave different oil recovery results, despite the identical values of shear viscosity at the equivalent shear rates in the core. The figure shows that the oil recovery started to differ from the early stage of the polymer flooding experiment, the more elastic HPAM solutions resulting in higher oil recovery compared to the xanthan

gum solution. Finally, the cumulative oil recovery differed significantly for the injected polymer solutions.

The difference in the polymer flooding results is also shown in Fig. 7-5, comparing the total oil recovery and the breakthrough oil recovery for the polymer solutions.

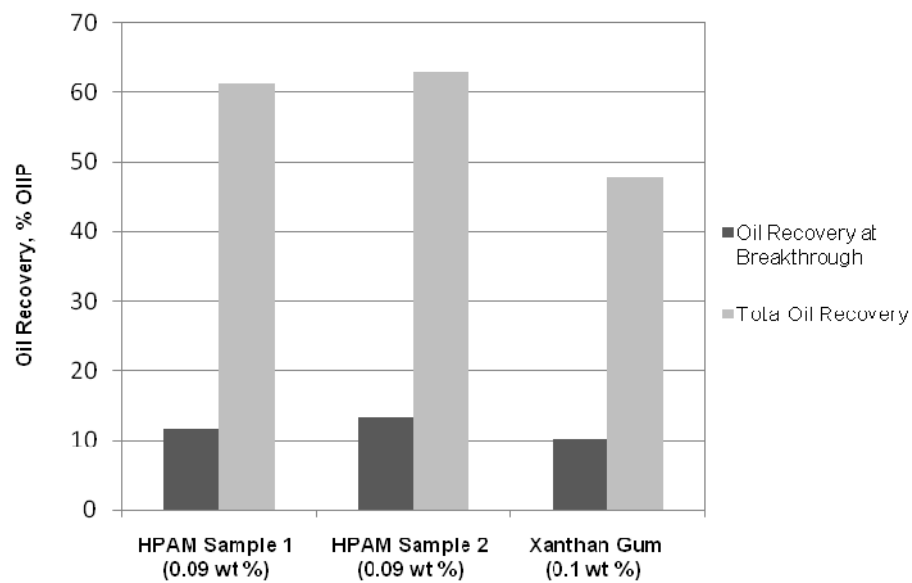


**Fig. 7-5—Breakthrough Recovery and Total Oil Recovery for the Xanthan Gum Solution and HPAM Samples 1 and 2**

As shown in the comparative column chart for the breakthrough and total oil recovery of the polymer solutions (and also mentioned in the respective chapters), the injection of the xanthan gum solution resulted in the oil recovery of 47.8 % OIIP, while HPAM Samples 1 and 2 gave 61.3 and 62.9% OIIP, respectively. Since the shear viscosity behavior of the polymer solutions was identical, the

significant difference in the total oil recovery can be explained by the difference in the elastic properties of the polymer solutions as reflected in the measured normal force values (Fig. 7-3).

## **7.2 Comparison of Experimental Data for PEO, HPAM and Xanthan Gum Solutions**

The oil recovery results obtained by flooding the PEO, HPAM and xanthan gum solutions are combined herein to determine any correlation between the rheological properties of the polymer solutions and the resultant oil recovery. An attempt was made to find a rheological parameter that would correlate better with oil recovery.

Table 7-1 shows the results of polymer flooding experiments with PEO, HPAM and xanthan gum solutions.

<b>TABLE 7-1—OIL RECOVERY DATA FOR AQUEOUS SOLUTIONS OF PEO, HPAM AND XANTHAN GUM</b>	
<u>Polymer Solution</u>	<u>Total Oil Recovery, % OIIP</u>
PEO Sample 1	51.5
PEO Sample 2	59.7
HPAM Sample 1	61.3
HPAM Sample 2	62.9
HPAM Sample 3	51.3
HPAM Sample 4	57.3
Xanthan Gum	47.8

The relation of the oil recovery to the weight average molecular weights and the polydispersity indices of the injected polymer solutions was analyzed. However, a there was found no clear correlation between those parameters and the resultant oil recovery that would hold true for all the polymer solutions independent of the polymer type, concentration, etc.

The ratio of normal force to shear stress was finally selected for the comparison of the oil recovery performance of various types of polymers. The ratio of normal force to shear stress can be defined as the equivalent Trouton ratio (Dehghanpour and Kuru, 2009).

Fig. 7-6 compares the equivalent Trouton ratio vs. shear rate for all the polymer solutions used in the experimental study. The equivalent Trouton ratio was calculated from the viscometry test results for each polymer solution.

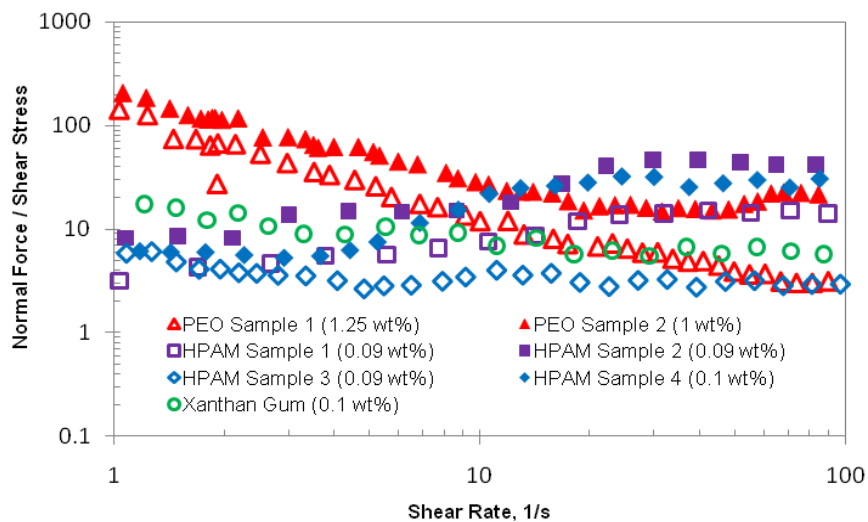


**Fig. 7-6—Equivalent Trouton Ratio of Aqueous Solutions of PEO, HPAM and Xanthan Gum**

It is clear from the figure that the equivalent Trouton ratio behavior of the polymer solutions used in the experimental studies is different. However, an attempt was made to correlate these values with the oil recovery data obtained from the polymer flooding experiments.

The relation of the equivalent Trouton ratio to the oil recovery was determined for a number of shear rate values falling within the range of the expected shear rates in the core:

- 1) Shear rate of 20 1/s
- 2) Shear rate of 14 1/s
- 3) Shear rate of 100 1/s.

The shear rate range of 20 1/s was expected at a radius of 70.7% of the core radius. The radius of 70.7% was selected based on the approach suggested in the API Recommended Practices for Evaluation of EOR Polymers, which stated “It is convenient to select the frontal advance rate at a radius where half of the pore volume of the core has been flooded. This radius is approximately 70.7% of the radius of the core” (API RP 63: Recommended Practices for Evaluation of Polymers Used in Enhanced Oil Recovery Operations, 1990, p. 30). Similarly, the 70.7% of core radius was calculated and the corresponding shear rate value (20 1/s) was selected for convenience to investigate the relationship between the equivalent Trouton ratio and oil recovery.

The total oil recovery vs. equivalent Trouton ratio at a shear rate of 20 1/s is given in Fig. 7-7 for all the polymer solutions used in the study.

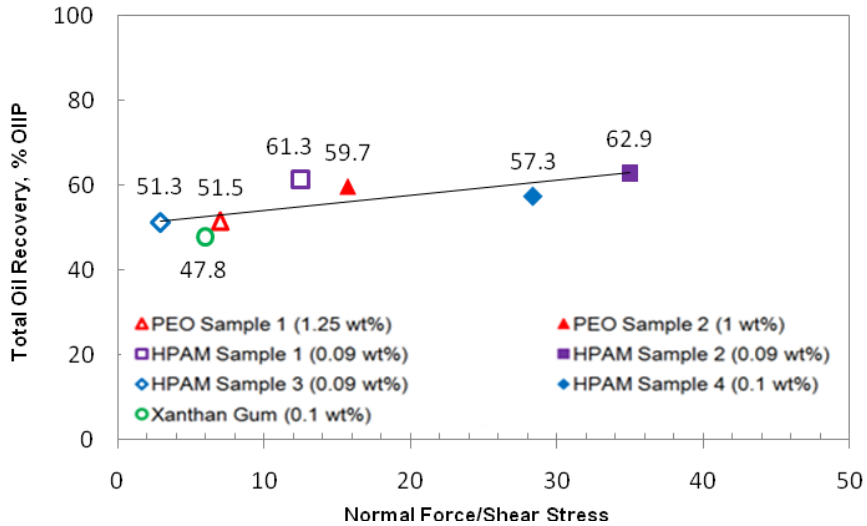


**Fig. 7-7—Total Oil Recovery vs. Equivalent Trouton Ratio of Aqueous Solutions of PEO, HPAM and Xanthan Gum at a Shear Rate of 20 1/s**

In Fig. 7-7, each point is a representative of each polymer solution used in the experimental study. It is clear that the experimental data are distributed around a line with a slope of 0.4. Thus, Fig. 7-7 shows that the total oil recovery increases with the increasing ratio of the normal force to shear stress. However, it should be noted here that more data are required to make the relation of the total oil recovery to the equivalent Trouton ratio conclusive.

The values of oil recovery vs. equivalent Trouton ratio are also given for shear rates of 14 and 100 1/s, which were expected at the wellbore and at the core walls according to Eq. 3-7.

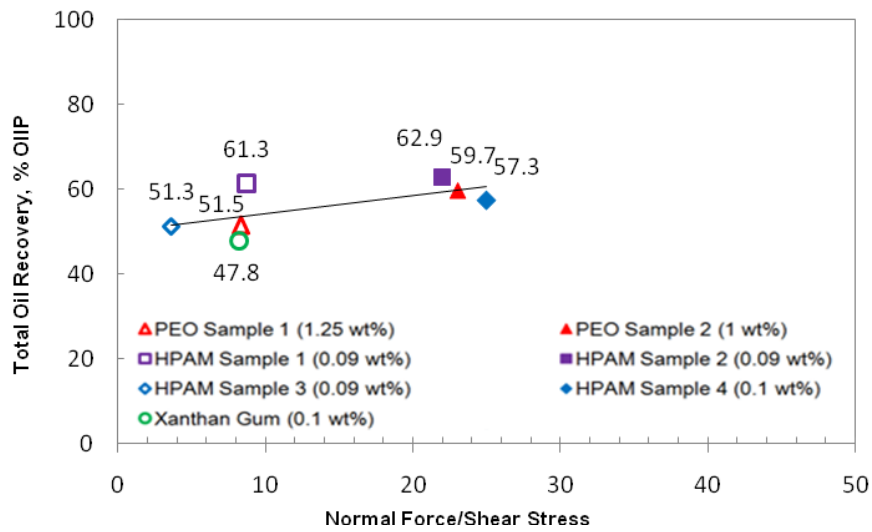


**Fig. 7-8—Total Oil Recovery vs. Equivalent Trouton Ratio of Aqueous Solutions of PEO, HPAM and Xanthan Gum at a Shear Rate of 14 1/s**

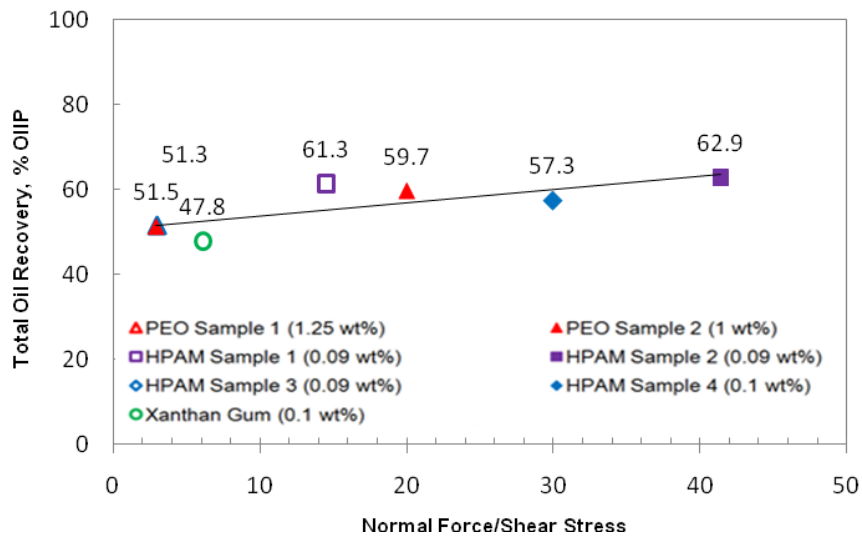


**Fig. 7-9—Total Oil Recovery vs. Equivalent Trouton Ratio of Aqueous Solutions of PEO, HPAM and Xanthan Gum at a Shear Rate of 100 1/s**

Fig. 7-8 and Fig. 7-9 show the same trend of the oil recovery curve. Thus oil recovery increases with the increasing ratio of the normal force to shear stress and, therefore, the equivalent Trouton ratio seems to correlate well with total oil recovery irrespective of the polymer type, molecular weight, concentration, etc.

It should also be noted that as polymer solution is injected into the reservoir (i.e. when shear rates are higher), the elastic behavior of the injected polymer solution becomes more prominent as seen by the normal force vs. shear rate data for all polymer solutions used in the experimental study. However, the correlation could serve as a good indication of EOR performance of polymer solutions away from the wellbore. Thus, the equivalent Trouton ratio could be a good criterion for screening polymers for polymer flood operations. However, it should be noted again that more data are required to make the results conclusive.

## CHAPTER 8

### CONCLUSIONS AND RECOMMENDATIONS

---

This chapter summarizes the results of the research study and suggests recommendations for future research in this area.

#### 8.1 Conclusions

The results of the conducted experimental study showed that elastic properties of injected polymeric fluids play an important role in polymer flood operations. The results were summarized and the following conclusions were drawn:

- The individual effect of elasticity on the microscopic sweep efficiency was investigated by injecting two polymer solutions with similar shear viscosity (i.e. similar weight average molecular weight) but significantly different elastic characteristics (i.e. different MWD). Thus, the effect of elasticity was isolated from the shear viscosity effect.
- A full-scale rheological characterization of the polymer solutions was carried out and the test results were compared. Shear viscosity behavior was presented by viscometry test results as well as viscous modulus measurements. Elasticity of the polymer solutions was presented in terms of normal force values, elastic modulus values and creep/recovery response of the solutions.

- Wider MWD of polymer solution was obtained at constant shear viscosity and polymer concentration. Although the polymer solutions had identical shear viscosity, the normal force and elastic modulus values of the polymer solutions with wider MWD were higher than those of the solutions with narrower MWD.
- The results of a full-scale rheological characterization of polymer solutions showed that the polydispersity index can be an adequate measure of MWD, which, in its turn, influences elastic properties of polymer solutions. Polymer solutions with different polydispersity indices were compared and the solution with higher polydispersity index was found to give higher oil recovery.
- It was found that the difference in the polydispersity index should be high enough to induce a notable difference in elastic properties. The moderate difference in the polydispersity indices of HPAM Samples 1 and 2 lead to the insignificant difference in the elastic properties of the solutions, and, correspondingly, in the moderate difference in the resultant oil recovery.
- The sweep efficiency of polymer flood operations could be improved by optimizing the MWD of polymer solution. The results of the experimental study showed that the wider MWD increased the elastic properties of the polymer solution, which, in its turn, provided additional resistance for the polymer solution to flow through porous media and led to higher oil recovery and lower residual oil saturation.

- Later breakthrough time and, correspondingly, higher breakthrough recovery was observed when flooding the polymer blends with higher elasticity compared to polymer solutions characterized by weaker elastic properties.
- Higher oil recovery was observed when flooding HPAM Samples 1 and 2 compared to other samples used in the experimental studies. This is explained by the higher weight average molecular weights of HPAM Samples 1 and 2.
- Xanthan gum characterized by very weak elastic properties showed the lowest oil recovery compared to the PEO and HPAM solutions.
- An attempt was made to find a rheological parameter that might be used as a screening criterion for polymer flooding operations irrespective of the polymer type, weight average molecular weight, concentration, etc. The equivalent Trouton ratio of the injected polymer solution seems to correlate with the resultant oil recovery. However, more data are needed to draw any conclusions regarding the correlation.

## 8.2 Recommendations

The following recommendations are suggested for future research work:

- The calculated polydispersity index values were used to present the MWD of the polymer solutions. It is suggested that the polydispersity index values be measured experimentally for each polymer blend.
- The effect of elasticity on the sweep efficiency was investigated. However, it is suggested that the effect of elasticity should be quantified.
- The individual effect of elasticity on the sweep efficiency was investigated by comparing the oil recovery results obtained by injecting polymer solutions with identical shear viscosity but different elasticity. However, residual resistance factors should also be determined to evaluate the effect of elasticity on the permeability reduction due to the flow of polymer solutions in porous media.
- Apparent viscosity of the polymer solutions in porous media should be redefined considering elastic properties of the solutions. The apparent viscosity values then can be readily used for modeling in a reservoir simulator.
- The polymer flooding experiments have been carried out at laboratory room temperature. The experimental set-up should be modified and refined to simulate more realistic subsurface conditions. It is suggested that polymer

flooding experiments with polymer solutions with identical shear viscosity but different elastic properties should also be conducted in such conditions to evaluate the effect of temperature and pressure.

- An attempt was made to find a rheological parameter that might be used as a screening criterion for polymer flooding operations irrespective of the polymer type, weight average molecular weight, concentration and etc. The relationship between the equivalent Trouton ratio and the resultant oil recovery was shown. However, more data are needed to make the suggested correlation conclusive.

## REFERENCES

---

Allen, E., and Boger, D.V. 1988. *The Influence of Rheological Properties on Mobility Control in Polymer-Augmented Waterflooding*. Paper SPE 18097 presented at the 63rd Annual Technical Conference and Exhibition of the Society of Petroleum Engineers, Houston, Texas, 2-5 October;

Allison, J.D., Wimberly, J.W., and Ely, T.L. 1985. *Automated and Manual Methods for the Determination of Polyacrylamide and Other Anionic Polymers*. Paper SPE 13589 presented at the SPE International Symposium on Oilfield and Geothermal Chemistry, Phoenix, Arizona, 9-11 April.

Bird, R.B., Armstrong, R.C., and Hassager, O. 1987. Second Edition. *Dynamics of Polymeric Liquids*. Vol.1: Fluid Dynamics, New York: John Wiley and Sons.

Bohlin Instruments. 2003. *User Manual for Bohlin Rheometers*, 2003, Issue 2.1. Gloucestershire, UK.

Carreau, P.J., De Kee, D., and Daroux, M. 1979. *An Analysis of the Viscous Behaviour of Polymeric Solutions*. The Canadian J. of Chem.Eng., Vol.57, April: 135-140.

Castagno, R.E., Shupe, R.D., Gregory, M.D., and Lescarbours, J.A. 1987. *Method for Laboratory and Field Evaluation of a Proposed Polymer Flood*. J. Res. Eng., November 1987: 452-460.

Chan, P.S.-K., Chen, J., Ettelaie, R., Law, Z., Alevisopoulos, S., Day, E., and Smith, S. 2007. *Study of the Shear and Extensional Rheology of Casein, Waxy Maize Starch and Their Mixtures*. Food Hydrocolloids, 21 (2007): 716-725.

Chang, H.L. 1978. *Polymer Flooding Technology—Yesterday, Today and Tomorrow*. J. Pet. Tech., 30 (8): 1113-1128.

Chauveteau, G. 1982. *Rodlike Polymer Solution Flow Through Fine Pores: Influence of Pore Size on Rheological Behaviour*. J. Rheology, 26(2): 111-142.

Chauveteau, G., and Kohler, N. 1974. *Polymer Flooding: the Essential Elements for Laboratory Evaluation*. SPE Paper 4745 presented at the Improved Oil Recovery Symposium of the Society of Petroleum Engineers of AIME, Tulsa, Oklahoma, 22-24 April.

Christopher, R.H., and Middleman, S. 1965. *Power-Law Flow Through a Packed Tube*. I&EC Fund., 4: 422-426.

Clay, T.D., and Menzie, D.E. 1966. *The Effect of Polymer Additives on Oil Recovery in Conventional Waterflooding*. Paper SPE 1670 presented at the SPE Four Corners Regional Meeting, Farmington, New Mexico, 9-10 September.

Dehghanpour, H.A. 2008. *Investigation of Viscoelastic Properties of Polymer Based Fluids as a Possible Mechanism of Internal Filter Cake Formation*. MS thesis, U of Alberta, Edmonton, Alberta, Canada.

Dehghanpour, H.A., and Kuru E. 2009. *A New Look at the Viscoelastic Fluid Flow in Porous Media—A Possible Mechanism of Internal Cake Formation and Formation Damage Control*. Paper SPE 121640 presented at the 2009 SPE International Symposium on Oilfield Chemistry, the Woodlands, Texas, 20-22 April.

Delshad, M., Kim, D.H., Magbagbeola, O.A., Huh, C., Pope, G.A. and Tarahhom, F. 2008. *Mechanistic Interpretation and Utilization of Viscoelastic Behaviour of Polymer Solutions for Improved Polymer-Flood Efficiency*. Paper SPE 113620 presented at the 2008 SPE/DOE Improved Oil Recovery Symposium, Tulsa, Oklahoma, 19-23 April.

Dominguez, J.G., and Willhite, G.P. 1976. *Retention and Flow Characteristics of Polymer Solutions in Porous Media*. Paper SPE 5835 presented at the SPE-AIME Fourth Symposium on Improved Oil Recovery, Tulsa, Oklahoma, 22-24 March.

Ferry, J.D. 1980. *Viscoelastic Properties of Polymers*. Third edition. New York: John Wiley & Sons, Inc.

Garrouch, A.A., and Gharbi, R.B. 2006. *A Novel Model for Viscoelastic Fluid Flow in Porous Media*. Paper SPE 102015 presented at the 2006 SPE Annual Technical Conference and Exhibition, San Antonio, Texas, 24-27 September.

Garrouch, A.A. 1999. *A Viscoelastic Model for Polymer Flow in Reservoir Rocks*. Paper SPE 54379 presented at the 1999 SPE Asia Pacific Oil and Gas Conference and Exhibition, Jakarta, Indonesia, 20-22 April.

Gleasure, R.W., and Phillips, C.R. 1990. *An Experimental Study of Non-Newtonian Polymer Rheology Effects on Oil Recovery and Injectivity*. SPE Res Eng, November: 481-486.

Gupta, R.K., and Sridhar, T. 1985. *Viscoelastic Effects in Non-Newtonian Flows Through Porous Media*. Rheol. Acta, 24: 148-151.

Heemskerk, J., Janssen-van Rosmalen, R., Holtslag, R.J., and Teeuw, D. 1984. *Quantification of Viscoelastic Effects of Polyacrylamide Solutions*. Paper SPE 12652 presented at the SPE/DOE Fourth Symposium on Enhanced Oil Recovery, Tulsa, Oklahoma, 15-18 April.

Hejri, S., Willhite, G.P., and Green, D.W. 1991. *Development of Correlations to Predict Biopolymer Mobility in Porous Media*. J. Res. Eng., February: 91-98.

Hill, H.J., Brew, J.R., Claridge, E.L., Hite, J.R., and Pope, G.A. 1974. *The Behavior of Polymers in Porous Media*. Paper SPE 4748 presented at the Improved Oil Recovery Symposium of the Society of Petroleum Engineers of AIME, Tulsa, Oklahoma, 22-24 April.

James, D.F., and Chandler, G.M. 1990. *Measurement of the Extensional Viscosity of M1 in a Converging Channel Rheometer*. J. of Non-Newtonian Fluid Mech., 35 (1990): 445-458.

Jennings, R.R., Rogers, J.H., and West, T.J. 1971. *Factors Influencing Mobility Control By Polymer Solutions*. J. Pet Tech, March: 391-401.

Jiang, H., Wu, W., Wang, D., Zeng, Y., Zhao, S., and Nie, J. 2008. *The Effect of Elasticity on Displacement Efficiency in the Lab and Results of High Concentration Polymer Flooding in the Field*. Paper SPE 115315 presented at the SPE Annual Technical Conference and Exhibition, Denver, Colorado, 21-24 September.

Jones, D.M., Walters, K., Williams, P.R. 1987. *On the Extensional Viscosity of Mobile Polymer Solutions*. Rheol Acta, 26 (20).

Kaminsky, R.D., Wattenbarger, R.C., Szafranski, R.C., and Coutee, A.S. 2007. *Guidelines for Polymer Flooding Evaluation and Development*. Paper IPTC 11200 presented at the International Petroleum Technology Conference, Dubai, U.A.E., 4-6 December.

Kozicki, W., Son, J.E., and Hanna, M.R. 1984. *Characterization of Adsorptional Phenomena in Polymer Solution Flows*. The Chem. Eng. J., 29 (1984): 171-181.

Kuehne, D.L., and Shaw, D.W. 1983. *Manual and Automated Turbidimetric Methods for the Determination of Polyacrylamides in the Presence of Sulfonates*. Paper SPE 11784 presented at the SPE Oilfield and Geothermal Chemistry Symposium, Denver, Colorado, 1-3 June.

Lake, L.W. 1989. *Enhanced Oil Recovery*. Englewood Cliffs, New Jersey: Prentice Hall.

Lee, S., Kim, D.H., Huh, C., and Pope, G.A. 2009. *Development of a Comprehensive Rheological Property Database for EOR Polymers*. Paper SPE 124798 presented at the 2009 SPE Annual Technical Conference and Exhibition, New Orleans, Louisiana, 4-7 October.

Levitt, D.B., and Pope, G.A. 2008. *Selection and Screening of Polymers for Enhanced-Oil Recovery*. Paper SPE 113845 presented at the SPE/DOE Improved Oil Recovery Symposium, Tulsa, Oklahoma, 19-23 April.

Littmann, W. 1988. *Polymer Flooding*. Amsterdam, The Netherlands: Elsevier Science Publishers B.V.

Marshall, R., and Metzner, A.B. 1967. *Flow of Viscoelastic Fluids Through Porous Media*. EC Fund., 6:393.

Martin, F.D., Hatch, M.J., Shepitka, J.S., and Ward, J.S. 1983. *Improved Water-Soluble Polymers for Enhanced Recovery*. Paper SPE 11786 presented at the International Symposium on Oilfield and Geothermal Chemistry, Denver, Colorado, 1-3 June.

Mezzomo, R.F., Moczydlower, P., Sanmartin, A.N., and Araujo, C.H.V. 2002. *A New Approach to the Determination of Polymer Concentration in Reservoir Rock Adsorption Tests*. Paper SPE 75204 presented at the SPE/DOE Thirteenth Symposium on Improved Oil Recovery, Tulsa, Oklahoma, 13-17 April.

Needham, R.B., and Doe, P.H. 1987. *Polymer Flooding Review*. J. Pet. Tech., 39 (12), 1503-1507.

Pandey, A., Beliveau, D., Kumar, M.S., Pitts, M.J., and Qi, J. 2008. *Evaluation of Chemical Flood Potential for Mangala Field, Rajasthan, India – Laboratory Experiment Design and Results*. Paper IPTC 12636 presented at the International Petroleum Technology Conference, Kuala Lumpur, Malaysia, 3-5 December.

Petrie, C.J. 2006. *Extensional Viscosity: A Critical Discussion*. J. Non-Newtonian Fluid Mech., 137 (2006): 15-23.

Pinaud, F. 1987. *Effect of Molecular Weight Parameters on the Viscoelastic Properties of Polymer Melts*. J. Non-Newtonian Fluid Mechanics, 23: 137-149.

Ranjbar, M., Rupp, J., Pusch, G., and Meyn, R. 1992. *Quantification and Optimization of Viscoelastic Effects of Polymer Solutions for Enhanced Oil Recovery*. Paper SPE 24154 presented at the SPE/DOE Eighth Symposium on Enhanced Oil Recovery, Tulsa, Oklahoma, 22-24 April.

Rogošić, M., Mencer, H.J., and Gomzi, Z. 1996. *Polydispersity Index and Molecular Weight Distributions of Polymers*. Eur. Polym. J., 32 (11): 1337-1344.

Saavedra, N.F., Gaviria, W., and Davitt, J. 2002. *Laboratory Testing of Polymer Flood Candidates: San Francisco Field*. Paper SPE 75182 presented at the SPE/DOE Improved Oil Recovery Symposium, Tulsa, Oklahoma, 13-17 April.

Sandiford, B.B. 1964. *Laboratory and Field Studies of Water Floods Using Polymer Solutions to Increase Oil Recoveries*. J. Pet. Tech. (August): 917-922.

Seright, R. S. 1983. *The Effects of Mechanical Degradation and Viscoelastic Behavior on Injectivity of Polyacrylamide Solutions*. SPE J. (June): 475-485.

Schumacher, M. M. ed. 1978. *Enhanced Oil Recovery*. Park Ridge, New Jersey: Noyes Data Corporation.

Shan, D.O., and Schechter, R.S., eds. 1977. *Improved Oil Recovery by Surfactant and Polymer Flooding*. London: Academic Press, Inc.

Shaw, M.T., and MacKnight, W.J. 2005. *Introduction to Polymer Viscoelasticity*. Third Edition. New York: John Wiley & Sons.

Sorbie, K.S. 1991. *Polymer-Improved Oil Recovery*. London: Blackie and Son Ltd.

Szabo, M.T. 1975. *Laboratory Investigations of Factors Influencing Polymer Flood Performance*. SPE J., August: 338-346.

Taber, J.J., Martin, F. D., and Seright, R. S. 1997. *EOR Screening Criteria Revisited – Part 1: Introduction to Screening Criteria and Enhanced Recovery Field Projects*. SPE Res. Eng., August.

Taber, J.J., Martin, F. D., and Seright, R. S. 1997. *EOR Screening Criteria Revisited – Part 2: Applications and Impact of Oil Prices*. SPE Res. Eng., August.

Trivedi, J. J. 2009. *EOR Screening. Lecture*. University of Alberta, Edmonton, Alberta, Canada, 17 September.

Vinogradov, G.V., and Malkin, A.Ya. 1980. *Rheology of Polymers*. Moscow: Mir Publishers.

Wang, D., Cheng, J., Xia, H., Li, Q., and Shi, J. 2001. *Viscous-Elastic Fluids Can Mobilize Oil Remaining After Water-Flood by Force Parallel to the Oil-Water Interface*. Paper SPE 72123 presented at the SPE Asia Pacific Improved Oil Recovery Conference, Kuala Lumpur, Malaysia, 8-9 October.

Wang, D., Cheng, J., Yang, Q., Gong, W., Li, Q, and Chen, F. 2000. *Viscous-Elastic Polymer Can Increase Microscale Displacement Efficiency in Cores*. Paper SPE 63227 presented at the 2000 SPE Annual Technical Conference and Exhibition, Dallas, Texas, 1-4 October.

Wang, D., Wang, G., Wu, W., Xia, H., and Yin, H. 2007. *The Influence of Viscoelasticity on Displacement Efficiency—from Micro- to Macroscale*. Paper SPE 109016 presented at the SPE Annual Technical Conference and Exhibition, Anaheim, California, 11-14 November.

Wang, D., Xia, H., Yang, S. and Wang, G. 2010. *The Influence of Visco-Elasticity on Micro Forces and Displacement Efficiency in Pores, Cores and in the Field*. Paper SPE 127453 presented at the SPE EOR Conference at Oil and Gas West Asia, Muscat, Oman, 11-13 April.

Wang, J., and Dong M. 2009. *Optimum Effective Viscosity of Polymer Solution for Improving Heavy Oil Recovery*. J. Pet. Sci. and Eng. 67: 155-158.

Willhite, G.P., and Uhl, J.T. 1986. *Correlation of the Mobility of Biopolymer with Polymer Concentration and Rock Properties in Sandstone*. Polymer Science and Engineering. 55:577.

Wreath, D., Pope, G., and Sepehrnoori, K. 1990. *Dependence of Polymer Apparent Viscosity on the Permeable Media and Flow Conditions*. In Situ, 14 (3): 263-284.

Xia, H., Ju, Y., Kong, F., and Wu, J. 2004. *Effect of Elastic Behavior of HPAM Solutions on Displacement Efficiency Under Mixed Wettability Conditions*. Paper SPE 90234 presented at the 2004 SPE International Petroleum Conference in Mexico, Puebla, Mexico, 8-9 November.

Yuan, C., Delshad, M., and Wheeler, M.F. 2010. *Parallel Simulations of Commercial-Scale Polymer Floods*. Paper SPE 132441 presented at the SPE Western Regional Meeting, Anaheim, California, 27-29 May.

RP 63, *Recommended Practices for Evaluation of Polymers Used in Enhanced Oil Recovery Operations*, First Edition. 1990. Washington, DC: API.